

# DEUTSCHES ELEKTRONEN – SYNCHROTRON **DESY**

DESY 88-180  
December 1988



## Radiative Effects and Flavor Mixing in the Standard Model

R.D. Peccei

*Deutsches Elektronen-Synchrotron DESY, Hamburg*

ISSN 0418-9833

NOTKESTRASSE 85 · 2 HAMBURG 52

**DESY behält sich alle Rechte für den Fall der Schutzrechtserteilung und für die wirtschaftliche Verwertung der in diesem Bericht enthaltenen Informationen vor.**

**DESY reserves all rights for commercial use of information included in this report, especially in case of filing application for or grant of patents.**

**To be sure that your preprints are promptly included in the  
HIGH ENERGY PHYSICS INDEX,  
send them to the following address (if possible by air mail):**

**DESY  
Bibliothek  
Notkestrasse 85  
2 Hamburg 52  
Germany**

# Radiative Effects and Flavor Mixing in the Standard Model

R.D. Peccei\*

Deutsches Elektronen Synchrotron DESY  
Hamburg, Fed. Rep. Germany

## Abstract

After a brief introduction to the standard model and a summary of some salient experimental results, a fairly extensive, but at the same time elementary, discussion of electroweak radiative corrections is given. Special attention is paid to the effect of having a large top and/or Higgs mass. Experimental constraints, both direct and indirect, for the presence of top are discussed and the present bounds on the number of generations are reviewed. Assuming the existence of only three generations, a detailed discussion is given of the uncertainties associated with the determination of the elements of the quark mixing matrix. Several issues in particle-antiparticle mixing and CP violation are also broached.

## 1 A Précis of the Standard Model

The standard model for the electroweak interactions [1] is based on an  $SU(2) \times U(1)$  gauge theory which is spontaneously broken to  $U(1)_{em}$ . The model has three distinct sectors:

1. The Gauge-Higgs sector
2. The Fermion-Gauge sector
3. The Fermion-Higgs sector

Experimentally, very little is known about the first sector. The only thing that has been established with some accuracy here is the interrelation between the  $W$  and the  $Z$  boson masses, which is predicted by Higgs doublet breaking. The Fermion-Gauge sector, on the contrary, is quite well checked by experiment. For instance, as I will discuss in some detail, it is already necessary to include electroweak radiative corrections, for a comparison of theory with experiment, testifying to the precision with which one understands this part of the standard model. The last sector above, has essentially no experimental support. The only evidence here is inferential. Quark mass generation, via the Fermion-Higgs Yukawa couplings, induces flavour mixing in the charged weak currents and such mixing has been observed. Indeed, the mixing matrix  $V$  plays a fundamental role in a variety of phenomena: CP violation, flavor oscillations, etc- topics which will occupy us for a fair fraction of these lectures.

\*Lectures presented at the TASI-88 Summer School, Brown University, Providence, Rhode Island, June 1988

## 1.1 The Gauge-Higgs Sector

The gauge Lagrangian for  $SU(2) \times U(1)$  is augmented by including a scalar field  $\Phi$ , whose self interactions lead to a breakdown of  $SU(2) \times U(1)$  to  $U(1)_{em}$ . The simplest such scalar field is a complex doublet and the Gauge-Higgs Lagrangian reads

$$\mathcal{L}_{GH} = -\frac{1}{4}F_a^{\mu\nu}F_{a\mu\nu} - \frac{1}{4}F_Y^{\mu\nu}F_{Y\mu\nu} - (D_\mu\Phi)^\dagger(D^\mu\Phi) - V(\Phi) \quad (1)$$

In the above  $F_a^{\mu\nu}$  and  $F_Y^{\mu\nu}$  are the  $SU(2)$  and  $U(1)$  field strengths, respectively:

$$F_a^{\mu\nu} = \partial^\mu W_a^\nu - \partial^\nu W_a^\mu + ig\epsilon_{abc}W_b^\mu W_c^\nu \quad (2)$$

$$F_Y^{\mu\nu} = \partial^\mu Y^\nu - \partial^\nu Y^\mu \quad (3)$$

and  $D_\mu\Phi$  is the  $SU(2) \times U(1)$  covariant derivative <sup>1</sup>

$$D_\mu\Phi = [\partial_\mu - ig\frac{\tau_a}{2}W_a^\mu + i\frac{g'}{2}Y_\mu]\Phi \quad (4)$$

Here  $g$  and  $g'$  are the  $SU(2)$  and  $U(1)$  coupling constants, respectively. The potential  $V(\Phi)$  is such that the doublet Higgs field  $\Phi$  acquires a vacuum expectation value, thereby causing the breakdown  $SU(2) \times U(1) \rightarrow U(1)_{em}$ . The vacuum expectation value

$$\langle \Phi \rangle = \frac{v}{\sqrt{2}} \begin{pmatrix} 1 \\ 0 \end{pmatrix} \quad (5)$$

breaks  $SU(2)$  and  $U(1)$  but conserves  $U(1)_{em}$ , since the charge

$$Q = T_3 + Y \quad (6)$$

acting on  $\langle \Phi \rangle$  vanishes:

$$Q \langle \Phi \rangle = \begin{pmatrix} 0 & 0 \\ 0 & -1 \end{pmatrix} \frac{v}{\sqrt{2}} \begin{pmatrix} 1 \\ 0 \end{pmatrix} = 0 \quad (7)$$

The breakdown of  $SU(2) \times U(1) \rightarrow U(1)_{em}$  gives mass to three of the gauge fields. These mass terms are readily computed from the Higgs field kinetic energy term by replacing  $\Phi$  by its vacuum expectation value  $\langle \Phi \rangle$ :

$$\mathcal{L}_{mass} = -(D_\mu \langle \Phi \rangle)^\dagger (D^\mu \langle \Phi \rangle) \quad (8)$$

With  $\langle \Phi \rangle$  given by Eq(5), one sees readily that the charged fields

$$W_\pm^\mu = \frac{1}{\sqrt{2}}[W_1^\mu \mp iW_2^\mu], \quad (9)$$

as well as

$$[\frac{\tau_3}{2}W_3^\mu - \frac{g'}{2}Y^\mu]_{11} = \frac{1}{2}[gW_3^\mu - g'Y^\mu] \quad (10)$$

<sup>1</sup>The field  $\Phi$  has hypercharge  $Y$  equal to  $-\frac{1}{2}$ .

The interactions of the Higgs field with the gauge fields are also fixed. The complex doublet  $\Phi$  is composed of four real fields. Of these, three are "eaten" by the Higgs mechanism to give longitudinal components to the  $W^\pm$  and  $Z$  fields. The remaining scalar field is the physical Higgs boson,  $H$ . It is possible to parameterize  $\Phi$  so as to make its physical content manifest. One writes  $\Phi$  as

$$\Phi = \frac{1}{\sqrt{2}} e^{i\xi} \begin{pmatrix} v - H \\ 0 \end{pmatrix} \quad (15)$$

In the above the fields  $\xi$  are unphysical. Indeed, since the potential  $V(\Phi)$  is really only a function of  $\Phi^\dagger\Phi$ , it is clear that  $\xi$  does not enter in  $V$  at all. Furthermore,  $\xi$  can be eliminated by a gauge choice from the covariant derivative  $D_\mu\Phi$  [2]. Hence, effectively, one can replace  $\Phi$  by

$$\Phi \equiv \frac{1}{\sqrt{2}} \begin{pmatrix} v + H \\ 0 \end{pmatrix} \quad (16)$$

The Gauge-Higgs interactions are immediately read off from the Higgs kinetic energy terms in (1), using the above representation. There are both trilinear and quadrilinear couplings. The trilinear couplings, for instance, are proportional to the mass of the gauge fields and one finds

$$\mathcal{L}_{\text{trilinear}} = -\frac{\epsilon}{2\sin\Theta_W \cos\Theta_W} M_Z Z^\mu Z_\mu H - \frac{\epsilon}{\sin\Theta_W} M_W W_\mu^+ W_\mu^- H \quad (17)$$

Note that there is no direct  $H A^\mu A_\mu$  coupling.

## 1.2 The Fermion-Gauge Sector

The interactions of the fermions (quarks and leptons) with the  $SU(2) \times U(1)$  fields are fixed, once their  $SU(2) \times U(1)$  quantum numbers are specified. The Gauge-Fermion Lagrangian is simply

$$\mathcal{L}_{GF} = -\sum_i \bar{\psi}_i \gamma^\mu \frac{1}{i} D_\mu \psi_i \quad (18)$$

where  $D_\mu \psi_i$  is the appropriate covariant derivative for the  $i^{\text{th}}$  fermion:

$$D_\mu \psi_i = [\partial_\mu - ig(t_a)_i W_{a\mu} - ig(y)_i Y_\mu] \psi_i \quad (19)$$

The known fermions have left handed helicity components<sup>2</sup> which transform as an  $SU(2)$  doublet ( $t_a = \frac{t_a}{2}$ ), while their right handed components are  $SU(2)$  singlets ( $t_a = 0$ ). Their hypercharge values follow directly from their charge, via Eq(6). Furthermore, fermions come in repetitive patterns (families, or generations) which have the same quantum numbers. I summarize the relevant  $SU(2) \times U(1)$  properties of the first generation of quarks and leptons in Table 1 below<sup>3</sup>.

<sup>2</sup>In my conventions  $\psi_L = \frac{1}{2}(1 - \gamma_5)\psi$ ;  $\psi_R = \frac{1}{2}(1 + \gamma_5)\psi$ .

<sup>3</sup>The right handed neutrino is usually omitted, since it has no  $SU(2) \times U(1)$  quantum numbers

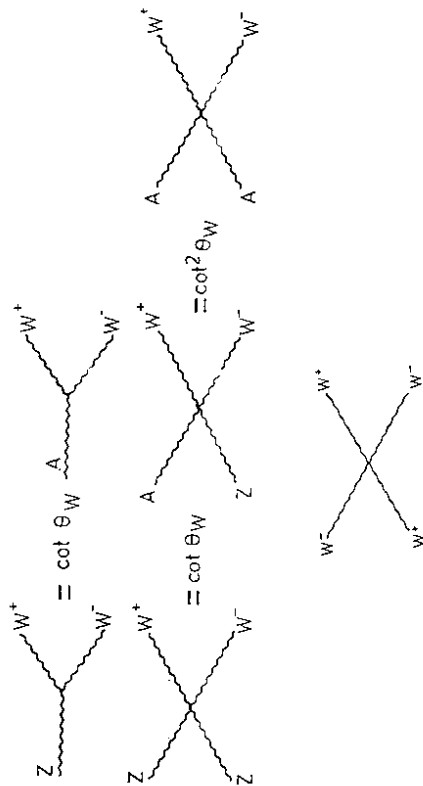


Figure 1: Non vanishing 3-gauge and 4-gauge vertices.

get mass. It is convenient to define two new neutral fields  $Z^\mu$  and  $A^\mu$ , related to  $W_3^\mu$  and  $Y^\mu$  by

$$\begin{pmatrix} W_3^\mu \\ Y^\mu \end{pmatrix} = \begin{pmatrix} \cos\Theta_W & \sin\Theta_W \\ -\sin\Theta_W & \cos\Theta_W \end{pmatrix} \begin{pmatrix} Z^\mu \\ A^\mu \end{pmatrix} \quad (11)$$

By picking the mixing angle  $\Theta_W$  - the Weinberg angle - as

$$\tan\Theta_W = \frac{g'}{g} \quad (12)$$

so that  $[gW_3^\mu - g'Y^\mu] = \frac{g}{\cos\Theta_W} Z^\mu$ , one insures that  $Z^\mu$  and  $A^\mu$  are the mass eigenstates. A simple calculation then gives

$$\mathcal{L}_{\text{mass}} = -\frac{1}{2} \frac{g^2 v^2}{2\cos\Theta_W} Z^\mu Z_\mu - \frac{g^2 v^2}{2} W_\mu^+ W_\mu^- \quad (13)$$

Since the  $A^\mu$  field has no mass term, it is naturally identified as the photon field. Furthermore, one learns that for doublet breaking there is a simple relation between the  $W$  and  $Z$  masses. Namely:

$$M_W = M_Z \cos\Theta_W = \frac{g'}{2} \quad (14)$$

The gauge interactions arise from the  $F_a^{\mu\nu} F_{a\mu\nu}$  term in the Lagrangian (1). Because of this they obey particular symmetry properties, due to the  $\epsilon_{abc}$  term in (2). Furthermore, the interactions of the photon and  $Z$  fields have fixed ratios, since  $W_3^\mu = \cos\Theta_W Z^\mu + \sin\Theta_W A^\mu$ . These interconnections, for the nonvanishing 3-gauge and 4-gauge vertices are shown in Fig 1.

Table 1: Fermion assignments in the standard model

Fermion	$SU(2)$	$U(1)$	$Q = T_3 + Y$
$\begin{pmatrix} \nu_e \\ e \end{pmatrix}_L$	2	$-\frac{1}{2}$	$\begin{pmatrix} 0 \\ -1 \end{pmatrix}$
$e_R$	1	-1	-1
$\begin{pmatrix} u \\ d \end{pmatrix}_L$	2	$\frac{1}{6}$	$\begin{pmatrix} \frac{2}{3} \\ -\frac{1}{3} \end{pmatrix}$
$u_R$	1	$\frac{2}{3}$	$\frac{2}{3}$
$d_R$	1	$-\frac{1}{3}$	$-\frac{1}{3}$

From Eq(18) it follows that the interactions between the gauge fields and the fermions can be written as

$$\mathcal{L} = g J_a^\mu W_{a\mu} + g' J_Y^\mu Y_\mu \quad (20)$$

where the  $SU(2)$  and  $U(1)$  fermionic currents are given by

$$J_a^\mu = \sum \bar{\psi}_i \gamma^\mu (t_a)_i \psi_i \quad (21)$$

$$J_Y^\mu = \sum \bar{\psi}_i \gamma^\mu (y)_i \psi_i \quad (22)$$

Using Eq.(12), Eq.(20) can be rewritten in terms of the physical fields  $Z^\mu$ ,  $A^\mu$  and  $W_\pm^\mu$  and their associated currents:

$$Z^\mu \leftrightarrow J_{NC}^\mu = 2(J_3^\mu - \sin^2 \Theta_W J_{em}^\mu) \quad (23)$$

$$A^\mu \leftrightarrow J_{em}^\mu = J_3^\mu + J_Y^\mu \quad (24)$$

$$W_\pm^\mu \leftrightarrow J_\pm^\mu = 2(J_1^\mu \pm iJ_2^\mu) \quad (25)$$

One finds in this way for  $\mathcal{L}_{int}$  the expression

$$\mathcal{L}_{int} = e J_{em}^\mu A_\mu + \frac{\epsilon}{2\sqrt{2}\sin\Theta_W} (W_+^\mu J_{-\mu} - W_-^\mu J_{+\mu}) + \frac{\epsilon}{2\cos\Theta_W \sin\Theta_W} Z_\mu J_{NC}^\mu \quad (26)$$

In the above, the identification of the electric charge  $e$  as the strenght of the coupling between the photon field and the electromagnetic current, has been used. This identification provides the coupling constant interrelation (unification condition)

$$\epsilon = g' \cos\Theta_W = g \sin\Theta_W \quad (27)$$

For weak interaction processes where the momentum transfer  $q^2$  is such that  $q^2 \ll M_W^2, M_Z^2$ , the effects of  $\mathcal{L}_{int}$  can be well approximated by a current-current effective Lagrangian

$$\mathcal{L}_{eff}^{weak} = \frac{i}{2!} \int \mathcal{L}_{int} \cdot \mathcal{L}_{int} \simeq \left( \frac{\epsilon}{2\sqrt{2}\sin\Theta_W} \right)^2 \frac{1}{M_W^2} J_{-\mu}^\mu J_{-\mu}^\mu + \frac{1}{2} \left( \frac{\epsilon}{2\cos\Theta_W \sin\Theta_W} \right)^2 \frac{1}{M_Z^2} J_{NC}^\mu J_{NC\mu} \quad (28)$$

In this limit the Glashow Salam Weinberg model reduces to the Fermi theory, plus an additional neutral current interaction contribution. This allows one to identify the Fermi constant  $G_F$  as

$$\frac{G_F}{\sqrt{2}} = \frac{\epsilon^2}{8 \sin^2 \Theta_W M_W^2} \quad (29)$$

It has become conventional to introduce a parameter

$$\rho = \frac{M_W^2}{M_Z^2 \cos^2 \Theta_W} \quad (30)$$

Then Eq(28) simplifies to

$$\mathcal{L}_{eff}^{weak} = \frac{G_F}{\sqrt{2}} [J_+^\mu J_{-\mu} + \rho J_{NC}^\mu J_{NC\mu}] \quad (31)$$

Note that, in the case of doublet Higgs breaking, Eq(14) gives  $\rho = 1$ .

### 1.3 The Fermion-Higgs Sector

Ordinary fermion mass terms, since they connect  $\bar{\psi}_L$  with  $\psi_R$ , are forbidden by  $SU(2)$ . However, a Yukawa coupling of  $\bar{\psi}_L$  and  $\psi_R$  to the doublet Higgs field  $\Phi$  is allowed. After the breakdown of  $SU(2) \times U(1)$  to  $U(1)_{em}$ , these interactions give rise to fermion mass terms. Thus a doublet Higgs field performs a dual role in the standard model: it gives mass to both gauge bosons and to the quarks and leptons. A general Yukawa interaction will mix fermions of different families, which have the same hypercharge. Thus, when  $\Phi$  gets replaced by its vacuum expectation value  $\langle \Phi \rangle$ , one obtains mass matrices for fermions of the same charge.

Let me discuss this point a bit more in detail. One considers besides  $\Phi$ , the Higgs doublet field of hypercharge  $-\frac{1}{2}$ , also its charge conjugate  $\bar{\Phi}$ , of hypercharge  $+\frac{1}{2}$ :

$$\bar{\Phi} = i\tau_2 \Phi^* \quad (32)$$

If  $i$  and  $j$  are family indices then, in an obvious notation, the most general  $SU(2) \times U(1)$  invariant Yukawa interaction is <sup>4</sup>

$$\mathcal{L}_{Yukawa} = -\Gamma_{ij}^u (\bar{u}_i, \bar{d}_i)_L \Phi u_{jR} - \Gamma_{ij}^d (\bar{u}_i, \bar{d}_i)_L \bar{\Phi} d_{jR} + \Gamma_{ij}^l (\bar{\nu}_i, \bar{e}_i)_L \bar{\Phi} l_{jR} + h.c. \quad (33)$$

The effective replacement of  $\Phi$  by Eq(16) and of  $\bar{\Phi}$  by

$$\bar{\Phi} = \frac{1}{\sqrt{2}} \begin{pmatrix} 0 \\ v + H \end{pmatrix} \quad (34)$$

yields mass terms for fermions of the same charge and couplings for the Higgs boson  $H$  with the fermions. Since the role of  $v$  and  $H$  in Eqs(6) and (34) are interchangeable, it suffices to focus on the mass terms, which read

$$\mathcal{L}_{Mass} = -\bar{u}_{iL} M_{ij}^u u_{jR} - \bar{d}_{iL} M_{ij}^d d_{jR} - \bar{l}_{iL} M_{ij}^l l_{jR} + h.c. \quad (35)$$

with

$$M_{ij}^f = \frac{1}{\sqrt{2}} \Gamma_{ij}^f v \quad (f = \{u, d, l\}) \quad (36)$$

<sup>4</sup>No Yukawa interactions containing right handed neutrinos are generally included, so as not to generate neutrino masses.

Because the above mass matrices are not necessarily diagonal or hermitean one needs to perform a basis change to get to the physical fermion fields. It is this basis change which causes the family mixing of the states probed by the weak interactions.

Specifically, the matrix  $M^f$  can be diagonalized by the bi-unitary transformation<sup>5</sup>

$$(U_L^f)^\dagger M^f (U_R^f) = M_{diag}^f \quad (37)$$

and the fermion fields are replaced by

$$\psi_{L,R}^f \rightarrow U_{L,R}^f \psi_{L,R}^f \quad (38)$$

These replacements introduce a mixing matrix for the charged currents, but do not affect the neutral currents. This is easily checked. For the case of three generations, for example, before the basis change the charged current  $J_\pm^\mu$  reads

$$J_\pm^\mu = 2(\bar{\nu}_e \bar{\nu}_\mu \bar{\nu}_\tau)_L \gamma^\mu \mathbf{1} \begin{pmatrix} c \\ \mu \\ \tau \end{pmatrix}_L + 2(\bar{u} \bar{c} \bar{t})_L \gamma^\mu \mathbf{1} \begin{pmatrix} d \\ s \\ b \end{pmatrix}_L \quad (39)$$

After the basis change Eq(38) this current becomes

$$J_\pm^\mu = 2(\bar{\nu}_e \bar{\nu}_\mu \bar{\nu}_\tau)_L \gamma^\mu U_L^\nu \begin{pmatrix} c \\ \mu \\ \tau \end{pmatrix}_L + 2(\bar{u} \bar{c} \bar{t})_L \gamma^\mu (U_L^q)^\dagger U_L^d \begin{pmatrix} d \\ s \\ b \end{pmatrix}_L \quad (40)$$

Because the neutrinos are massless, the matrix  $U_L^\nu$  above can be eliminated by a redefinition of the neutrino fields. The matrix  $(U_L^q)^\dagger U_L^d$  appearing in the quark sector, on the other hand, remains. It is the  $3 \times 3$  unitary mixing matrix of the charged current sector - the Cabibbo Kobayashi Maskawa matrix  $V$  [3]. It is clear that the basis change of Eq(38) will not change the form of the neutral or electromagnetic currents, since these currents always involve fermions of the same charge and  $(U_L^f)^\dagger U_L^f = (U_R^f)^\dagger U_R^f = 1$ .

The basis change (38) which diagonalizes the mass matrices  $M^f$ , obviously diagonalizes also the Yukawa couplings  $\Gamma^f$ . Clearly, therefore, after the basis change to physical fermion fields, the coupling of the Higgs boson  $H$  to the fermions is purely diagonal and the Higgs-Fermion Lagrangian is simply

$$\mathcal{L}_{HF} = - \sum_i [m_i \bar{\psi}_i \psi_i + \frac{m_i}{v} H \bar{\psi}_i \psi_i] \quad (41)$$

Note that here also the Higgs couplings are proportional to the mass of the particles with which it interacts. The only remnant of the mass generation mechanism coming from the Yukawa interactions Eq(33) in the mixing matrix  $V$  entering in the charged currents. As can be seen from Eq(40)  $V$  is a unitary matrix

$$V^\dagger V = V V^\dagger = 1 \quad (42)$$

For the case of  $n$  families, such a matrix is described by  $\frac{1}{2}n(n-1)$  real angles and  $\frac{1}{2}n(n+1)$  phases. However, by further diagonal phase redefinitions of the quark fields one can always remove  $2n-1$  of the phases<sup>6</sup>. Thus physically the Cabibbo Kobayashi Maskawa mixing matrix  $V$  is described by  $\frac{1}{2}n(n-1)$  real angles and  $\frac{1}{2}n(n-2)$  phases. In particular, one needs at least three generations to have a phase in  $V$ . As we shall see later in these lectures, this phase can account for the CP violating phenomena seen in the Kaon system.

<sup>5</sup>If  $M^f$  is hermitean, then  $U_L^f = U_R^f$ .

<sup>6</sup> $2n-1$ , not  $2n$  because an overall phase has no physical meaning.

## 2 Testing the Standard Model

Since the standard model, by construction, reproduces the low  $q^2$  charged current weak interactions [cf Eq(31)], tests of the standard model have necessarily focused on neutral current processes. These interactions, if one has no prejudice on the Higgs sector, depend on two parameters:  $\sin^2 \Theta_W$  and  $\rho$ . On the other hand, if one assumes that the breakdown  $SU(2) \times U(1) \rightarrow U(1)_{em}$  is effected by a Higgs doublet, then  $\rho = 1$  and the only parameter to describe neutral current processes is the Weinberg angle. In a nutshell, the electroweak model of Glashow Salam and Weinberg [1] has become the standard model since all neutral current experiments [Neutrino deep inelastic scattering; polarized lepton deep inelastic scattering;  $W$  and  $Z$  properties; neutrino electron scattering; elastic neutrino nucleon scattering; parity violation in atoms] lead, within errors, to the same values of  $\sin^2 \Theta_W$  and  $\rho$ .

### 2.1 Resumé of Salient Experimental Results

In this subsection, I want to summarize the present experimental status of the most accurate neutral current experiments to:

- show the "state of the art" testing to which the standard model has been subjected
- indicate the beginning importance which electroweak radiative corrections are playing in comparing standard model predictions with experiment

I will focus particularly, therefore, on deep inelastic experiments involving neutrinos ( $\nu_\mu$ ) and antineutrinos ( $\bar{\nu}_\mu$ ) and on the experimentally determined properties of the  $W$  and  $Z$  bosons.

The comparison of the neutral current processes  $\nu_\mu \bar{N} \rightarrow \nu_\mu \bar{X}$  and  $\bar{\nu}_\mu N \rightarrow \bar{\nu}_\mu X$  with the charged current processes  $\nu_\mu \bar{N} \rightarrow \mu^- X$  and  $\bar{\nu}_\mu N \rightarrow \mu^+ X$  allows the determination of both  $\rho$  and  $\sin^2 \Theta_W$ . For the case of scattering on an isoscalar target, as provided by a nucleus with an equal number of neutrons and protons, so that  $N = \frac{1}{2}(n+p)$ , and in a world of only one generation [so that the quark "flavors" in a nucleon are only  $u, d$  and their antiparticles  $\bar{u}, \bar{d}$ ] there is a simple connection between the charged and neutral current processes, shown in Fig 2. Defining as usual the kinematical variables  $x$  and  $y$  by

$$x = \frac{q^2}{-2P \cdot q} ; \quad y = \frac{P \cdot q}{P \cdot l} \quad (43)$$

there are three possible ratios measured experimentally:

$$R_\mu = \frac{\int dx dy < \frac{d\sigma}{dx dy} >_{\nu_\mu N \rightarrow \nu_\mu X}}{\int dx dy < \frac{d\sigma}{dx dy} >_{\nu_\mu N \rightarrow \mu^- X}} \quad (44)$$

$$R_{\bar{\mu}} = \frac{\int dx dy < \frac{d\sigma}{dx dy} >_{\bar{\nu}_\mu N \rightarrow \bar{\nu}_\mu X}}{\int dx dy < \frac{d\sigma}{dx dy} >_{\bar{\nu}_\mu N \rightarrow \mu^+ X}} \quad (45)$$

and

$$r = \frac{\int dx dy < \frac{d\sigma}{dx dy} >_{\nu_\mu N \rightarrow \mu^+ X}}{\int dx dy < \frac{d\sigma}{dx dy} >_{\nu_\mu N \rightarrow \mu^- X}} \quad (46)$$

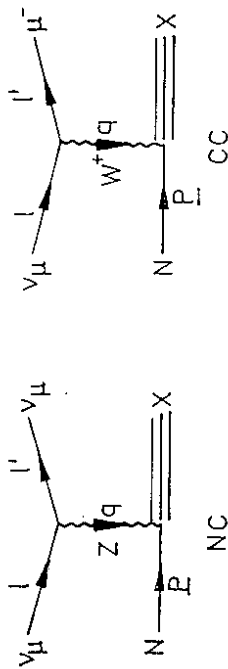


Figure 2: Deep inelastic neutral current and charged current processes involving neutrinos.

For  $q^2 \ll M_W^2, M_Z^2$  and for scattering off isoscalar targets assumed to be composed only of quarks and antiquarks of the first family, one can readily establish the, so called, Llewellyn Smith relations [4] among these ratios:

$$R_L = \rho^2 \left[ \left( \frac{1}{2} - \sin^2 \Theta_W \right) + \frac{5}{9} \sin^4 \Theta_W (1 + r) \right] \quad (47)$$

$$R_F = \rho^2 \left[ \left( \frac{1}{2} - \sin^2 \Theta_W \right) + \frac{5}{9} \sin^4 \Theta_W (1 + r^{-1}) \right] \quad (48)$$

That is, for this simplified situation, one can altogether bypass the structure functions to compute the neutral current cross sections, provided one measures at the same time the charged current cross sections. Of course, in real life, scattering is done on not purely isoscalar targets. Furthermore, one must also take into account that nucleons have also a sea of strange quarks, charm quarks, etc. These real life effects, however, give rise to small corrections, which one can account for in a systematic way.

As an illustration, I indicate briefly the procedure followed by the CDHS collaboration [5] to extract  $\sin^2 \Theta_W$ . Analogous corrections have been also applied in other deep inelastic experiments [6,7,8]. What was measured by the CDHS collaboration are the ratios  $R_L$  and  $R_F$ , with the results

$$R_L = 0.3072 \pm 0.0025 \pm 0.0020 \quad (49)$$

$$r = 0.39 \pm 0.01 \quad (50)$$

where the two errors in Eq(49) are, respectively, statistical and systematic. Assuming  $\rho = 1$ , the Llewellyn Smith relation Eq(47) implies a value

$$(\sin^2 \Theta_W)_{\text{uncorr}} = 0.236 \pm 0.005 \quad (51)$$

To obtain a final value for the Weinberg angle, however, a number of corrections must be applied. The major "experimental" correction comes from the fact that the target,  $FC$ , is

not purely isoscalar. This lowers the value of  $\sin^2 \Theta_W$  by  $-0.009$  [5]. There are, on the other hand, a number of smaller "experimental" corrections, connected with the presence of strange and charm quarks in the nucleon, which essentially cancel this shift. In addition, however, one must apply electroweak radiative corrections to the data and when this is done - in the manner which I shall explain below - one lowers  $\sin^2 \Theta_W$  by  $-0.011$  [5]. In performing all of these corrections one incurs a certain theoretical error, because one needs to estimate many things which are not precisely known (e.g. the amount of strange sea). The biggest error in the final value one obtains for  $\sin^2 \Theta_W$  is due to the uncertainty in the value of the charm quark mass, which affects particularly the ratio  $r$ . Carrying through all these corrections CDHS obtains finally a value for  $\sin^2 \Theta_W$

$$\sin^2 \Theta_W = 0.225 \pm 0.005 \pm [0.003 \pm 0.013(m_c - 1.5 \text{ GeV})] \quad (52)$$

The error in the square bracket is an estimate of the theoretical uncertainty. Assuming, as is reasonable, that  $m_c = 1.5 \pm 0.3 \text{ GeV}$ , then the full  $m_c$  uncertainty gives a theoretical error of [0.005]. The electroweak radiative effects included in Eq(52) are computed using a definition of  $\sin^2 \Theta_W$  in which

$$\sin^2 \Theta_W = 1 - \frac{M_W^2}{M_Z^2} \quad (53)$$

I will explain shortly why one needs to specify precisely what one means by  $\sin^2 \Theta_W$ , when one computes radiative corrections. Here I note only that these radiative effects have lowered the raw experimental value for  $\sin^2 \Theta_W$  by about 4%.

The results of CDHS are in perfect agreement with results obtained at Fermilab [7] [8] and by the other large neutrino scattering experiment at CERN, CHARM [6]. Assuming that  $\rho = 1$ , the results of all these experiments, including CDHS, are reported in Table 2. The error in brackets in this Table is an estimate of the theoretical uncertainty.

Table 2: Results of Deep Inelastic Neutrino Experiments for  $\sin^2 \Theta_W$

$\sin^2 \Theta_W = 0.235 \pm 0.005 \pm [0.005]$	CDHS[5]
$\sin^2 \Theta_W = 0.236 \pm 0.005 \pm [0.005]$	CHARM[6]
$\sin^2 \Theta_W = 0.239 \pm 0.010$	CCFR[7]
$\sin^2 \Theta_W = 0.246 \pm 0.016$	FHH[8]

Recently a global reanalysis of these inelastic experiments, and of all other neutral current experiments, has been performed by two groups [9] [10]. I will give below, for definitiveness, the results of Amaldi et al [9]. However, those of Costa et al [10] are quite similar. Correcting the raw experimental value of  $\sin^2 \Theta_W$  for all experimental effects, but not including radiative corrections, Amaldi et al [9] arrive at a "bare" average value for the Weinberg angle [9] of

$$(\sin^2 \Theta_W)_{\text{DIS}} = 0.242 \pm 0.006 \quad (54)$$

Applying radiative corrections, adopting the definitions Eq(53) for  $\sin^2 \Theta_W$  and using in addition the values  $m_t = 45 \text{ GeV}$  and  $M_H = 100 \text{ GeV}$ , for the yet unknown top and Higgs masses, gives a downward shift

$$\delta s^2 = -0.009 \pm 0.001 \quad (55)$$

The final value quoted by Amaldi et al [9] from their global fit of all neutrino deep inelastic data, assuming  $\rho = 1$ , is

$$(\sin^2 \Theta_W)_{DIS} = 0.233 \pm 0.003 \pm [0.005] \quad (56)$$

which is in perfect agreement with the values given by the individual experiments in Table 2.

To determine  $\rho$  in addition one needs to measure also  $R_\rho$ . The most accurate values for  $R_\rho$  come from the CERN experiments [11, 12]:

$$\begin{aligned} R_\rho &= 0.363 \pm 0.015 \quad CDHS[11] \\ R_\rho &= 0.377 \pm 0.020 \quad CHARM[12] \end{aligned} \quad (57)$$

Including also experimental information on  $R_\rho$ , Amaldi et al [9] obtain values for both  $\rho$  and  $\sin^2 \Theta_W$ . A two parameter fit of all data yields:

$$\sin^2 \Theta_W = 0.232 \pm 0.014 \pm [0.008] \quad (58)$$

$$\rho = 0.999 \pm 0.013 \pm [0.008] \quad (59)$$

One sees that the above is quite consistent with the fit obtained by fixing  $\rho = 1$ . Furthermore, Eq(59) shows that the hypothesis of doublet Higgs breaking is well established experimentally.

A second set of precision measurements for testing the electroweak theory comes from the CERN collider measurements of the  $W$  and  $Z$  properties. The mass values for the  $W^\pm$  and the  $Z$  bosons, measured by the  $UA1$  and  $UA2$  collaborations, have been summarized by Jenni [13] and are displayed in Table 3 below.

Table 3: Values of  $W$  and  $Z$  Masses [13]

$M_W = (82.7 \pm 1.0 \pm 2.7) GeV$	$UA1(e\nu)$	Average	$(80.8 \pm 1.3) GeV$
$M_W = (80.2 \pm 0.6 \pm 1.7) GeV$	$UA2(e\nu)$	$M_W =$	$(80.8 \pm 1.3) GeV$
$M_Z = (93.1 \pm 1.0 \pm 3.1) GeV$	$UA1(e^+e^-)$	Average	$(92.0 \pm 1.8) GeV$
$M_Z = (91.5 \pm 1.2 \pm 1.7) GeV$	$UA2$	$M_Z =$	$(92.0 \pm 1.8) GeV$

Using Eq(53) one can compute  $\sin^2 \Theta_W$  directly from the  $W$  and  $Z$  mass values. In so doing, the large systematic errors in Table 3 largely cancel. However, the statistical accuracy is still not good enough to obtain a really significant number. One finds in this way that

$$\sin^2 \Theta_W = 1 - \frac{M_W^2}{M_Z^2} = \left\{ \begin{array}{l} 0.211 \pm 0.025 \quad UA1(e\nu) \\ 0.232 \pm 0.025 \pm 0.010 \quad UA2 \end{array} \right\} \quad (60)$$

These values agree with those of Eq(56), but the errors are such that not much more can be said.

One can, however, do a much more accurate comparison between different determinations of  $\sin^2 \Theta_W$  by using a radiatively corrected version of the formula [cf Eq(29)] relating

the Fermi constant to  $M_W$  and  $\sin^2 \Theta_W$ . One can write this formula as an equation for  $\sin^2 \Theta_W$ :

$$\sin^2 \Theta_W = \frac{\pi\alpha}{\sqrt{2}G_F M_W^2} \left[ \frac{1}{1 - \Delta r} \right] = \frac{(37.281 GeV)^2}{M_W^2 [1 - \Delta r]} \quad (61)$$

In the above  $\alpha$  is the fine structure constant  $\alpha = \frac{e^2}{4\pi}$ , measured at zero momentum transfer. The quantity  $\Delta r$  contains the effects of the radiative corrections and we shall discuss it shortly in detail. For the definition Eq(53) of  $\sin^2 \Theta_W$ ,  $\Delta r$  is rather large. Adopting again as canonical values  $m_t = 45 GeV$  and  $M_H = 100 GeV$ , one finds [14, 9]:

$$\Delta r = 0.0713 \pm 0.0013 \quad (62)$$

Using the  $UA1$  and  $UA2$  vector boson masses and Eq(61), one obtains

$$\begin{aligned} \sin^2 \Theta_W &= 0.218 \pm 0.005 \pm 0.014 \quad UA1(e\nu) \\ \sin^2 \Theta_W &= 0.232 \pm 0.003 \pm 0.008 \quad UA2 \end{aligned} \quad (63)$$

which lead to an average value - indicating also an estimate of possible theoretical uncertainties [9] - of

$$(\sin^2 \Theta_W)_{M_W/M_Z} = 0.228 \pm 0.007 \pm [0.002], \quad (64)$$

The values for  $\sin^2 \Theta_W$  obtained in deep inelastic scattering experiments, Eq(56), is in very good agreement with that of Eq(64), which follows from the measurements of the  $W$  and  $Z$  masses. I should note, however, that this comparison is very much aided by the inclusion of radiative corrections. If one had set in Eq(61)  $\Delta r = 0$ , then the "bare" value of  $\sin^2 \Theta_W$  one would have obtained would have been

$$(\sin^2 \Theta_W)_{M_W/M_Z} = 0.212 \pm 0.007 \quad (65)$$

The effect of radiative corrections is to **increase** this value by about 7%. In the case of deep inelastic scattering, however, the effect of the radiative corrections was to **decrease** the value of  $\sin^2 \Theta_W$  by about 4%. So the bare values, Eqs(54) and (65), are actually quite far apart. This is summarized in Table 4.

Table 4: Radiative effects for  $\Theta_W$ .

	$\sin^2 \Theta_W^0$	$\sin^2 \Theta_W$
Deep Inelastic	$0.242 \pm 0.006$	$0.233 \pm 0.003 \pm [0.005]$
W/Z Masses	$0.212 \pm 0.007$	$0.228 \pm 0.007 \pm [0.002]$

As a final point I display in Fig 3 the results in the  $\rho - \sin^2 \Theta_W$  plane of the global fit of Amaldi et al [9] of all neutral current experiments. As can be seen, the most accurate determinations for  $\rho$  and  $\sin^2 \Theta_W$  come from the two processes discussed above. However, all neutral current experiments find a consistent value of  $\rho$  and  $\sin^2 \Theta_W$ , testifying to the validity of the standard model - at least to the level of accuracy to which it is probed today. Setting  $\rho = 1$ , this global fit yield for  $\sin^2 \Theta_W$  the value

$$\sin^2 \Theta_W = 0.230 \pm 0.0048 \quad (66)$$

<sup>†</sup>The error here is due to uncertainties in the cross section  $e^+e^- \rightarrow hadrons$  at low energy, needed for a full estimate of  $\Delta r$ .



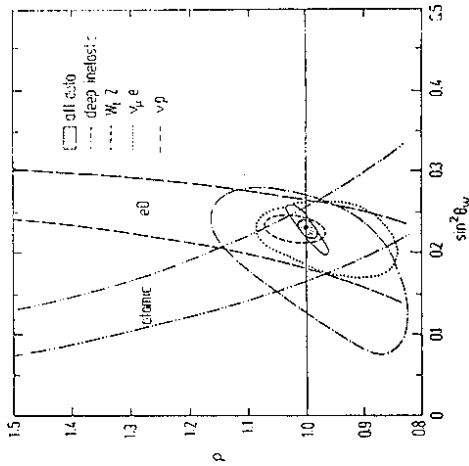


Figure 3: Allowed regions in the  $\rho - \sin^2 \Theta_W$  plane at 90% C.L. for various neutral current processes. From [9]

## 2.2 Electroweak Radiative Corrections and the Renormalization Group

I have indicated briefly earlier than when considering radiative corrections one must specify how  $\sin^2 \Theta_W$  is defined. In the 0<sup>th</sup> order discussion of Sec.1 we have defined  $\sin^2 \Theta_W$  in a number of different - but to this order, equivalent - ways:

- Through the unification condition, Eq(27):

$$\epsilon = g' \cos \Theta_W = g \sin \Theta_W \quad (67)$$

- Via the interrelation of the  $W$  and  $Z$  masses, corresponding to doublet Higgs breaking, Eq(14):

$$\sin^2 \Theta_W = 1 - \frac{M_W^2}{M_Z^2} \quad (68)$$

- By comparing the low energy charged current interactions with the Fermi theory, Eq(29):

$$\frac{G_F}{\sqrt{2}} = \frac{c^2}{8 \sin^2 \Theta_W M_W^2} \quad (69)$$

- From the structure of the neutral current itself, Eq(23):

$$J_{NC}^\mu = 2(J_3^\mu - \sin^2 \Theta_W J_{em}^\mu) \quad (70)$$

Although these ways of specifying the Weinberg angle are equivalent in lowest order in  $\alpha$ , each of these definitions will get different corrections in higher order, with the corrections depending precisely on how the Weinberg's angle is physically defined. Thus one must agree on some definition of  $\sin^2 \Theta_W$ , and then all other definitions will be related in a calculable way to this conventionally picked value.

Sirlin [15] suggested in 1980 that a particularly useful definition for  $\sin^2 \Theta_W$  would tie this parameter directly with the measured values of the  $W$  and  $Z$  masses, also at  $O(\alpha)$ . That is, he suggested that one should adopt Eq(68) as the definition of  $\sin^2 \Theta_W$  also in higher order. Once one defines  $\sin^2 \Theta_W$  this way, then one fixes the way in which one absorbs infinities in higher order calculations and one can express all corrections to the lowest order results in terms of a well defined power series in  $\alpha$ . The advantage of using Sirlin's definition of  $\sin^2 \Theta_W$ , which is the definition I shall use in these lectures, is that one can estimate in most instances the dominant electroweak radiative corrections by means of the renormalization group [16]. Radiative corrections in the  $SU(2) \times U(1)$  theory can only be large if the electromagnetic coupling constant squared is accompanied by a large logarithm. A non logarithmic correction is proportional to  $\frac{\alpha}{\pi} \sim \frac{1}{500}$  and is negligible. A logarithmic correction, on the other hand, is enhanced since  $M_W^2 \gg \langle q^2 \rangle$ , with  $\langle q^2 \rangle >$  being the relevant momentum or energy transfer in the process, so that, typically,

$$\frac{\alpha}{\pi} \ln \frac{M_W^2}{\langle q^2 \rangle} \sim (2-3) \times 10^{-2} \quad (71)$$

These logarithmic factors in the calculation can be tracked by means of the renormalization group.

To understand the idea behind this, it is useful to look at the formula I used earlier connecting  $G_F$  with  $\sin^2 \Theta_W$ , in which the effects of radiative corrections are included [Eq(61)]:

$$M_W^2 \sin^2 \Theta_W = \frac{\pi \alpha}{\sqrt{2} G_F} \left[ \frac{1}{1 - \Delta r} \right] \quad (72)$$

On the left-hand side of this equation, using Sirlin's [15] definition of  $\sin^2 \Theta_W$ , all the parameters are fixed at a large scale ( $M_W, M_Z \sim 100 GeV$ ). On the right-hand side of this equation, on the other hand, the parameters  $\alpha$  and  $G_F$  are fixed by low energy processes (Thomson scattering for  $\alpha$  and  $\mu$ -decay for  $G_F$ ). Thus it is not surprising the correction  $\Delta r$  is large. One should be able to account for the dominant electroweak radiative corrections  $\Delta r$  by replacing  $\alpha$  and  $G_F$  by their "running" counterparts, evaluated at the large scale  $M_W$ . That is, the replacement of  $\alpha$  by  $\alpha(M_W)$  and  $G_F$  by  $G_F(M_W)$  (the running electromagnetic coupling and the running Fermi constant, respectively) should remove the bulk of the electroweak radiative corrections, since no large logarithms can then appear. Thus one expects, approximately,

$$M_W^2 \sin^2 \Theta_W = \frac{\pi \alpha(M_W)}{\sqrt{2} G_F(M_W)} \left[ \frac{1}{1 - \Delta r} \right] \approx \frac{\pi \alpha(M_W)}{\sqrt{2} G_F(M_W)} \quad (73)$$

which gives the estimate for  $\Delta r$ :

$$\Delta r \approx 1 - \left( \frac{\alpha}{\alpha(M_W)} \right) \left( \frac{G_F(M_W)}{G_F} \right) \quad (74)$$

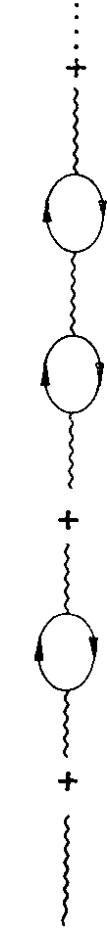


Figure 4: Graphs giving rise to the running of  $\alpha$

The computation of the running electromagnetic constant  $\alpha$  proceeds through the summation of the usual QED vacuum polarization graphs, which include all the charged fermions  $f$  in the model (see Fig. 4). This yields the standard result [17]:

$$\alpha(M_W) = \frac{\alpha}{1 - \frac{\alpha}{3\pi} \sum_f e_f^2 \ln \frac{M_W^2}{m_f^2}} \quad (75)$$

which, for the three generation electroweak model gives  $\alpha(M_W) \simeq \frac{1}{128}$ <sup>8</sup>. The Fermi constant in  $\mu$ -decay, as I will discuss immediately below, does not in fact run, so that  $G_F(M_W) \simeq G_F$ . Thus our considerations lead us to predict that

$$\Delta r \simeq 1 - \left( \frac{\alpha}{\alpha(M_W)} \right) \left( \frac{G_F(M_W)}{G_F} \right) \simeq 1 - \frac{128}{137} \simeq 0.066 \quad (76)$$

This number is very near the result of the exact  $\mathcal{O}(\alpha)$  calculation in [9,14] quoted in Eq(62). Thus one sees that via these renormalization group considerations one has got the main effect.

It remains to understand why the Fermi constant does not run. To see this, one must look at the photonic corrections to  $\mu$ -decay in the Fermi theory. If these corrections are infinite in the Fermi theory - that is, proportional to  $A \ln \Lambda$ , where  $\Lambda$  is a high energy cutoff introduced to regularize the theory - then one expects in the  $SU(2) \times U(1)$  model, which is less singular at short distances, that there will be corrections proportional to  $A \ln M_W$ . So if there are no infinite photonic corrections in the Fermi theory, one should also have no logarithmic dependences on  $M_W$ . So for  $G_F$  not to run, it must be that the photonic corrections to  $\mu$ -decay in the Fermi theory, indicated in Fig. 5, including the contributions from the fermion wave function renormalization, are in fact finite.

<sup>8</sup>This value actually uses the experimental cross section for the process  $e^+e^- \rightarrow \text{hadrons}$  to take more carefully into account the effects of the light quarks. For a careful discussion, see [18].

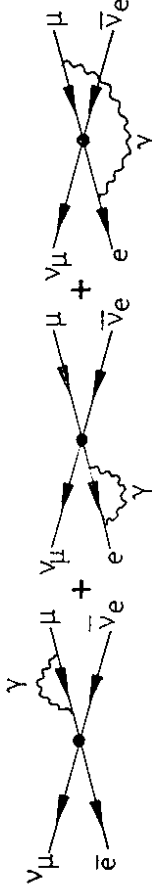


Figure 5: Photonic corrections to  $\mu$ -decay in the Fermi theory

One can express this somewhat more formally, as follows. Higher order corrections modify the coefficient  $\frac{G_F}{\sqrt{2}}$  of the 4 Fermi operator  $\bar{\mu} \gamma_\mu (1 - \gamma_5) \nu_\mu \bar{\nu}_e \gamma^\mu (1 - \gamma_5) e$  in the effective current-current Lagrangian of Eq(31). To define this operator properly one must introduce a scale  $\mu$  where the operator is normalized. The corresponding coefficient will also depend on  $\mu$  and one has in general a power series expansion in powers of  $\alpha \ln M_W^2 / \mu^2$  for this coefficient

$$G_F(\mu^2) = G_F(M_W^2) \left\{ 1 + a \frac{\alpha}{\pi} \ln \frac{M_W^2}{\mu^2} + \dots \right\} \quad (77)$$

where  $a$  is a numerical constant. This logarithmic series can be summed by making use of the renormalization group equation [19], so that one relates the Fermi constant at different scales

$$G_F(\mu^2) = G_F(M_W^2) \left[ \frac{\alpha(\mu^2)}{\alpha(M_W^2)} \right] \quad (78)$$

where  $\bar{d}$  is the anomalous dimension of the operator entering in  $\mu$ -decay. It is simple to see that this anomalous dimension vanishes - or equivalently that  $a$  in Eq(77) vanishes. Thus the Fermi constant does not run:

$$G_F(\mu^2) = G_F(M_W^2) \quad (79)$$

The above can be demonstrated in two ways, either by making use of a Fierz transformation trick, or by direct calculation. The operator entering in  $\mu$  decay can be readily transformed to one where the neutrino fields are contracted with one another:

$$\bar{\mu} \gamma^\mu (1 - \gamma_5) \nu_\mu \bar{\nu}_e \gamma_\mu (1 - \gamma_5) e = \bar{\mu} \gamma^\mu (1 - \gamma_5) e \bar{\nu}_e \gamma_\mu (1 - \gamma_5) \nu_\mu \quad (80)$$

Only the  $\bar{\mu}e$  term above is affected by photonic corrections. However, the anomalous dimension of this current, like that of the ordinary electromagnetic current, vanishes. Hence the anomalous dimension  $\bar{d}$  in Eq(78) must also vanish.

Thus the potentially logarithmic divergent piece of the photonic corrections to  $\mu$  decay vanishes, which establishes, in a different way, the assertion that  $G_F$  does not run.

Having understood the magnitude of  $\Delta r$ , using these renormalization group techniques, I want to apply this same method to compute the electroweak corrections to the Llewellyn Smith formulas, Eqs (47) and (48). For definitiveness, I will consider the case where the symmetry breaking is caused by a Higgs doublet, so that  $\rho = 1$ . Thus it suffices to look only at  $R_\nu$ , whose 0<sup>th</sup> order expression, reads

$$R_\nu = \frac{\int dx dy \frac{d\epsilon}{dx dy} < \nu_\mu N \rightarrow \nu_\mu X >}{\int dx dy \frac{d\sigma}{dx dy} < \nu_\mu N \rightarrow \mu^- X >} = \left( \frac{1}{2} - \sin^2 \Theta_W \right) + \frac{5}{9} \sin^4 \Theta_W (1 + \tau) \quad (86)$$

Now  $R_\nu$ , experimentally involves rather low momentum transfers ( $q^2 < M_W^2, M_Z^2$ ). Thus one expects that if one had used for  $\sin^2 \Theta_W$  a definition which related it to a low energy scale measurement - call it  $\sin^2 \Theta_W(m^2)$  - then one could have just used Eq(86) also to  $0(\alpha)$ . However, since I want to use Sirin's definition for  $\sin^2 \Theta_W$ , I need to derive a relation between this  $\sin^2 \Theta_W$  and  $\sin^2 \Theta_W(m^2)$ .

There is a further subtlety that needs also to be accounted for. Eq(86) hides the fact that both the neutral current cross section and the charged current cross section are proportional to the Fermi constant. Now the neutral current Fermi constant, just like the Fermi constant for  $\mu$  decay does not run. This is because the relevant operator  $(\bar{\nu}_\mu \gamma_\alpha (1 - \gamma_5) \nu_\mu) (\bar{q} \gamma_\alpha \gamma_5 q)$  also has zero anomalous dimension, for precisely the same reasons as were discussed in  $\mu$  decay. On the other hand, the Fermi constant associated with the charged current interactions involving quarks **does** run. The relevant operator now contains three charged fields - the  $\mu$  and two quarks - and the Fierz identity trick is not of any use anymore. Thus, apart from corrections arising out of reexpressing  $\sin^2 \Theta_W(m^2)$  in terms of  $\sin^2 \Theta_W$ , there is a correction due to the fact that

$$R_\nu \sim \frac{(G_F^{NC})^2}{(G_F^{CC})^2} \neq 1 \quad (87)$$

Let me examine this last point first. For the charged current process  $\nu_\mu \rightarrow \mu^- + u$ , even in Landau gauge, there exist a divergent graph among the diagrams shown in Fig 7. The self energy diagrams and the vertex diagrams are finite in Landau gauge. Furthermore, the potentially divergent 5<sup>th</sup> diagram is also finite, since it is precisely the same as the one we considered for  $\mu$  decay. However, the last diagram in Fig 7 is divergent. To calculate the running of  $G_F^{CC}$ :

$$G_F^{CC}(\mu^2) = G_F^{CC}(M_W^2) \left[ 1 + \frac{\alpha}{\pi} a_\nu \ln \frac{M_W^2}{\mu^2} \right] \quad (88)$$

it suffices to get the coefficient of the logarithmic divergence in this diagram, using as a cutoff  $\Lambda \leftrightarrow M_W$ . For the above computation it is enough again to set all external momenta to zero and drop all masses. The relevant diagram to evaluate is that indicated in Fig 8, whose amplitude, in the Landau gauge and setting all masses to zero, is given by

$$A^{CC} = \int \frac{d^4 p}{(2\pi)^4} \frac{-i}{p^2} (\eta^{\mu\nu} - \frac{p^\mu p^\nu}{p^2}) [i \epsilon_\mu \gamma_\mu (\frac{i \gamma p}{p^2}) \gamma_\alpha (1 - \gamma_5)] [i \epsilon_\nu \gamma_\nu (\frac{-i \gamma p}{p^2}) \gamma_\alpha (1 - \gamma_5)] \quad (89)$$

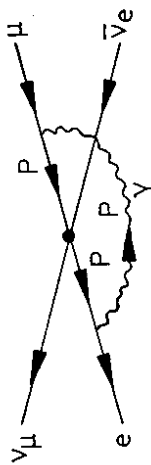


Figure 6: Momentum flow for the amplitude of Eq(81)

Although the above argument suffices to prove the desired non running of  $G_F$ , as I will need to perform similar computations again later on, it is useful to demonstrate this explicitly by evaluating directly the photonic diagrams of Fig 5. It is particularly convenient to perform this computation in the Landau gauge, where the photonic self energies are finite. In this way one needs not to worry about any wavefunction renormalization factors and the only diagram that needs to be examined for  $\mu$  decay is the last one in Fig 5. What I want to show is that this diagram is not ultraviolet divergent. For these limited purposes I can simplify my task further by also setting all external momenta to zero and dropping all masses. The relevant diagram to evaluate then is that indicated in Fig 6. The amplitude associated with Fig 6, in Landau gauge and setting all masses to zero, is given by:

$$A = \int \frac{d^4 p}{(2\pi)^4} \frac{-i}{p^2} (\eta^{\mu\nu} - \frac{p^\mu p^\nu}{p^2}) [\gamma_\alpha (1 - \gamma_5)] \frac{i \gamma p}{p^2} [i \epsilon_\mu \gamma_\mu] [i \epsilon_\nu \gamma_\nu (\frac{i \gamma p}{p^2}) \gamma_\alpha (1 - \gamma_5)] \quad (81)$$

This expression can be simplified by using the fact that under the integral sign

$$p_\alpha p_\beta = \frac{1}{4} p^2 \eta_{\alpha\beta} \quad (82)$$

so that

$$A = -i \epsilon_\mu \epsilon_\nu \int \frac{d^4 p}{(2\pi)^4} \frac{1}{p^2} \left\{ \frac{1}{4} [\gamma_\alpha \gamma_\beta \gamma_\alpha (1 - \gamma_5)] [\gamma^\mu \gamma^\beta \gamma^\alpha (1 - \gamma_5)] - [\gamma_\alpha (1 - \gamma_5)] [\gamma^\alpha (1 - \gamma_5)] \right\} \quad (83)$$

The quantity in the curly bracket can be shown to vanish by making use of the  $\gamma$ -matrix identity<sup>9</sup>

$$\gamma_\alpha \gamma_\beta \gamma_\rho = -\eta_{\alpha\beta} \gamma_\rho + \eta_{\alpha\rho} \gamma_\beta - \eta_{\beta\rho} \gamma_\alpha - i \epsilon_{\alpha\beta\rho\delta} \gamma^\delta \quad (84)$$

as well as the usual relations

$$\gamma^\alpha \gamma_\alpha = -4; \quad \gamma^\alpha \gamma_\mu \gamma_\alpha = 2\gamma_\mu; \quad \epsilon_{\alpha\beta\gamma\delta} \epsilon^{\alpha\beta\gamma\rho} = -6\eta_\rho^\delta \quad (85)$$

<sup>9</sup>My  $\gamma$ -matrices obey  $\{\gamma_\alpha, \gamma_\beta\} = -2\eta_{\alpha\beta}$  and my metric is  $-1 + 1 + 1 + 1$ .

This expression can be simplified as before, but now the resulting integrand does not vanish identically. One has

$$\begin{aligned}
 A^{CC} &= \frac{i\alpha}{4\pi^3} [\epsilon_\mu \epsilon_\nu] \int \frac{d^4 p}{(p^2)^2} \{ [\gamma_\mu \gamma_\nu \gamma_\alpha (1 - \gamma_5)] [\gamma^\mu \gamma^\nu \gamma^\alpha (1 - \gamma_5)] - [\gamma_\alpha (1 - \gamma_5)] [\gamma^\alpha (1 - \gamma_5)] \} \\
 &= \frac{3\alpha i}{4\pi^3} [\epsilon_\mu \epsilon_\nu] \int \frac{d^4 p}{(p^2)^2} [\gamma_\alpha (1 - \gamma_5)] [\gamma^\alpha (1 - \gamma_5)]
 \end{aligned}
 \tag{90}$$

In the above  $\epsilon_\mu$  and  $\epsilon_\nu$  are the charges of the  $\mu$  and the  $\nu$  quarks in units of  $e$ . The divergent integral in (90), evaluated with a cutoff  $\Lambda = M_W$  gives

$$\int \frac{d^4 p}{(p^2)^2} \leftrightarrow i\pi^2 \ln M_W^2
 \tag{91}$$

Hence one identifies the coefficient  $a_\nu$  in Eq(88) as

$$a_\nu = -\frac{3}{4} \epsilon_\mu \epsilon_\nu = \frac{1}{2}
 \tag{92}$$

and one has

$$G_F^{CC}(\mu^2) = G_F^{CC}(M_W^2) \left[ 1 + \frac{\alpha}{2\pi} \ln \frac{M_W^2}{\mu^2} \right] \equiv \rho^{CC} G_F^{CC}(M_W^2)
 \tag{93}$$

It remains to compute the running of  $\sin^2 \Theta_W$ . For these purposes it suffices to consider some convenient subprocess and look at the relevant photonic corrections. A particularly nice reaction to study is  $\nu_\mu e \rightarrow \nu_\mu e$  scattering, where there are only two different types of corrections to consider, as depicted in Fig 9. The correction to the electron vertex -  $G_F$  correction - are identical to those in  $\mu$ -decay (after the Fierz transformation) and obviously do not produce any logarithmic modifications. The, so called, Penguin contribution, on the other hand, modify  $\sin^2 \Theta_W$ . This correction corresponds, essentially, to an electromagnetic neutrino charge radius, giving rise to a multiplicative modification of the local 4-Fermi interaction. The neutrino-neutrino-photon vertex of Fig 10, given that the neutrino charge vanishes, has the gauge invariant form.

$$\Gamma^\lambda(q) = \bar{\nu}_\mu [q^2 \gamma^\lambda - q^\lambda \gamma^\mu (1 - \gamma_5) \nu_\mu] F(q^2)
 \tag{94}$$

However, the 2<sup>nd</sup> term above does not contribute, since  $m_{\nu_\mu} = 0$ . Hence, effectively, the Penguin contribution gives a correction to the  $\nu_\mu e \rightarrow \nu_\mu e$   $T$ -matrix of the form

$$T_{\text{Penguin}} = \bar{\nu}_\mu \gamma_\mu (1 - \gamma_5) \nu_\mu \bar{e} \gamma^\mu e F(q^2)
 \tag{95}$$

Clearly the above corresponds to a correction to  $\sin^2 \Theta_W$ , since the lowest order contribution to the  $T$ -matrix contains a term of the same form as (95) but proportional to  $\sin^2 \Theta_W$ :

$$T_{l.o.} = \bar{\nu}_\mu \gamma_\mu (1 - \gamma_5) \nu_\mu \bar{e} \gamma^\mu e [G_F \sqrt{2} \sin^2 \Theta_W] + \dots
 \tag{96}$$

The contributions to the Penguin vertex of Fig 10 are of two kinds, as indicated in Fig 11. Both these terms are technically divergent, but can be made convergent by subtracting at zero momentum transfer, since the Penguin vertex must vanish there (cf Eq(94)). I will illustrate the relevant calculations by considering the CC contribution of Fig 11. Neglecting

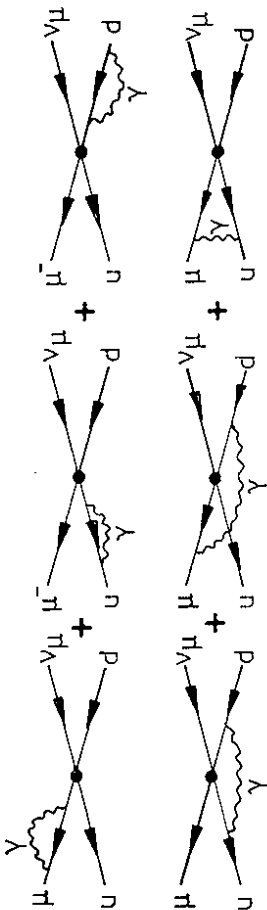


Figure 7: Photonic corrections to the process  $\nu_\mu + d \rightarrow \mu^- + u$  in the Fermi theory

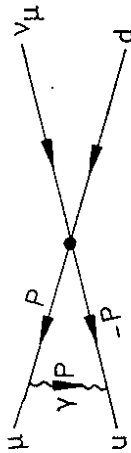


Figure 8: Momentum flow for the amplitude of Eq(89)

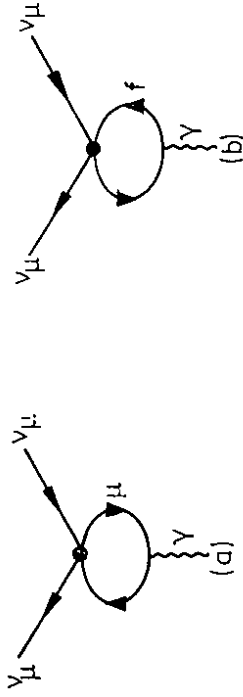


Figure 11: Contribution to the neutrino-neutrino photon vertex, to lowest order in the weak interactions: (a) CC contribution; (b) NC contribution

again mass terms, which are irrelevant for these purposes, the charged current vertex correction is

$$\Gamma_\lambda^{CC}(q) = \frac{G_F}{\sqrt{2}} \bar{\nu}_\mu \left\{ \int \frac{d^4 p}{(2\pi)^4} \gamma_\alpha (1 - \gamma_5) \frac{i\gamma(p+q)}{(p+q)^2} i e_\mu \gamma_\lambda \frac{i\gamma p}{p^2} \gamma^\alpha (1 - \gamma_5) \right\} \nu_\mu - \{q=0\} \quad (97)$$

The quantity in the  $\{ \}$  curly bracket can be rewritten as

$$\begin{aligned} \{ \}_\lambda &= -4i e_\mu \int \frac{d^4 p}{(2\pi)^4} \frac{\gamma p \gamma_\lambda \gamma (p+q) (1 - \gamma_5)}{p^2 (p+q)^2} \\ &= -4i e_\mu \int \frac{d^4 p}{(2\pi)^4} \int_0^1 dx \frac{[\gamma p - \gamma q(1-x)] \gamma_\lambda [\gamma p + \gamma q x] (1 - \gamma_5)}{[p^2 + q^2 x(1-x)]^2} \end{aligned} \quad (98)$$

Since all terms odd in  $p$  vanish and

$$\gamma q \gamma^\lambda \gamma q = q^2 \gamma^\lambda - 2q^\lambda \gamma q, \quad (99)$$

with the  $2^{nd}$  term above not contributing between the neutrino spinors, one has effectively

$$\{ \}_\lambda^{eff} = -4i e_\mu \int_0^1 dx \int \frac{d^4 p}{(2\pi)^4} \frac{\frac{1}{2} p^2 - q^2 x(1-x)}{[p^2 + q^2 x(1-x)]^2} \gamma^\lambda (1 - \gamma_5) \quad (100)$$

The quadratically divergent piece arising from Eq(100) vanishes if one subtracts the  $q^2 = 0$  contribution, but one still has a remaining logarithmic divergence. It is this divergence which details the running of  $\sin^2 \Theta_W$ . One has

$$\Gamma_\lambda^{CC}(q^2) = \bar{\nu}_\mu \gamma_\lambda (1 - \gamma_5) q^\mu \nu_\mu \left\{ 4i e_\mu \sqrt{2} G_F \int_0^1 dx x(1-x) \int \frac{d^4 p}{(2\pi)^4} \frac{1}{[p^2 - q^2 x(1-x)]^2} \right\} \quad (101)$$

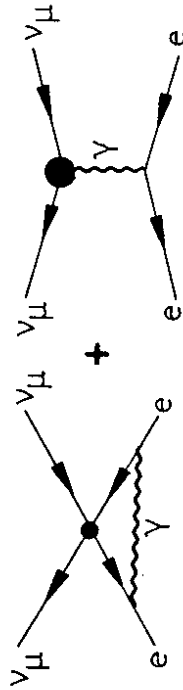


Figure 9: Photonic corrections to  $\nu_\mu e \rightarrow \nu_\mu e$  scattering: (a)  $G_F$  correction; (b) Penguin correction



Figure 10: The neutrino-neutrino-photon vertex

Cutting off the divergence as before with a cutoff  $\Lambda = M_W$  gives for the integral over momentum in Eq(101) [ cf Eq. (91) ]  $\frac{1}{16\pi} \ln M_H^2$ . Hence, using that  $\epsilon_\mu = -\epsilon$ ,

$$\Gamma_\lambda^{CC}(q^2) = \bar{\nu}_\mu \gamma_\lambda (1 - \gamma_5) q^\mu \nu_\mu [\sqrt{2} G_F \frac{\epsilon}{24\pi^2} \ln M_W^2] \quad (102)$$

This result can be used to compute the modification to the  $\nu_\mu \epsilon \rightarrow \nu_\mu \epsilon$  scattering amplitude due to the CC Penguin contribution. One has

$$T_{\text{Penguin}}^{CC} = \bar{\nu}_\mu \gamma_\mu (1 - \gamma_5) \nu_\mu \bar{\epsilon} \gamma^\mu \epsilon [G_F \sqrt{2} \sin^2 \Theta_W] \left\{ -\frac{\alpha}{6\pi \sin^2 \Theta_W} \ln M_W^2 \right\} \quad (103)$$

Whence one obtains immediately the form of the running  $\sin^2 \Theta_W$ , arising from these contributions<sup>10</sup>

$$\sin^2 \Theta_W(m^2) = \sin^2 \Theta_W \left\{ 1 - \frac{1}{\sin^2 \Theta_W} \frac{\alpha}{6\pi} \ln \frac{M_W^2}{m^2} \right\} \quad (104)$$

One can evaluate in an analogous way the NC contributions to the neutrino-neutrino-photon vertex, with the result involving a sum over all the flavours  $f$  entering in the loop in Fig 11. Adding the result of this calculation in, one obtains finally the desired formula detailing the running of  $\sin^2 \Theta_W$ :

$$\sin^2 \Theta_W(m^2) = \sin^2 \Theta_W \left\{ 1 - \frac{\alpha}{6\pi \sin^2 \Theta_W} \left[ 1 + \sum_f (2e_f^2 \sin^2 \Theta_W - T_{3f} e_f) \right] \ln \frac{M_W^2}{m^2} \right\} \quad (105)$$

In the above  $T_{3f}$  is the  $T_3$  value of the fermions in question. It turns out that there is a fairly large cancellation in the quantity in the square bracket in Eq(105), since

$$\sum_f (2e_f^2 \sin^2 \Theta_W - T_{3f} e_f) + 1 = N g \left[ \frac{16}{3} \sin^2 \Theta_W - 2 \right] + 1 \simeq -1.32 \quad (106)$$

where the 2<sup>nd</sup> line applies for three generations ( $Ng = 3$ ) and  $\sin^2 \Theta_W = 0.23$ . Thus, approximately,

$$\sin^2 \Theta_W(m^2) = \sin^2 \Theta_W \left[ 1 + 0.96 \frac{\alpha}{\pi} \ln \frac{M_W^2}{m^2} \right] \equiv \kappa \sin^2 \Theta_W \quad (107)$$

We have now all the elements to compute  $\sin^2 \Theta_W$  from the measured value for  $R_\nu$ , in the leading logarithmic approximation. Instead of the lowest order approximation of Eq(86), if we want to extract  $\sin^2 \Theta_W$  - given by Sirlin's definition Eq(68) - from  $R_\nu$ , we must reexpress  $\sin^2 \Theta_W(m^2)$  in terms of  $\sin^2 \Theta_W$ , using Eq(107), and correct for the mismatch between the neutral and charged current Fermi constants. That is, one has

$$R_\nu \simeq \frac{1}{(\rho^{CC})^2} \left\{ \frac{1}{2} - \kappa \sin^2 \Theta_W \right\} + \frac{5}{9} \kappa^2 \sin^4 \Theta_W (1 + r) \quad (108)$$

Comparing the above with Eq(68) one deduces for the shift  $\delta s^2$  [ cf Eq(55) ] the formula

$$\delta s^2 \simeq -\sin^2 \Theta_W |\kappa - 1| - \frac{R_\nu [(\rho^{CC})^2 - 1]}{[1 - \frac{20(1+r)(R_\nu - \frac{1}{2})}{9}]} \simeq -0.23[\kappa - 1] - 0.48[(\rho^{CC})^2 - 1] \quad (109)$$

<sup>10</sup>Here the scale  $m^2$  is defined so that, if  $m = M_W$ , then  $\sin^2 \Theta_W(m^2) = \sin^2 \Theta_W$ .

where to obtain the last line we have used the approximate numerical values of the various physical parameters. Using Eq(93) and Eq(107) one has, approximately,

$$\delta s^2 \simeq -0.7 \frac{\alpha}{\pi} \ln \frac{M_H^2}{\mu^2} \simeq -0.007 \quad (110)$$

where the last result uses for  $\mu^2 \simeq 100 \text{GeV}^2$ , which is a typical momentum transfer for the deep inelastic neutrino scattering experiments. The value just computed in the leading log approximation, Eq(110), is in excellent agreement with the result of the exact calculation, quoted in Eq(55). This reasserts the contention that the dominant effects of the electroweak radiative corrections can be computed by retaining just the logarithmic corrections.

### 2.3 Effects of $m_t$ and $M_H$

The actual numbers for  $\delta s^2$  and  $\Delta r$  used to compare theory and experiment took, as canonical values,  $m_t = 45 \text{GeV}$  and  $M_H = 100 \text{GeV}$  for the two still unknown parameters in the standard model. It is interesting to ask how sensitively does the good agreement obtained with experiment depend on these choices. We shall see that both  $\delta s^2$  and  $\Delta r$  are quite sensitive to  $m_t$ , once it becomes much bigger than  $M_W$ , but they are rather insensitive to the Higgs mass. Indeed, one finds

$$\delta s^2, \Delta r \sim \left\{ \left( \frac{m_t}{M_W} \right)^2 \right. \quad (111)$$

Furthermore, it turns out that the correction to  $\delta s^2$  is positive as  $m_t$  increases, while it is negative for  $\Delta r$ . This gives rise to a bound on  $m_t$ , since as this parameter grows so does the discrepancy between the values of  $\sin^2 \Theta_W$  obtained in deep inelastic scattering and that obtained through the values of the  $W$  and  $Z$  masses [9]. This bound on  $m_t$  lies in the range of 200 GeV, with the actual value depending slightly on the Higgs mass.

The quadratic behaviour in  $m_t$ ,<sup>11</sup> shown in Eq(111) comes from the failure of a total cancellation between the  $W$  and  $Z$  propagator corrections. This is perhaps most simply demonstrated by considering the effect of fermion loops to the neutral current (NC) to charged current (CC) ratio in  $R_\nu$ . The relevant graphs in both cases are shown in Fig 12. For  $q^2 \ll M_H^2, M_Z^2$  these graphs modify the NC and CC amplitudes as follows

$$\begin{aligned} A^{NC} &\rightarrow \frac{\epsilon^2}{8 \sin^2 \Theta_W \cos^2 \Theta_W} \left[ M_Z^2 + \frac{1}{M_Z^2} \pi_f^Z(0) \right] \\ A^{CC} &\rightarrow \frac{\epsilon^2}{8 \sin^2 \Theta_W} \left[ \frac{1}{M_W^2} + \frac{1}{M_W^2} \pi_f^W(0) \right] \end{aligned} \quad (112)$$

where  $\pi_f^Z(0)$  and  $\pi_f^W(0)$  are the  $Z$  and  $W$  self energy contributions, due to the fermion(s) in question, at zero momentum transfer<sup>12</sup>. Obviously, these modifications change the ratio of these amplitudes from unity in lowest order ( $\rho_0^{NC} = 1$ ) to:

$$\rho^{NC} = 1 + \left[ \frac{\pi_f^Z(0)}{M_Z^2} - \frac{\pi_f^W(0)}{M_W^2} \right] \quad (113)$$

<sup>11</sup>More correctly, this behaviour concerns the top-bottom mass squared difference:  $m_t^2 - m_b^2$ . However, since  $m_b \ll M_W$ , I shall consistently set  $m_b = 0$  in our discussion.

<sup>12</sup>More precisely, they are the coefficients of the  $\gamma^{\mu\nu}$  piece of the weak boson vacuum polarization tensors

bottom - like quarks, the unitarity of the mixing matrix  $V$  implies that the sum of these three contributions is equivalent to that of one loop with unit strength:

$$V_{it}(V^\dagger)_{it} = 1 \quad (116)$$

Hence, effectively one has

$$\begin{aligned} [\pi_f^W(0)]^{\mu\nu} &= -i(-1)3 \int \frac{d^4 p}{(2\pi)^4} \{ T r \frac{i e \gamma^\mu (1 - \gamma_5)}{2\sqrt{2} \sin \Theta_W} \frac{i(\gamma p - m_t)}{p^2 + m_t^2} \frac{i e \gamma^\nu (1 - \gamma_5)}{2\sqrt{2} \sin \Theta_W} \frac{i \gamma p}{p^2} \} \\ &= \frac{3i\alpha}{32\pi^3 \sin^2 \Theta_W} \int d^4 p \frac{2}{p^2(p^2 + m_t^2)} T r \gamma^\mu \gamma p^\nu \gamma p(1 - \gamma_5) \end{aligned} \quad (117)$$

Although Eqs(115) and (117) are individually divergent, the difference appearing in Eq(113) for  $\rho^{NC}$  is perfectly finite. One has

$$\begin{aligned} \frac{1}{M_W^2} [\pi_f^Z(0)]^{\mu\nu} - \frac{1}{M_W^2} [\pi_f^W(0)]^{\mu\nu} &= \frac{3i\alpha}{32\pi^3 M_W^2 \sin^2 \Theta_W} \int d^4 p \left\{ \frac{1}{(p^2 + m_t^2)^2} + \frac{1}{(p^2)^2} - \frac{2}{p^2(p^2 + m_t^2)} \right\} \\ &\quad \cdot T r \gamma^\mu \gamma p^\nu \gamma p(1 - \gamma_5) \\ &= \frac{3i\alpha}{32\pi^3 M_W^2 \sin^2 \Theta_W} \int d^4 p \frac{T r \gamma^\mu \gamma p^\nu \gamma p(1 - \gamma_5)}{(p^2)^2(p^2 + m_t^2)^2} \end{aligned} \quad (118)$$

The resulting integral is clearly convergent and a simple calculation secures

$$\int d^4 p \frac{T r \gamma^\mu \gamma p^\nu \gamma p(1 - \gamma_5)}{(p^2)^2(p^2 + m_t^2)^2} = \frac{2\pi^2}{i m_t^2} \eta^{\mu\nu} \quad (119)$$

Hence one finds [20]

$$[\rho^{NC}]_{loop} = 1 + \frac{3\alpha}{16\pi \sin^2 \Theta_W} \left( \frac{m_t}{M_W} \right)^2 \quad (120)$$

Eq(120) shows that the  $\rho$  parameter departs strongly from unity if the  $t$ -quark is very heavy - or more precisely if the mass squared difference between  $t$  and  $b$  quarks is much greater than  $M_W^2$ .

Quite similar considerations give the  $t$ -dependence of  $\Delta r$  and  $\kappa$  [21]. To trace the sensitivity of these corrections to  $m_t$ , let me look again at the radiative corrected formula, Eq(61), for  $M_W^2$ :

$$M_W^2 = \frac{\pi\alpha}{\sqrt{2} G_F \sin^2 \Theta_W} \frac{1}{1 - \Delta r} \quad (121)$$

This formula can be obtained from the "bare" expression

$$(M_W^0)^2 = \frac{\pi\alpha^0}{\sqrt{2} G_F \sin^2 \theta_W^0} \quad (122)$$

by shifting all the bare values by a certain amount:

$$M_W^2 = (M_W^0)^2 + \delta M_W^2; \quad G_F = G_F^0 + \delta G_F; \quad etc \quad (123)$$

Hence the correction  $\Delta r$  can be written as

$$\Delta r = -\frac{\delta\alpha}{\alpha} + G_F^{-1} \frac{\delta \sin^2 \Theta_W}{\sin^2 \Theta_W} + \frac{\delta M_W^2}{M_W^2} \quad (124)$$

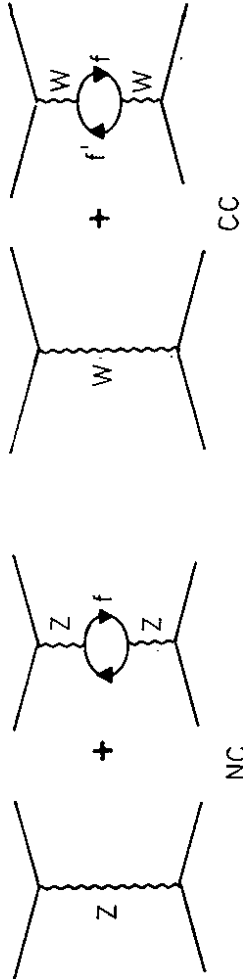


Figure 12: Fermion loop modifications to the NC and CC amplitudes

Let me consider first the modification to the Z propagator. What enters at each vertex in the fermion loop of Fig 12 is the expectation for this fermion of  $2(J_3^\mu - \sin^2 \Theta_W J_{em}^\mu)$ . However, since purely electromagnetic contributions do not give rise to terms proportional to fermion masses, one needs only concern oneself with the  $J_3^\mu$  pieces<sup>13</sup>. These contributions are quite divergent individually and one must be a bit careful. In particular, it is important to consider **simultaneously** both the top and bottom corrections to the  $Z^0$  propagator. Thus the  $\pi_f^Z(0)$  contribution of Eq(113) which needs to be studied contains both the  $t$  and  $b$  quark loops.

Using only the expectation of  $(2J_3^\mu)$  at each vertex the  $Z^0$  self energy due to both  $t$  and  $b$  quark loops is given by

$$[\pi_f^Z(0)]^{\mu\nu} = -i(-1)3 \int \frac{d^4 p}{(2\pi)^4} \left\{ T r \frac{i e \gamma^\mu (1 - \gamma_5)}{4 \sin \Theta_W \cos \Theta_W} \frac{i(\gamma p - m_t)}{p^2 - m_t^2} 4 \sin \Theta_W \cos \Theta_W \frac{i(\gamma p - m_t)}{p^2 + m_t^2} \right\} + \{m_t = 0\} \quad (114)$$

In the above the  $(-i)$  factor is the one appropriate to the definition of  $\pi_f^Z$  used in Eq(112), while the factors of  $(-1)$  and 3 are Pauli principle and color factors of the fermion loops in questions. A little algebra reduces Eq(114) to

$$[\pi_f^Z(0)]^{\mu\nu} = \frac{3i\alpha}{32\pi^3 \sin^2 \Theta_W \cos^2 \Theta_W} \int d^4 p \frac{1}{(p^2 + m_t^2)^2} + \frac{1}{(p^2)^2} T r \gamma^\mu \gamma p^\nu \gamma p(1 - \gamma_5) \quad (115)$$

A similar calculation must be performed for the corrections to the W propagator. Here what enter are the  $t - b$ ,  $t - s$  and  $t - d$  loops. However, if one neglects the masses of the

<sup>13</sup>The cross term between  $J_3^\mu$  and  $J_{em}^\mu$  also does not contribute.

On the other hand, by the definition of  $\sin^2 \Theta_W$ , one has also that

$$M_Z^2 = \frac{\pi\alpha}{\sqrt{2}GF \sin^2 \Theta_W \cos^2 \Theta_W} \frac{1}{1 - \Delta r} \quad (125)$$

Thus one can compute an alternative expression for  $\Delta r$ :

$$\Delta r = -\frac{\delta\alpha}{\alpha} - \frac{\delta GF}{GF} \frac{\cos^2 \Theta_W - \sin^2 \Theta_W}{\cos^2 \Theta_W \sin^2 \Theta_W} \delta \sin^2 \Theta_W - \frac{\delta M_Z^2}{M_Z^2} \quad (126)$$

Comparison of Eqs(124) and (126) yields a connection between the shift needed for  $\sin^2 \Theta_W$  and the shifts associated with the  $W$  and  $Z$  masses:

$$\delta \sin^2 \Theta_W = \cos^2 \Theta_W \left( \frac{\delta M_Z^2}{M_Z^2} - \frac{\delta M_W^2}{M_W^2} \right) \quad (127)$$

We have already computed the shift of the Fermi constant, defined through the  $CC$  process, due to the presence of a heavy  $t$ -quark loops (c.f. Fig 12)

$$\frac{\delta GF}{GF} = \frac{\pi_f^W(0)}{M_f^2 W} \quad (128)$$

The mass shifts  $\delta M_W^2$  and  $\delta M_Z^2$ , on the other hand, are related to the relevant self energy functions on their mass shells

$$\delta M_W^2 = -\pi_f^W(M_W^2); \quad \delta M_Z^2 = -\pi_f^Z(M_Z^2) \quad (129)$$

However, in the limit when  $m_t \gg M_W^2$ , the self energy contribution due to heavy  $t$ -quarks on shell, is approximately equal to that evaluated at zero momentum transfer. Thus for the shifts due to heavy  $t$ -quarks one has also, approximately

$$\delta M_W^2 \simeq -\pi_f^W(0); \quad \delta M_Z^2 \simeq -\pi_f^Z(0) \quad (130)$$

Using Eqs(128) and (130) the large  $m_t$  dependence of  $\Delta r$  simplifies to

$$[\Delta r]_{top} \simeq -\frac{\delta\alpha}{\alpha} + \frac{\delta \sin^2 \Theta_W}{\sin^2 \Theta_W} \quad (131)$$

However, as I remarked earlier, purely electromagnetic corrections never give rise to quadratic mass shifts. Thus using Eq(127) and Eq(130) one has [21]

$$[\Delta r]_{top} \simeq \frac{\delta \sin^2 \Theta_W}{\sin^2 \Theta_W} \simeq -\frac{\cos^2 \Theta_W \cdot \pi_f^Z(0)}{\sin^2 \Theta_W \cdot M_Z^2} - \frac{\pi_f^W(0)}{M_W^2} \simeq -\frac{3\alpha \cos^2 \Theta_W}{16\pi \sin^4 \Theta_W} \left( \frac{m_t}{M_W} \right)^2, \quad (132)$$

where to obtain the last line, I have used the result previously obtained for  $\rho^{NC}$ , Eq(120). Furthermore, recalling the definition of  $\kappa$ , Eq(107), one sees that for  $\kappa$  the large  $m_t$  contribution produces a shift opposite to the shift in  $\Delta r$  [21]

$$[\kappa]_{top} = -\frac{\delta \sin^2 \theta_W}{\sin^2 \Theta_W} = \frac{3\alpha \cos^2 \Theta_W}{16\pi \sin^4 \Theta_W} \left( \frac{m_t}{M_W} \right)^2 \quad (133)$$

We have now all the relevant formulas to explore the effects of having a large  $t$ -quark mass in the standard model. Recall that the change in  $\sin^2 \Theta_W$  for deep inelastic scattering,  $\delta s^2$ , was given by the approximate formula Eq(109). Since  $R_V \sim [\rho^{NC}/\rho^{CC}]^2$  it follows therefore also that

$$\delta s^2 \simeq -\sin^2 \theta_W (R_V - 1) = 0.48([\rho^{NC}]^2 - 1). \quad (134)$$

Using our results the large  $m_t$  shift is given by

$$[\delta s^2]_{top} \simeq \frac{3\alpha}{16\pi \sin^2 \Theta_W} \left\{ -\cos^2 \theta_W - 2(0.48)^2 \right\} \left( \frac{m_t}{M_W} \right)^2 \simeq 4.4 \times 10^{-4} \left( \frac{m_t}{M_W} \right)^2 \quad (135)$$

Note that the net effect is not particularly big, because of the large cancellation among the two terms in the curly bracket above. Recall that for  $m_t = 45GeV$ ,  $\delta s^2 = -0.009$  [9]. Using Eq(135), this shift is partially cancelled for  $m_t = 200GeV$ , where one would obtain only  $\delta s^2 = -0.006$ .

The effects of a large top mass are more severe for  $\Delta r$ . Using Eq(132) one has, numerically,

$$[\Delta r]_{top} \simeq -6.3 \times 10^{-3} \left( \frac{m_t}{M_W} \right)^2 \quad (136)$$

Hence the value for  $\Delta r$ , obtained with the canonical value of  $m_t = 45GeV$ ,  $\Delta r = 0.071$ , [9] is more than halved at  $m_t = 200GeV$  where, using Eq(136), one obtains only  $\Delta r = 0.031$ . The good agreement between  $(\sin^2 \Theta_W)_{DIS}$  and  $(\sin^2 \Theta_W)_{M_W/M_Z}$  of Table 4 is spoiled for large  $m_t$ , since the former goes up and the latter goes down as  $m_t$  grows. This is illustrated in Table 5

Table 5: Effects of  $m_t$  on  $\sin^2 \Theta_W$ .

	$m_t = 45GeV$	$m_t = 200GeV$
Deep Inelastic	$0.233 \pm 0.003 \pm [0.005]$	$0.236 \pm 0.003 \pm [0.005]$
$W/Z$ Masses	$0.228 \pm 0.007 \pm [0.002]$	$0.219 \pm 0.007 \pm [0.002]$

This phenomena has been analyzed in detail by Amaldi et al [9], who have studied the variations of  $\sin^2 \Theta_W$  as a function of  $m_t$  for a variety of neutral current processes besides those discussed here [4]. They obtain in this way a 90 % C.L. region for  $\sin^2 \Theta_W$  and  $m_t$ , as shown in Fig 13. The actual precise limits on  $m_t$  depend slightly on the choice one takes for the Higgs mass, but one sees that, roughly speaking, values of  $m_t$  above  $200GeV$  are not allowed.

The weak dependence of the bound on  $m_t$  on the Higgs mass follows since, as I have previously noted (c.f. Eq(111)), the corrections  $\delta s^2$  and  $\Delta r$  only depend logarithmically on this parameter. As a last point in this already long section, I will demonstrate this explicitly for  $\Delta r$ . Similar considerations apply for  $\delta s^2$ . Using Eqs(127) - (129) one can rewrite  $\Delta r$  entirely in terms of differences of  $W$  and  $Z$  self energies, plus the purely electromagnetic contribution  $-\frac{\delta\alpha}{\alpha}$ . However, this last term gives no  $M_H$  dependence and I will drop it entirely. Hence, effectively, one has

$$(\Delta r)_{Higgs} = -\left\{ \frac{\pi_f^W(M_W^2)}{M_W^2} - \frac{\pi_f^W(0)}{M_W^2} \right\} + \frac{\cos^2 \Theta_W}{\sin^2 \Theta_W} \left\{ \frac{\pi_f^Z(M_Z^2)}{M_Z^2} - \frac{\pi_f^Z(M_W^2)}{M_W^2} \right\} \quad (137)$$

Because the formula for  $(\Delta r)_{Higgs}$ , involves differences in self energies, there are some simplifications. In particular, the seagull self energy graphs of Fig 14 do not contribute



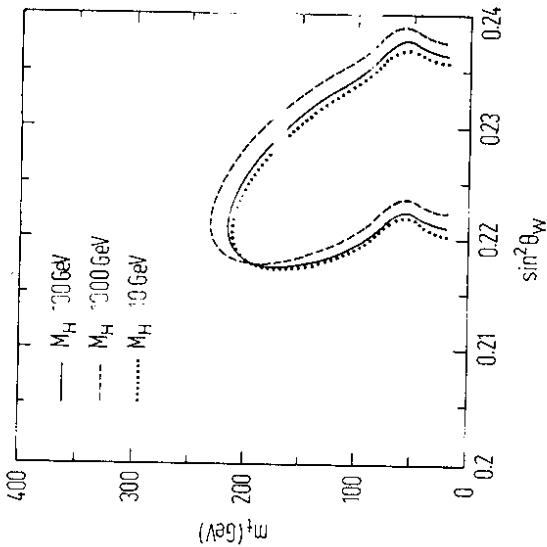


Figure 13: Allowed 90 % C.L. region for  $\sin^2 \Theta_W$ , for Higgs boson masses of 10, 100 and 1000 GeV. From [9].



Figure 14: Seagull self energy graphs

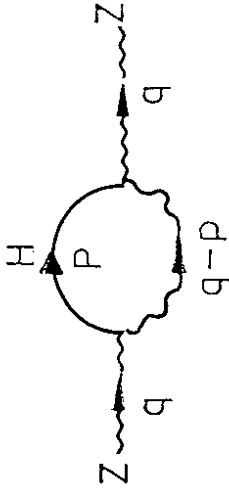


Figure 15: Higgs contribution to the Z self energy

at all. This is certainly clear for the first difference in Eq(137), since these contributions are  $q^2$  independent. The second difference in Eq(137) also vanishes because the Z and W terms, divided by their respective masses, cancel. As is the case with the gauge mass terms [c.f. Eq(13)], the  $WWHH$  and  $ZZHH$  vertices just differ by a factor of  $\cos^2 \Theta_W$ . This factor is compensated by  $M_Z^2$  in the difference appearing in Eq(137).

Hence one needs only consider the  $H - W/Z$  loop contributions to the self energies, arising out of the trilinear interactions detailed in Eq(17). The answer for  $\Delta r$  is gauge invariant and so can be evaluated in any gauge. I will do the computation in the unitary gauge, which is the physical gauge where the W and Z propagators contain a projection  $(\eta^{\mu\nu} + q^\mu q^\nu / M^2)$ , with  $M^2$  being the appropriate mass. The integrals which enter in the computation diverge and must be regularized. It is convenient to use dimensional regularization, where the divergent contributions are segregated in terms proportional to  $(n-4)^{-1}$ , with  $n$  being the continued dimension. When one adds up all the contributions in  $\Delta r$ , of course, these terms cancel. In our limited calculation, we shall show that there are no singular terms depending on  $M_H$  and shall extract the finite contributions proportional to  $\ln M_H$ .

The contribution to the Z self energy due to the graph shown in Fig 15 is given by, in n-dimensions.

$$i\pi^2 (-q^2)_{,\mu\nu} = -i \int \frac{d^n p}{(2\pi)^4} \frac{ieM_Z}{\sin^2 \Theta_W \cos \Theta_W} \frac{-i \{ \eta_{\mu\nu} - \frac{(q-p)_\mu (q-p)_\nu}{M_Z^2} \}}{p^2 + M_H^2 (q-p)^2 + M_Z^2} \quad (138)$$

What is needed is the  $\eta_{\mu\nu}$  coefficient in the above. To proceed we Feynman parametrize the denominator in Eq(138) and shift to a new integration variable  $p' = p - qx$ . Then the denominator becomes

$$Den = \int_0^1 dx [p'^2 + D_Z]^{-2} \quad (139)$$

<sup>14</sup>The processes I have discussed, however, are the most significant, since they are the most precise

where

$$D_Z = M_Z^2 x + M_H^2(1-x) - q^2 x(1-x) \quad (140)$$

In the numerator, since we need only the  $\eta_{\mu\nu}$  coefficient, effectively one can replace

$$[q(1-x) - p']_{\mu} [q(1-x) - p']_{\nu} \rightarrow p_{\mu} p'_{\nu} \equiv \frac{p^2}{n} \eta_{\mu\nu} \quad (141)$$

Thus, going to Euclidean space  $[-i \int d^n p' \rightarrow \int d^n p_E]$  and doing the trivial angular integral  $[\Omega_n = \frac{2\pi^{n/2}}{\Gamma(n/2)}]$  yields

$$\pi^Z(-q^2) = \frac{\alpha M_Z^2}{4\pi^3 \sin^2 \Theta_W \cos^2 \Theta_W} \left\{ \Omega_n \int_0^1 dx \int_0^\infty dp p^{n-1} \frac{1 - \frac{p^2}{nM_Z^2}}{[p^2 + D_Z]^2} \right\} \quad (142)$$

Using

$$\int_0^\infty dp \frac{p^{2\beta+n-1}}{[p^2 + D]^{\alpha}} = \frac{\Gamma(\beta + \frac{n}{2}) \Gamma(\alpha - 3 - \frac{n}{2})}{2\Gamma(\alpha) D^{\alpha-\beta-\frac{n}{2}}} \quad (143)$$

the curly bracket in Eq(142) reduces to

$$\left\{ \right\} = \frac{\pi^{n/2} \Gamma(2 - \frac{n}{2})}{D_Z^{2-\frac{n}{2}}} \int_0^1 dx \left[ 1 - \frac{D_Z}{M_Z^2(n-2)} \right] \quad (144)$$

The singularity is isolated in  $\Gamma(2 - \frac{n}{2})$ . Using

$$\frac{\Gamma(2 - \frac{n}{2})}{D_Z^{2-\frac{n}{2}}} = -\frac{2}{(n-4)} - \ln D_Z \quad (145)$$

one has, as  $n \rightarrow 4$ :

$$\left\{ \right\} = -\frac{2\pi^2}{(n-4)} \int_0^1 dx \left[ 1 - \frac{D_Z}{2M_Z^2} \right] - \pi^2 \int_0^1 dx \left[ 1 - \frac{D_Z}{2M_Z^2} \right] \ln D_Z \quad (146)$$

Since  $D_Z$  contains  $M_H$  there is a potentially, Higgs mass dependent, divergent term. However, it is easy to see that in  $\Delta r$  these divergent terms cancel. An analogous calculation for the Higgs correction to the  $W$  propagator secures a formula akin to Eq(142)

$$\pi^W(-q^2) = \frac{\alpha M_W^2}{4\pi^3 \sin^2 \Theta_W} \left\{ \right\}^W \quad (147)$$

where  $\left\{ \right\}^W$  is identical to  $\left\{ \right\}^Z$ , except that  $M_W \leftrightarrow M_Z$ . Thus the singular contributions for  $\pi^W$  and  $\pi^Z$  depending on  $M_H$  are

$$\begin{aligned} \pi^W(-q^2)_{sing}^{sing} / M_H &= \frac{\alpha M_H^2}{8\pi \sin^2 \Theta_W} \frac{1}{(n-4)} \\ \pi^Z(-q^2)_{sing}^{sing} / M_H &= \frac{\alpha M_H^2}{8\pi \sin^2 \Theta_W \cos^2 \Theta_W} \frac{1}{(n-4)} \end{aligned} \quad (148)$$

Obviously, given the mass weighting in Eq(137), the Higgs mass dependent singular terms in  $\Delta r$  cancel.

It remains to detail the finite  $M_H$  dependence in  $\Delta r$ . This can be extracted from the formulas just obtained for  $\pi^W$  and  $\pi^Z$ , using Eq(137). Collecting terms, one finds

$$\left[ \pi^W(-q^2) \right]_{Higgs} = \frac{\alpha M_W^2}{4\pi \sin^2 \Theta_W} \int_0^1 dx \left[ 1 - \frac{M_W^2 x + M_H^2(1-x) + q^2 x(1-x)}{M_W^2} \right] \ln M_W^2 x - M_H^2(1-x) + q^2 x(1-x) \quad (149)$$

$$\left[ \pi^Z(-q^2) \right]_{Higgs} = -\frac{\alpha M_W^2}{4\pi \sin^2 \Theta_W \cos^2 \Theta_W} \int_0^1 dx \left[ 1 - \frac{M_Z^2 x + M_H^2(1-x) + q^2 x(1-x)}{M_Z^2} \right] \ln M_Z^2 x - M_H^2(1-x) + q^2 x(1-x) \quad (150)$$

Using the above, the Higgs mass dependence of  $\Delta r$  is readily computable. One finds, in particular, for large  $M_H$  [21],

$$(\Delta r)_{Higgs} = \frac{11\alpha}{48\pi \sin^2 \Theta_W} \ln \frac{M_H^2}{M_Z^2} \simeq 0.0023 \ln \frac{M_H^2}{M_Z^2} \quad (151)$$

From Eq(151) one sees that a  $1T\epsilon^V$  Higgs would increase, approximately,  $\Delta r$  by 0.01. Such a shift is clearly well below the present experimental accuracy. Using the value of  $\sin^2 \Theta_W$  obtained in deep inelastic scattering, Eq(56), and the present experimental value for  $M_W$ , given in Table 3, Eq(61) implies for  $\Delta r$ :

$$(\Delta r)_{exp} = 0.077 \pm 0.037 \quad (152)$$

This value is in perfect agreement with the theoretical prediction given in Eq(62), which uses  $m_t = 45\text{GeV}$  and  $M_H = 100\text{GeV}$ . However, it is too inaccurate to be able to test Eq(151), even if one were to know  $m_t$  precisely. Only when the new  $c^+c^-$  colliders at the Z energy, LEP and SLC, come into operation will one hope to achieve the accuracy needed ( $\delta\Delta r < 0.01$ ) to be able to test for virtual Higgs boson effects [22].

### 3 Counting Flavors

I want to begin discussing a different aspect of the standard model, connected with the observed family repetition of the fundamental fermions. I shall start by looking at issues connected with the top quark.

#### 3.1 Why there is Top

Demanding agreement between the standard model predictions and experiment is a sophisticated way to infer that top must exist. Indeed, as we saw in the last section,  $m_t < 200\text{GeV}$  was needed to make sure that the radiatively corrected values of  $\sin^2 \Theta_W$  measured in different experiments agree, within errors, with each other. Langacker [23] has pointed out a much more direct and simpler way by which one can tell from experiment that top exists, even though top has not been directly observed! His observation makes use of the measurement of the axial charge of  $b$ -quarks in  $e^+e^-$  annihilation experiments.

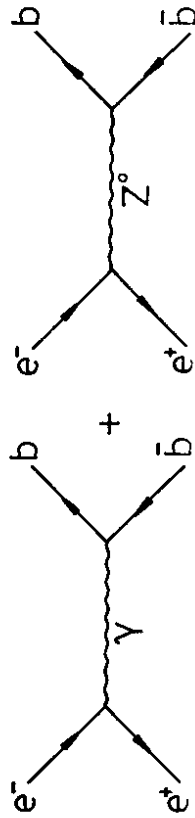


Figure 16: Feynman graph contributions to  $e^+e^- \rightarrow b\bar{b}$

In the standard model, where the left handed components of  $b$  and  $t$  quarks sit together in a doublet, the neutral current of  $b$ -quarks has an axial piece:

$$[J_{NC}^\mu]_b = 2[J_3^\mu - \sin^2\theta_W J_{em}^\mu]_b = \bar{b}\left(-\frac{1}{2}\right)\gamma^\mu\gamma_5 b + \dots \quad (153)$$

Conventionally, the axial charge  $a_b$  of the  $b$ -quark is defined as twice the coefficient of  $\gamma^\mu\gamma_5$  in the neutral current. Thus in the standard model

$$a_b = 2\left[-\frac{1}{2}\right] = -1 \quad (154)$$

Obviously, if the  $b$ -quark had a different assignment in the standard model, the value of  $a_b$  would change. In particular, if the top quark did not exist and  $b$ -quarks were  $SU(2)$  singlets then  $a_b = 0$ .

The axial charge  $a_b$  has been measured experimentally by studying the forward-backward asymmetry in the process  $e^+e^- \rightarrow b\bar{b}$ . Events originating from  $b$ -quarks are identified from the high transverse momentum leptons produced in semileptonic decays  $b \rightarrow c\ell\nu$ . Experimentally, a large  $pt$  cut serves to discriminate between the  $b$  and the  $c$  semileptonic decay sample. In the process  $e^+e^- \rightarrow b\bar{b}$ , the existence of a  $Z$  exchange contribution, besides the usual photon annihilation term, (see Fig 16) gives an asymmetry in the angular distribution of the produced  $b$  quarks. Let  $\Theta$  be the angle in the CM system between the direction of the incoming electron and the outgoing  $b$ -quark, as shown in Fig 17. Then the differential angular distribution has the form

$$\frac{d\sigma}{d\cos\Theta} = \frac{\pi\alpha^2}{2s} [A(1 + \cos^2\Theta) + B\cos\Theta] \quad (155)$$

It is the presence of the  $B$  coefficient, due to the  $Z$  graph, which causes a forward-backward asymmetry

$$A_{FB}(s) = \frac{\int_0^1 d\cos\Theta \left(\frac{d\sigma}{d\cos\Theta}\right) - \int_{-1}^0 d\cos\Theta \left(\frac{d\sigma}{d\cos\Theta}\right)}{\int_0^1 d\cos\Theta \left(\frac{d\sigma}{d\cos\Theta}\right) + \int_{-1}^0 d\cos\Theta \left(\frac{d\sigma}{d\cos\Theta}\right)} = \frac{3B}{8A} \quad (156)$$

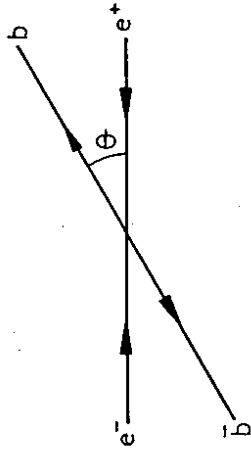


Figure 17: Definition of the angle  $\Theta$  for  $e^+e^- \rightarrow b\bar{b}$

In the PEP/PETRA energy range, where this asymmetry has been measured, since  $s \ll M_Z^2$ ,  $B$  is determined by the  $Z - \gamma$  interference term, as the  $|Z|^2$  term is negligible. A straightforward calculation of the graphs in Fig 16 gives

$$A_{FB}^b(s) \simeq \frac{9G_F}{16\pi\sqrt{2}\alpha} \left| \frac{sM_W^2}{M_Z^2 - s} \right| a_b \simeq 0.29a_b \quad (157)$$

The numerical value above is that appropriate for  $\sqrt{s} = 35\text{GeV}$ , which is the energy where most of the data on this asymmetry has been gathered. Clearly, at this energy, the asymmetry expected in the standard model is sizable.

In Fig 18, I show the data of the JADE collaboration [24], which are the most accurate. The measured distribution shows a substantial asymmetry and the data is backward peaked, implying  $a_b < 0$ . The result of JADE for  $a_b$  ( $a_b = -0.90 \pm 0.24 \pm 0.10$ ); combined with those of the other PEP and PETRA experiments [25] yields an average experimental value for the axial charge of the  $b$ -quark

$$a_b = -0.84 \pm 0.21 \quad (158)$$

Actually, this raw number needs to be corrected for  $B - \bar{B}$  mixing - a subject which I'll discuss, in detail in Sec. 5. When this is done, the final central value for  $a_b$  is slightly higher, but the error has also increased. One finds [25]

$$a_b = -1.08 \pm 0.29 \quad (159)$$

Clearly Eq(159) is in perfect agreement with the expectations of the standard model, in which the left handed  $b$  quark is part of an  $SU(2)$  doublet. So top must exist, but where is it?

### 3.2 Where is Top?

The safest lower bound for top is provided by the study of the process  $e^+e^- \rightarrow \text{hadrons}$  at high energy at TRISTAN. The ratio of the cross section for this process to that for

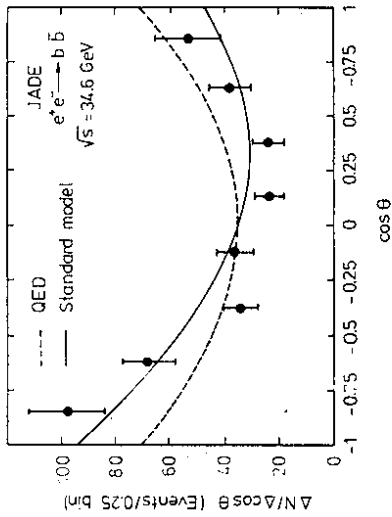


Figure 18: The angular distribution for the process  $e^+e^- \rightarrow b\bar{b}$ , measured by JADE [24].

producing  $\mu$ -pairs is proportional to the charged squared of the quarks being produced:

$$R = \frac{\sigma(e^+e^- \rightarrow \text{hadrons})}{\sigma(e^+e^- \rightarrow \mu^+\mu^-)} \simeq 3 \sum_q^2 e_q^2 \quad (160)$$

where the factor of 3 above is a color factor. Thus one expects a step in  $R$  of  $(\Delta R)_{\text{top}} = \frac{4}{3}$ , after one goes above the threshold in energy for producing  $t-\bar{t}$  pairs. Although  $R$  rises due to the tail of the  $Z$  pole, no sign of this threshold jump can be seen at the highest TRISTAN energies [26], as Fig 11 demonstrates. This allows the various collaborations working at TRISTAN to set a lower bound on  $m_t$  of about 28 GeV. More precisely, the 95% C.L. TRISTAN bounds are [27]:

$$m_t \geq \begin{cases} 27.4 \text{ GeV} & \text{TOPAZ} \\ 28.0 \text{ GeV} & \text{VENUS} \\ 27.6 \text{ GeV} & \text{AMY} \end{cases} \quad (161)$$

The strongest experimental bound on top comes from the UA1 collaboration, working at the Sp $\bar{p}$ S collider [28]. In  $p\bar{p}$  collisions top can be produced either as a byproduct of  $W$  decay, if its mass is below the  $W \rightarrow t\bar{b}$  threshold, or in association with a  $t$ , by gluon fusion, as shown in Fig. 20. The first process has a well determined rate, which can be inferred from the experimentally measured  $W$  production and the known  $W \rightarrow t\bar{b}$  branching fraction in the standard model. The rate for the second process, however, is more uncertain, since it depends on the knowledge of the gluon structure functions and of higher order QCD corrections. The signal for both these sources of top is an isolated muon with large transverse momentum, from the semileptonic decay of top, plus jets resulting from

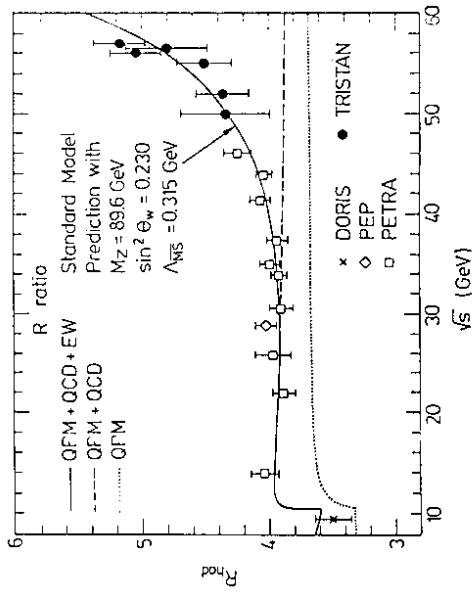


Figure 19:  $R$  values measured by the VENUS, AMY and TOPAZ detectors at TRISTAN, from [26]. Data from DESY and SLAC is also plotted. The solid curve is the prediction of the standard model, in which the tail of the  $Z$  propagator is beginning to be noticeable.

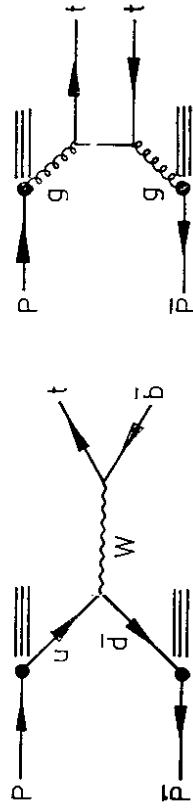


Figure 20: Mechanisms for producing top in  $p\bar{p}$  collisions: (a) through  $W$  decay; (b) by gluon-gluon fusion.

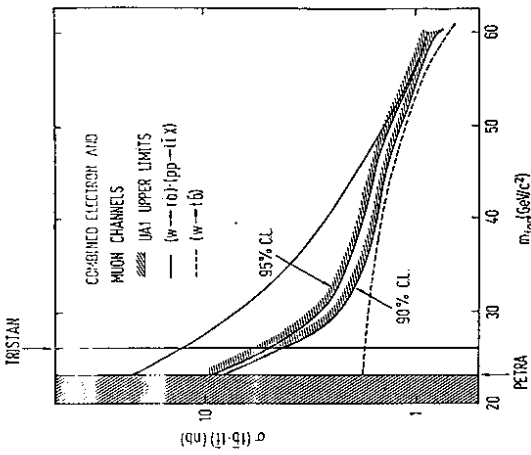


Figure 21: Expected top signal for the UA1 cuts [28], as a function of  $m_t$ . The dashed line is the signal from  $W \rightarrow tb$ .

the accompanying debris. This signal, although characteristic, is not without background and a careful Monte Carlo study is needed to ascertain the presence of top.

Fig. 21, taken from [28], shows the expected signal, as a function of  $m_t$ , for the cuts imposed by the UA1 collaboration. As can be seen, for  $m_t \leq 50$  GeV the main source of the signal is the gluon-gluon fusion process. The signal in Fig. 21 lies above the calculated background for  $m_t \geq 56$  GeV (at 90% confidence) and this allows the setting of a lower bound on  $m_t$ .

Because the predicted rate is dominated by the (somewhat) theoretically uncertain QCD process, this bound is not the most conservative one can set. UA1 sets a more cautious lower bound of  $m_t \geq 44$  GeV [28], by varying the QCD inputs for the theoretically predicted top cross section and selecting the lowest value among these. A similar result has also been obtained recently by Altarelli et al. [29], who incorporated the effects of higher order QCD corrections for heavy quark production [30] and obtained  $m_t \geq 41$  GeV. In summary, from the nonobservation of a clear signal in high energy  $p\bar{p}$  scattering one can deduce - subject to the above mentioned theoretical ambiguities - an experimental lower bound for the top mass, in the range

$$m_t \geq (41 - 56) \text{ GeV} \quad (162)$$

The measurement of  $\alpha_s$  gives us the reasonable certitude that top exists and so that there are three generations of quarks and leptons. The above lower bound on  $m_t$ , along with the upper bound provided by the electroweak radiative corrections, tell us that there is a range of about  $150 \text{ GeV}$  open for top-hunting:  $50 \text{ GeV} \leq m_t \leq 200 \text{ GeV}$ . The interesting and still open question, however, is if there are more generations? Direct evidence against

more generations is rather scant, with the best bounds again being those of UA1 [28] of  $m_b \geq 32 \text{ GeV}$  (90% C.L.) and  $m_t \geq 41 \text{ GeV}$  (90% C.L.) for a fourth generation charge  $-\frac{1}{3}$  quark and a fourth generation lepton, respectively. On the other hand, rather good limits are beginning to emerge from  $e^+e^-$  experiments and from the CERN collider on the number of light neutrinos. These limits, which are becoming of comparable quality to the cosmological bound from nucleosynthesis [31] ( $N_\nu \leq 4$ ), can be taken to be limits on the number of families, under the reasonable assumption that all neutrinos species are either massless, or at least very much lighter than the corresponding charged fermions. I discuss these interesting limits below.

### 3.3 Neutrino Counting Experiments

The idea of neutrino counting experiments is very simple. In the standard model the coupling of the  $Z$  boson to each neutrino species is universal [c.f. Eq(26)]

$$\mathcal{L}_{Z\nu\rho} = \frac{e}{4 \sin \Theta_W \cos \Theta_W} Z^\mu \sum_i \bar{\nu}_i \gamma_\mu (1 - \gamma_5) \nu_i \quad (163)$$

Thus if the neutrinos are light,  $m_\nu \simeq 0$ , all types of neutrinos are able to be produced via their coupling to the  $Z$ . Two experimental particle physics bounds exist on the number of neutrino species. One of these, the PEP/PETRA limit, arising from the study of the process  $e^+\epsilon^- \rightarrow \gamma \text{ Nothing}$ , makes use of the coupling of a virtual  $Z$  to neutrinos. The other, coming from the CERN collider, measures indirectly the total  $Z$  width, and hence can bound in this way the number of neutrinos. I want to describe briefly both of these bounds, since they also illustrate nicely various general features of the standard model.

#### 3.3.1 $e^+\epsilon^- \rightarrow \gamma \text{ Nothing}$

At PEP and PETRA the production of photons unaccompanied by other charged or neutral interacting particles - the process  $e^+\epsilon^- \rightarrow \gamma \text{ Nothing}$  - has been studied. This reaction in the standard model can occur by pair producing neutrinos, along with some bremsstrahlung photon:  $e^+\epsilon^- \rightarrow \nu_i \bar{\nu}_i \gamma$ . Clearly, the more neutrino species there are, the larger the contribution one expects from this process to the total cross section for  $e^+\epsilon^- \rightarrow \gamma \text{ Nothing}$ . Experimentally, however, the situation is complicated, since the signal can also be faked by radiative  $e^+\epsilon^-$  production, in which the final charged particles never come out of the beam pipe. To minimize this background one must require that the produced photon comes out at a rather large angle, with respect to the incident  $e^+\epsilon^-$  direction. This cut, however, also reduces the expected signal and, typically, one is left with just a handful of events.

The two graphs that contribute to the process  $e^+\epsilon^- \rightarrow \nu_i \bar{\nu}_i \gamma$  are shown in Fig 22. Since the coupling of the  $Z$  is universal, it is obvious that the total rate will be the same for each species. There is, however, a complication for the case in which  $\nu_i$  is an electron neutrino ( $\nu_i = \nu_e$ ). For the process  $e^+\epsilon^- \rightarrow \nu_e \bar{\nu}_e \gamma$ , in addition to the  $s$ -channel NC contribution, there is also a  $t$ -channel CC contribution, as Fig 23 shows. For the energies of PEP and PETRA, where  $\sqrt{s} \ll M_Z$ , one can compute all processes in the Fermi approximation, where all gauge boson propagators are just replaced by constants. This has two consequences:

1. The internal photon emission graph for the process  $e^+e^- \rightarrow \nu_e \bar{\nu}_e \gamma$  is totally negligible, since it involves two weak propagators, and can be omitted.

2. By means of a Fierz transformation one can recast the  $\nu_e$  calculation in a similar form as that appropriate for arbitrary neutrinos.

Let me expand a bit on the last point. In the Fermi approximation, the effective neutral current Lagrangian describing  $e^+e^- \rightarrow \nu_i \bar{\nu}_i$  is given by [c.f. Eq(31)]<sup>15</sup>

$$\mathcal{L}_{NC}^{eff} = \frac{G_F}{\sqrt{2}} \bar{\nu}_i \gamma^\mu (1 - \gamma_5) \nu_i [\bar{e} (Q_L^e \gamma_\mu (1 - \gamma_5) + Q_R^e \gamma_\mu (1 + \gamma_5)) e] \quad (164)$$

where the chiral charges  $Q_{L,R}^e$  are

$$Q_L^e = -\frac{1}{2} + \sin^2 \Theta_W; \quad Q_R^e = \sin^2 \Theta_W \quad (165)$$

The charged current Lagrangian, corresponding to the process  $e^+e^- \rightarrow \nu_e \bar{\nu}_e$  on the other hand, is given by

$$\mathcal{L}_{CC}^{eff} = \frac{G_F}{\sqrt{2}} \bar{\nu}_e \gamma^\mu (1 - \gamma_5) e [\bar{e} \gamma_\mu (1 - \gamma_5) \nu_e] \quad (166)$$

This Lagrangian, however, can be rewritten as that appearing in Eq(164), after a Fierz transformation:

$$[\mathcal{L}_{CC}^{eff}]_{Fierz} = \frac{G_F}{\sqrt{2}} \bar{\nu}_e \gamma^\mu (1 - \gamma_5) \nu_e [\bar{e} \gamma_\mu (1 - \gamma_5) e] \quad (167)$$

Clearly, therefore, the result of the computation for producing electron neutrinos is just like that for producing any other neutrino, but with the replacement

$$Q_L^e \rightarrow (Q_L^i)_{eff} = Q_L^i + 1; \quad Q_R^e \rightarrow (Q_R^i)_{eff} = Q_R^i \quad (168)$$

The calculation of the process  $e^+e^- \rightarrow \nu \bar{\nu} \gamma$  was done originally by Ma and Okada [32] and it was repeated soon after by Gaemers, Gastmans and Renard [33], who corrected some errors in the first calculation. If one denotes by  $x$  the ratio of the photon energy to the incident electron energy in the CM system:  $x = \frac{2E_\gamma}{\sqrt{s}}$  and by  $y$  the cosine of the angle that the photon makes with respect to the  $e^-$  direction:  $y = \cos \Theta_\gamma$  (see Fig 24), one finds [33]

$$\frac{d\sigma}{dx dy} = \frac{\alpha G_F^2 s (1-x)}{3\pi^2 x (1-y)^2} \left[ \left(1 - \frac{1}{2}x\right)^2 + \frac{1}{4}x^2 y^2 \right] F \quad (169)$$

One sees that this cross section has the typical  $x^{-1}$  behaviour of a bremsstrahlung process. The factor  $F$ , in the Fermi approximation, is simply given by

$$F = (N_\nu - 1) [(Q_L^i)^2 + (Q_R^i)^2] + [(Q_L^i)_{eff}^2 - (Q_R^i)_{eff}^2] \\ = N_\nu \left[ \frac{1}{4} - \sin^2 \Theta_W + 2 \sin^4 \Theta_W \right] + 2 \sin^4 \Theta_W \approx 0.126 N_\nu + 0.46 \quad (170)$$

That is, all neutrinos contribute equally, except for the electron neutrino which has just some different effective chiral charges. Unfortunately, as can be seen from Eq(170), the

<sup>15</sup>I have taken  $\rho = 1$  here, as that is what experiment indicates.

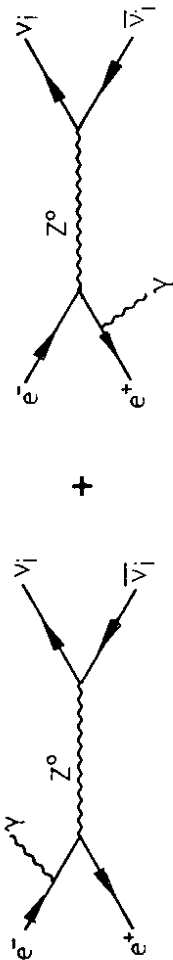


Figure 22: Graphs contributing to the process  $e^+e^- \rightarrow \nu_i \bar{\nu}_i \gamma$ , with  $\nu_i \neq \nu_e$ .

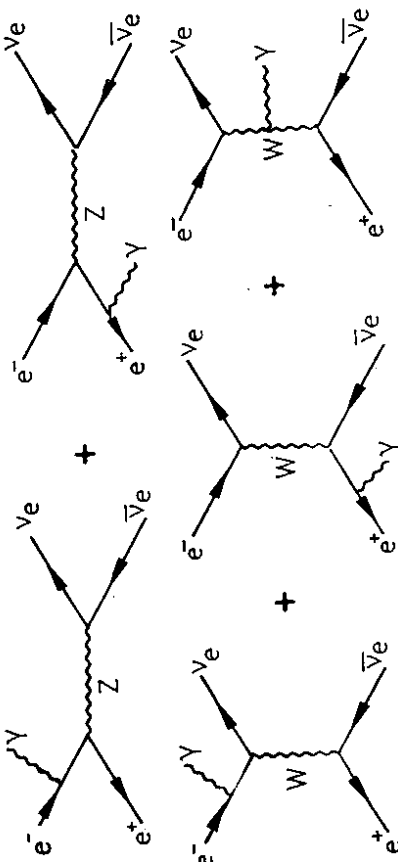


Figure 23: Graphs contributing to the process  $e^+e^- \rightarrow \nu_e \bar{\nu}_e \gamma$ .

This leads to an average value [38] of  $R$ :

$$\langle R \rangle = 8.4^{+1.2}_{-0.9} \quad (174)$$

and a 90 % confidence limit

$$R < 10.1 \quad (90\% C.L.) \quad (175)$$

The ratio  $R$  depends on the number of neutrinos  $N_\nu$  and on the top mass,  $m_t$ . This is easily seen by rewriting Eq(172) as a function of the total  $Z$  and  $W$  widths:

$$R = \left[ \frac{\sigma_W}{\sigma_Z} \right] \left[ \frac{\Gamma(W \rightarrow e\nu_e)}{\Gamma(Z \rightarrow e^+e^-)} \right] \left[ \frac{\Gamma_{tot}^Z}{\Gamma_W} \right] \quad (176)$$

The first two factors in square brackets above are fixed by our present theoretical knowledge. The ratio of the  $W$  and  $Z$  production cross sections is calculable in QCD, with reasonably good accuracy, while the ratio of the partial widths of  $W \rightarrow e\nu_e$  to  $Z \rightarrow e^+e^-$  is fixed by the  $SU(2) \times U(1)$  model. The total width ratio, however, is affected by the unknown parameters in the standard model. Since  $\Gamma_{tot}^Z$  goes up the more neutrino species there are, it is clear that the bound on  $R$  of Eq(175) also gives a bound on  $N_\nu$ . However, since the total widths depend on whether the decays  $Z \rightarrow t\bar{t}$  and  $W \rightarrow t\bar{b}$  are possible and on how big their respective contributions are- the bound on  $N_\nu$  depends also on the value of the  $t$ -quark mass.

To make the above remarks more quantitative, one needs to calculate the three quantities in square brackets in Eq(176). The widths  $\Gamma(W \rightarrow e\nu_e)$  and  $\Gamma(Z^0 \rightarrow e^+e^-)$  are straightforward to compute from the interaction Lagrangian of Eq(26). Neglecting the electron mass, a simple calculation gives

$$\Gamma(W \rightarrow e\nu_e) = \frac{\sqrt{2}G_F M_W^3}{12\pi} \quad (177)$$

$$\Gamma(Z^0 \rightarrow e^+e^-) = \frac{\sqrt{2}G_F M_Z^2}{6\pi} [(Q_L^e)^2 + (Q_R^e)^2] \quad (178)$$

In the above, I have replaced the factor of  $\frac{1}{\sin^2 \Theta_W}$  which comes from a direct calculation using the Lagrangian of Eq(26), by  $\frac{\sqrt{2}G_F M_Z^2}{\pi}$ . This replacement, effectively, takes care of the leading logarithmic radiative effects because, as can be seen in Eqs(177) and (178), both sides contain only quantities at large scales, or quantities like  $G_F$  which do not run. Using Eqs(177) and (178) one has

$$\frac{\Gamma(W \rightarrow e\nu_e)}{\Gamma(Z \rightarrow e^+e^-)} = \frac{2M_W^3}{M_Z^3 [1 - 4 \sin^2 \Theta_W + 8 \sin^4 \Theta_W]} = 2.08 \quad (179)$$

The numerical value above uses a set of values for the parameters in the standard model which correspond to the central values presently measured, consistent with Eq(53):  $\sin^2 \Theta_W = 0.23$ ;  $M_Z = 92 \text{ GeV}$ ;  $M_W = 80.7 \text{ GeV}$ .

To calculate the total  $Z$  width, in the standard model, one just needs to sum over the individual fermionic channels:

$$\Gamma_{tot}^Z = \sum_f \Gamma(Z \rightarrow ff) \quad (180)$$

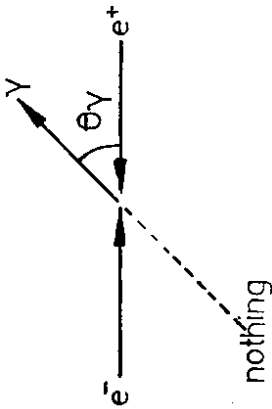


Figure 24: Definition of the angle  $\Theta_\gamma$

part in  $F$  not proportional to  $N_\nu$  is rather large. Thus the difference between having three ( $F \simeq 0.84$ ) or four ( $F \simeq 0.96$ ) families is only about 15%.

Because of the cuts on  $y$  imposed to get rid of background at PEP and PETRA <sup>16</sup>, very few events of the type  $e^+e^- \rightarrow \gamma$  Nothing are expected and very few are observed. Nevertheless, one has been able to set rather good limits on the number of neutrino species. The most sensitive results come from ASP at PEP [34] and CELLO at PETRA [35], giving 90 % C.L. of  $N_\nu \leq 7.5$  and  $N_\nu \leq 8.7$ , respectively. An analysis of all  $e^+e^-$  data, done by the CELLO collaboration [35], gives a stronger combined limit

$$N_\nu < 4.6 \quad (90\% C.L.) \quad (171)$$

### 3.3.2 Neutrino Counting in Collider Experiments

A bound on the number of neutrino species has also been obtained at the Sp $\bar{p}$ S collider through the measurement of the ratio of the production of  $W$  bosons, decaying into an electron and a neutrino [ $W \rightarrow e\nu_e$ ], to that of  $Z$  bosons, decaying into  $e^+e^-$  pairs [ $Z \rightarrow e^+e^-$ ]:

$$R = \frac{\sigma_W B(W \rightarrow e\nu_e)}{\sigma_Z B(Z \rightarrow e^+e^-)} \quad (172)$$

This ratio has been measured by both the UA1 and UA2 collaborations with the result

$$R = \begin{cases} 9.1^{+1.7}_{-1.2} & \text{UA1[36]} \\ 7.2^{+1.7}_{-1.2} & \text{UA2[37]} \end{cases} \quad (173)$$

<sup>16</sup>Typically  $\Theta_{\text{gamma}} > 20^\circ$ .

$B(Z \rightarrow \epsilon^+ \epsilon^-)$  is actually very small: the  $\alpha_s$  uncertainty implies  $\delta\Gamma_{tot}^Z = \pm 20 \text{ MeV}$ , while the uncertainty in  $\sin^2 \Theta_W$  of Eq(66), only gives  $\delta\Gamma_{tot}^Z = \pm 12 \text{ MeV}$ .

A similar analysis yields  $\Gamma_{tot}^W$ . If one again neglects all fermion masses, except  $m_t$ , then  $\Gamma_{tot}^W$  is independent of the Cabibbo Kobayashi Maskawa matrix  $V$ . A simple calculation, using Eqs(25) and (26), yields

$$\Gamma_{tot}^W = \Gamma(W \rightarrow e\nu_e) \left\{ 3 + 2 \cdot 3 \left( 1 + \frac{\alpha_s}{\pi} \right) \right\} + \Gamma(W \rightarrow t\bar{b}) \quad (188)$$

Using the standard model parameters adopted earlier, Eq(177) implies

$$\Gamma(W \rightarrow e\nu_e) = 229 \text{ MeV} \quad (189)$$

For  $W \rightarrow t\bar{b}$ , on the other hand, one cannot forget phase space effects which kinematically suppress the rate. Neglecting again  $m_b$ , one finds

$$\Gamma(W \rightarrow t\bar{b}) = 3 \left( 1 + \frac{\alpha_s}{\pi} \right) \Gamma(W \rightarrow e\nu_e) \left\{ \left( 1 + \frac{m_t^2}{2M_W^2} \right) \left( 1 - \frac{m_t^2}{M_W^2} \right)^2 \right\} \quad (190)$$

The above formula implies  $\Gamma(W \rightarrow t\bar{b}) = 395 \text{ MeV}$  for  $m_t = 45 \text{ GeV}$ , but  $\Gamma(W \rightarrow t\bar{b}) \rightarrow 0$  as  $m_t \rightarrow M_W$ . For the standard model parameters adopted one has

$$\Gamma_{tot}^W = 2120 \text{ MeV} + \Gamma(W \rightarrow t\bar{b}) \quad (191)$$

with again little error - except for the error on  $M_W$ , but this error is irrelevant in the branching ratio that enters in  $R$ .

Collecting all the results one finds, in the standard model:

$$\frac{B(W \rightarrow e\nu_e)}{B(Z \rightarrow \epsilon^+ \epsilon^-)} = \frac{\Gamma(W \rightarrow e\nu_e) \Gamma_{tot}^Z}{\Gamma(Z \rightarrow \epsilon^+ \epsilon^-) \Gamma_{tot}^W} \approx 2.68 \left\{ \frac{2560 + 170(N_c - 3)}{2120 + \Gamma(W \rightarrow t\bar{b})(\text{MeV})} \right\} \quad (192)$$

It is clear from the above that this ratio increases as  $N_c$  increases and that the ratio also grows as  $m_t \rightarrow M_W$ , since then  $\Gamma(W \rightarrow t\bar{b}) \rightarrow 0$ . This behaviour is depicted in Fig 26

To complete the calculation of  $R$  one needs an estimate of the ratio  $\frac{\sigma_W}{\sigma_Z}$ . This is the place where the theoretical uncertainty is the largest. There are basically two sources of error in this ratio:

1. The actual estimates for  $\sigma_W$  and  $\sigma_Z$  need values for the probability of finding  $u$  and  $d$  quarks in the proton. These probabilities are related to the corresponding structure functions and these, in turn, have some uncertainty.
2. In addition, the production cross sections for  $W$  and  $Z$  bosons are affected by QCD corrections, arising from either real or virtual emission of gluons- the so called  $K$ -factor.

Because one is dealing with a ratio of cross sections, it turns out that  $\frac{\sigma_W}{\sigma_Z}$  is not very much affected by QCD corrections, since the  $W$  and  $Z$   $K$ -factors tend to cancel out. On the other hand, the actual value for  $\frac{\sigma_W}{\sigma_Z}$  depends to some extent on what structure functions one uses <sup>17</sup>.

<sup>17</sup> $\sigma_W$  requires a knowledge of  $f_d \otimes f_u$ , while  $\sigma_Z$  is proportional to  $(f_d \otimes f_d) \oplus (f_u \otimes f_u)$ , so there is not a complete cancellation in the ratio.

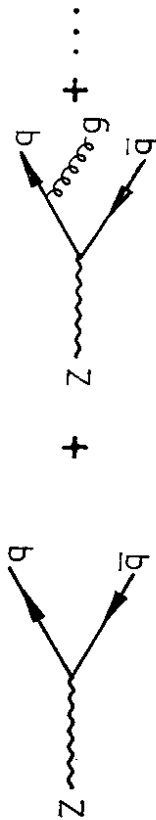


Figure 25: QCD corrected decays of the  $Z$  boson, including gluon emission.

From the UA1 bound on  $m_t$ , Eq(162), presumably the decay  $Z \rightarrow t\bar{t}$  is not kinematically allowed. Thus the fermions  $f$  in Eq(180) include all those in the first three generations, except top, plus any extra (light) neutrinos of subsequent generations. Neglecting fermion masses again, which is an excellent approximation, and using Eqs(23) and (26) one finds

$$\Gamma(Z \rightarrow f\bar{f}) = \frac{\sqrt{2}G_F M_Z^2}{6\pi} \left[ (Q_L^f)^2 + (Q_R^f)^2 \right] \begin{cases} 1 & \text{leptons} \\ 3(1 + \frac{\alpha_s}{\pi}) & \text{quarks} \end{cases} \quad (181)$$

In the above the chiral charges  $Q_L^f$ ,  $Q_R^f$  are given by

$$Q_L^f = T_{3f} - e_f \sin^2 \Theta_W; \quad Q_R^f = -e_f \sin^2 \Theta_W \quad (182)$$

where  $T_{3f}$  are the  $SU(2)$  quantum numbers of the left-handed fermions and  $e_f$  are the fermion charges. The extra factor entering in Eq(181) for the quarks is a color factor of 3, times a QCD correction which accounts for the fact that, as shown in Fig 25, a  $Z$  boson not only can decay into a  $q\bar{q}$  pair but it can also have decays involving gluon emission. Using the estimate [39]  $\frac{\alpha_s(M_Z)}{\pi} = 0.04 \pm 0.01$  and the standard values of  $M_Z$  and  $\sin^2 \Theta_W$  given above, one finds:

$$\Gamma(Z \rightarrow \nu\bar{\nu}) = 170 \text{ MeV} \quad (183)$$

$$\Gamma(Z \rightarrow \epsilon^+ \epsilon^-) = 86 \text{ MeV} \quad (184)$$

$$\Gamma(Z \rightarrow u\bar{u}) = 306 \text{ MeV} \quad (185)$$

$$\Gamma(Z \rightarrow d\bar{d}) = 393 \text{ MeV} \quad (186)$$

Using these results, the total  $Z$  width is

$$\Gamma_{tot}^Z = 2560 \text{ MeV} + (N_c - 3) 170 \text{ MeV} \quad (187)$$

I note that the error on this prediction - apart from the uncertainty in  $M_Z$  which is irrelevant for our considerations, since the value of  $M_Z$  does **not** affect the branching ratio



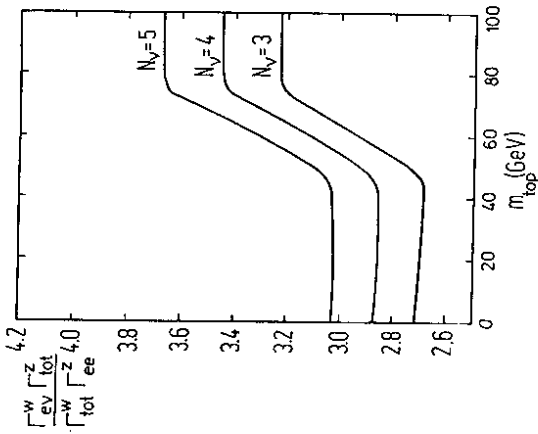


Figure 26: The ratio of the  $W \rightarrow \nu_e$  to  $Z \rightarrow e^+e^-$  branching ratios as a function of  $m_t$ , for various values of  $N_\nu$ .

Recently, Colas, Denegri and Stubenrauch [38] have done an extensive reanalysis of existing deep inelastic data from the BCDMS and EMC collaborations to try to determine  $\frac{\sigma_W}{\sigma_Z}$  accurately. Their results, which are shown pictorially in Fig 27 along with some other determinations, lead to a value

$$\frac{\sigma_W}{\sigma_Z} = 3.25 \pm 0.10 \quad (193)$$

Using Eqs(192) and (193) and the experimental bound on  $R$  of Eq(175), the bound on  $N_\nu$ , as a function of the top quark mass, follows immediately. In effect, for the bound, what is important in the lowest value for  $\frac{\sigma_W}{\sigma_Z}$  assumed. Using the  $1\sigma$  value of  $\frac{\sigma_W}{\sigma_Z}$  of Eq(193),  $\frac{\sigma_W}{\sigma_Z} = 3.15$ , Colas, Denegri and Stubenrauch obtain the results displayed in Fig 28. One sees that for  $m_t > M_W$  one has rather tight limits. These limits are displayed in a different form in Fig 29. From this figure, one sees that one can allow a few extra families if  $m_t \simeq 50 GeV$ , but there is essentially no freedom left if  $m_t > 80 GeV$ . To keep the above limits in perspective, however, one should note that if the minimum value assumed for  $\frac{\sigma_W}{\sigma_Z}$  goes down by 5% (i.e.  $\frac{\sigma_W}{\sigma_Z} = 3$  and not 3.15) then the allowed value for  $N_\nu$  rises by one unit.

I close this Section with a remark on the future. Namely, that very accurate neutrino counting can be expected at LEP and SLC. First of all, at these colliders operating at the  $Z$  energy, one is expected to measure  $M_Z$  to an accuracy of better than 50 MeV [40]. With this measurement the actual error on  $\Gamma_{tot}^Z$ , due to the uncertainty in the  $Z$  mass is tiny. Hence, one can really hope to keep

$$(\delta\Gamma_{tot}^Z)_{LEP/SLC} \lesssim 30 MeV \quad (194)$$

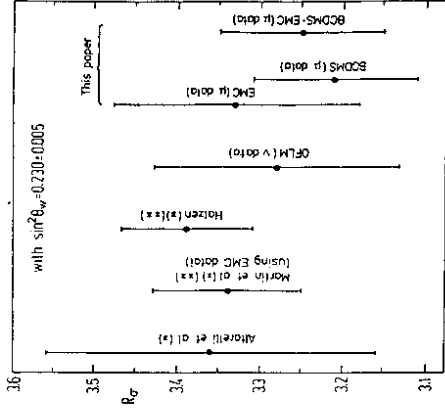


Figure 27: Compilation of the results on  $\frac{\sigma_W}{\sigma_Z}$ , from [38].

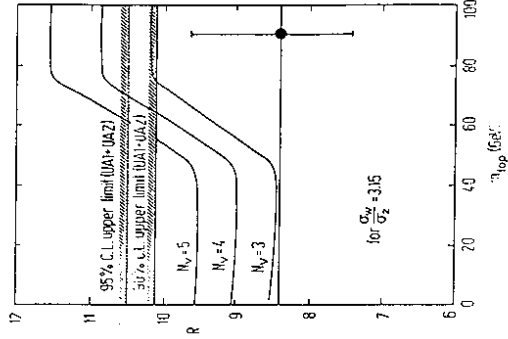


Figure 28: Values of  $N_\nu$  allowed by the combined UA1 and UA2 data on  $R$ , as a function of  $m_t$ , from [38].

The advantages of the above parametrization for the mixing matrix  $V$  is that, experimentally, the mixing angles  $\theta_i$  appear to have a natural hierarchy of values:

$$\theta_1 \gg \theta_2 \gg \theta_1^2 \gg \theta_3 \simeq \theta_3^2 \quad (198)$$

Thus, it is possible to write Eq(197) in a convenient approximate form [42], which is easy to remember. For this purpose one defines

$$\sin \theta_1 = \lambda, \quad \sin \theta_2 = A\lambda^2 \quad \sin \theta_3 = A\rho\lambda^3 \quad (199)$$

Then to  $O(\lambda^4)$ , but keeping all the phase information, Eq(197) becomes

$$V = \begin{pmatrix} 1 - \frac{\lambda^2}{2} & \lambda & A\rho\lambda^3 e^{-i\delta} \\ -\lambda(1 + A^2\rho\lambda^4 e^{i\delta}) & 1 - \frac{\lambda^2}{2} - A^2\rho\lambda^6 e^{i\delta} & A\lambda^2 \\ A\lambda^3(1 - \rho e^{i\delta}) & -A\lambda^2(1 - \rho\lambda^2 e^{i\delta}) & 1 \end{pmatrix} \quad (200)$$

Experiment provides information on the parameters  $\lambda$ ,  $A$ ,  $\rho$  and  $\delta$ . I shall discuss how their values, or allowed ranges, are determined below.

#### 4.1 $V_{ud}$ and Radiative Effects

The matrix element  $V_{ud}$  is the one which is known with the greatest precision. It is determined by comparing the rate for  $\beta$ -decay in nuclei to that for  $\mu$ -decay. The ratio of these decay rates is proportional to  $|V_{ud}|^2$ . However, to extract a precise value for  $|V_{ud}|$  one must:

1. make sure that in the comparison between theory and experiment, electroweak radiative corrections are taken into account;
2. pick appropriate decays, where hadronic and nuclear effects do not obscure the situation.

Recall from our discussion in Sec. 2 that electroweak radiative corrections affect, at leading logarithmic level, charged current processes involving hadrons but not  $\mu$ -decay. The relevant correction for the rate of  $d \rightarrow u + e^- + \bar{\nu}_e$ , relative to that for  $\mu^- \rightarrow \nu_\mu + e^- + \bar{\nu}_e$ , is the CC coefficient  $\rho^{CC}$  of Eq(93):

$$\frac{\Gamma(d \rightarrow u + e^- + \bar{\nu}_e)}{\Gamma(\mu^- \rightarrow \nu_\mu + e^- + \bar{\nu}_e)} \sim |V_{ud}|^2 |\rho^{CC}|^2 \quad (201)$$

Now

$$|\rho^{CC}|^2 = \left| 1 + \frac{3\alpha}{4\pi} \epsilon_u \ln \frac{M_W^2}{\mu^2} \right|^2 \simeq 1 + \frac{2\alpha}{\pi} \ln \frac{M_W}{\mu} \quad (202)$$

If  $\mu$  is taken of the order of the typical energies involved in nuclear decays ( $\mu \sim \text{few MeV's}$ ), one sees that the correction of Eq(202) is of the order of 3–4%. As Sirini[43] has emphasized, neglecting these effects would lead to a violation of unitarity of the CKM matrix. Hence, here one has another example where the physical importance of the electroweak radiative corrections is manifest.

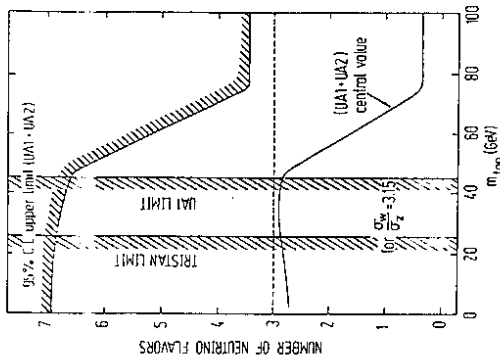


Figure 29: Bounds on  $N_\nu$  versus  $m_t$ , from [38].

Experimentally, furthermore, one believes that one can measure  $\Gamma_{tot}^Z$  very accurately, with perhaps [40]

$$(\delta\Gamma_{tot}^Z)_{\text{experiment}}^{LEP/SLC} \leq 10 \text{ MeV} \oplus 15 \text{ MeV} \quad (195)$$

where the first error is statistical and the second is an estimate of the expected systematic error. Given Eqs(194) and (195), one should have no trouble establishing if there are any extra neutrino species, since each extra neutrino type contributes:

$$\Gamma(Z \rightarrow \nu_i \bar{\nu}_i) = 170 \text{ MeV} \gg (\delta\Gamma_{tot}^Z)_{\text{theory}}^{LEP/SLC} \oplus (\delta\Gamma_{tot}^Z)_{\text{experiment}}^{LEP/SLC} \quad (196)$$

## 4 The Flavor Mixing Matrix

In this section I want to discuss in some detail one of the crucial elements that enter in the standard model: the flavor mixing matrix  $V$ . I will consider here only the case of 3 generations, where  $V$  is described by 3 angles and one phase. Many equivalent parametrizations of the Cabibbo Kobayashi Maskawa matrix exist in the literature. I shall use a parametrization which is related to the one suggested by Maiani [41] and is the form of the CKM matrix now adopted by the Particle Data Group:

$$V = \begin{pmatrix} V_{ud} & V_{us} & V_{ub} \\ V_{cd} & V_{cs} & V_{cb} \\ V_{td} & V_{ts} & V_{tb} \end{pmatrix} = \begin{pmatrix} c_1 c_3 & s_1 c_3 & s_3 e^{-i\delta} \\ -s_1 c_2 - c_1 s_2 s_3 e^{i\delta} & c_1 c_2 - s_1 s_2 s_3 e^{i\delta} & s_2 c_3 \\ s_1 s_2 - c_1 c_2 s_3 e^{i\delta} & -c_1 s_2 - s_1 c_2 s_3 e^{i\delta} & c_2 c_3 \end{pmatrix} \quad (197)$$

Here  $c_i = \cos \theta_i$ ,  $s_i = \sin \theta_i$ .

The quark level ratio of Eq(201), characterized by  $V_{ud}$  and  $\rho^{CC}$ , can be obscured when one is dealing with a transition in a nucleus. The current

$$J_+^\mu = V_{ud}\bar{u}\gamma^\mu(1 - \gamma_5)d, \quad (203)$$

written in terms of quarks, receives different corrections for its vector and axial pieces in a hadronic matrix element. In general, between nucleon states, one can write

$$\langle p; p_1 | \bar{u}\gamma_\mu d | n; p_2 \rangle = \bar{u}(p_1) [\gamma_\mu F_1(q^2) + \frac{i\sigma_{\mu\nu}q^\nu}{2M_N} F_2(q^2)] u(p_2) \quad (204)$$

$$\langle p; p_1 | \bar{u}\gamma_\mu\gamma_5 d | n; p_2 \rangle = \bar{u}(p_1) [\gamma_\mu\gamma_5 G_A(q^2) + \frac{i\hat{q}_\mu\gamma_5}{M_N} G_P(q^2)] u(p_2) \quad (205)$$

where  $q^\mu = (p_1 - p_2)^\mu$  is the momentum transfer and  $F_1$ ,  $F_2$ ,  $G_A$  and  $G_P$  are form factors. Since the momentum transfers in nuclear decays are small compared to  $M_N$ , the  $F_2$  and  $G_P$  form factors are not very important. Of the two remaining form factors, the axial form factor  $G_A(0)$  is affected by the strong interactions and one finds experimentally that, at zero momentum transfer  $G_A(0) \simeq 1.25$ . The vector form factor  $F_1$ , on the other hand, is not affected by the strong interactions and one has

$$F_1(0) = 1 \quad (206)$$

The result Eq(206), which follows from the conserved vector current hypothesis (CVC) [44], is easy to understand. The weak current  $J_+^\mu$ , of Eq(203), apart from  $V_{ud}$ , is also the  $1+1/2$  component of the strong isospin current for the  $u$  and  $d$  quarks. Indeed, at the quark level, since  $u$  and  $d$  form an isospin doublet, the strong isospin current is just

$$J_+^\mu = (\bar{u}\vec{d})\gamma^\mu \frac{\tau_1}{2} \begin{pmatrix} u \\ d \end{pmatrix} \quad (207)$$

To the extent that strong isospin is a good symmetry, so that the current Eq(207) is conserved

$$\partial_\mu J_+^\mu = 0 \quad (208)$$

it follows that  $F_1(0) = 1$ . This is easily seen, by computing the matrix element of the isospin raising operator, between a neutron and proton state, using Eq(204). By definition one has that <sup>18</sup>

$$\langle p; p_1 | J_{1+1/2} | n; p_2 \rangle = (2\pi)^3 2p_1^0 \delta^3(\vec{p}_1 - \vec{p}_2) \equiv \langle p; p_1 | p; p_2 \rangle \quad (209)$$

However, one has also that

$$\langle p; p_1 | J_{1+1/2} | n; p_2 \rangle = \langle p; p_1 | \int d^3x J_{1+1/2}^0 | n; p_2 \rangle = F_1(0) (2\pi)^3 2p_1^0 \delta^3(\vec{p}_1 - \vec{p}_2) \quad (210)$$

One can show, and I will sketch the proof of this in the next subsection, that corrections to the CVC result, Eq(206), only occur at  $2^{nd}$  order in isospin breaking [45]. This result,

<sup>18</sup> I use a covariant normalization for my states.

known as the Behrends, Sirlin, Ademollo, Gatto (BSAG) theorem, means that for nuclear transitions the corrections for  $F_1(0)$  are really negligible

$$F_1(0) = 1 + 0 \left( \frac{\Delta M_N}{M_N} \right)^2 \quad (211)$$

So one can essentially eliminate all the hadronic uncertainties, if one can focus on transitions where only  $F_1$  enters. Experimentally, to get rid of the axial vector contributions one studies Fermi transitions, where parity is conserved. Furthermore, one can also get rid of the contributions from  $F_2$  - the, so called, weak magnetism term - by studying transitions from a spin zero state to another spin zero state (0-0 transitions).

The ideal prototype for a 0-0 transition is the  $\beta$ -decay of the  $\pi^+$ . Unfortunately, the three body decay mode  $\pi^+ \rightarrow \pi^0 e^+ \bar{\nu}_e$ , is so rare that there is not enough experimental precision yet to match that which can be obtained by studying nuclear transitions. The nuclear decays studied are the superallowed Fermi  $0^+ \rightarrow 0^+$  transitions, of which 8 have been measured experimentally [47] and analyzed theoretically. In particular, Sirlin [46] has made a full comparison between theory and experiment, including the effects of the electroweak corrections. He finds, using only the best measured  $^{14}\text{O}$  transition,  $V_{ud} = 0.9739 \pm 0.0015$ . Using all 8 decays, the value quoted by Sirlin is slightly more accurate:

$$V_{ud} = 0.9744 \pm 0.0010 \quad (212)$$

I remark that, using the unitarity of the CKM matrix, the above allows one to determine  $\lambda$ , since  $V_{ud} \simeq 1 - \frac{\lambda^2}{2}$ . The value for  $\lambda$  obtained this way

$$\lambda = 0.226 \pm 0.004 \quad (213)$$

is in very good agreement with the direct determination of  $V_{us}$ , which I will discuss below. If one had not applied any electroweak radiative corrections, then one would have found  $V_{ud} \simeq 1$  and  $|V_{ud}|^2 + |V_{us}|^2 > 1$ , which would have violated the unitarity of the Cabibbo Kobayashi Maskawa matrix!

## 4.2 Fixing the Cabibbo Angle

The comparison of the rate for strangeness changing weak decays to that for  $\mu$ -decay allows a direct determination of  $V_{us} \simeq \lambda$ . This parameter, for the case of two generations, is just the sine of the Cabibbo angle,  $\sin \theta_C$  - introduced long ago by Cabibbo [48] to restore universality between hadronic and leptonic weak interactions. For analogous reasons to those discussed above, it is again safer to consider  $\Delta S = 1$  decays where only the vector currents enter [ $K \rightarrow \pi l \bar{\nu}_l$ ], rather than Hyperon  $\beta$ -decays.

The most comprehensive and careful analysis to date on how to extract  $\lambda$  from physical data on  $K_{e3}$  decays is due to Leutwyler and Roos [49] and I will base my discussion mostly on their work. In the decay  $K \rightarrow \pi l \bar{\nu}_l$ , shown in Fig 30, only the vector piece of the  $\Delta S = 1$  charged current contributes. The matrix element of this current, between a Kaon and a pion, is described by two form factors:

$$\langle K, p_1 | \bar{u}\gamma^\mu s | \pi, p_2 \rangle = C [(p_1 + p_2)^\mu f_+(q^2) + (p_1 - p_2)^\mu f_-(q^2)] \quad (214)$$

$$\Gamma(K_L^0 \rightarrow \pi^+ \pi^- \nu_e) = (4.915 \pm 0.733) \times 10^{-15} M e V \quad (220)$$

Leutwyler and Roos [49] deduce that

$$f_{\pm}^{K^+}(0) |V_{us}| = 0.2161 \pm 0.0017 \quad (221)$$

$$f_{\pm}^{K^0}(0) |V_{us}| = 0.2103 \pm 0.0020 \quad (222)$$

In obtaining these results, the authors of [49] ignored the, difficult to calculate and model dependent, correction  $\delta$  and just augmented the error brackets in Eq(221) and (222).

To proceed one must be able to estimate  $f_{\pm}(0)$ . Of course, since the  $\Delta S = 1$  current  $J_{\Delta S=1}^{\mu} = \bar{u}\gamma^{\mu}s$  is conserved in the  $SU(3)$  limit  $m_s = m_u = m_d$ , one expects that  $f_{\pm}(0) \simeq 1$ . However, the correction to this relation, coming from an  $SU(3)$  version of the BSAG theorem, naively appear to be quite large, since  $\frac{(m_u - m_d)^2}{(m_u + m_d)^2} \sim 0(1)$ ! Thus a more careful analysis is warranted. I will briefly go into this analysis here as it will serve to demonstrate the difficulties inherent in extracting weak interaction information in hadronic processes. Furthermore, it will give me a chance to indicate how the BSAG theorem comes about, although, for the case of pions and Kaons, in fact, the theorem is violated by mass singularities! When all the theoretical smoke clears, however, we shall see that indeed  $f_{\pm}(0)$  is very near unity, so that the value of  $|V_{us}|$  is close to that indicated on the right hand side of Eqs(221) and (222).

Corrections to the  $SU(3)$  limit result,  $f_{\pm}(0) = 1$ , are more complicated for the  $0^-$  mesons, since these particles are quasi Goldstone bosons and one expects that their masses vanish, as the quark masses vanish. Thus, in calculating corrections to  $f_{\pm}(0)$ , one can encounter factors of  $m_q^{-1}$ , coming from virtual exchanges of these mesons, which alter the ordinary mass power counting. Indeed, these mass singularities will also give some logarithmic, and therefore non analytical, dependence on  $m_q$ . Because of these circumstances, the correct expansion for  $f_{\pm}(0)$  is of the form [51]:

$$f_{\pm}(0) = 1 + 0(m_q \ln m_q) + 0(m_q) + \dots \quad (223)$$

Given Eq(223), it is obvious that for mesons the BSAG theorem [45] must be modified. Furthermore, at first sight, things look even worse than one would have naively expected. However, an actual computation shows that the coefficient of the  $0(m_q \ln m_q)$  term is of  $0(10^{-2})$  and thus these corrections are small [49].

The  $0(m_q)$  corrections above have a rather trivial origin. If  $m_u \neq m_d$  then there is some  $\pi^0 - \eta$  mixing. That is, the  $\pi^0$  is not purely the third component of an octet, but one has [52]

$$|\pi^0\rangle \simeq |\beta\rangle + \frac{\sqrt{3}(m_d - m_u)}{2(2m_s - m_d - m_u)} |\beta\rangle \simeq |\beta\rangle + \epsilon |\beta\rangle \quad (224)$$

Then a simple calculation gives [49]

$$f_{\pm}^{K^0}(0) = 1; \quad f_{\pm}^{K^+}(0) = 1 + \sqrt{3}\epsilon \quad (225)$$

Note that using the present estimates of the quark masses [52]  $\epsilon \simeq 2 \times 10^{-2}$ .

To understand the origin of the mass singularities - and to derive the BSAG theorem in ordinary circumstances! - one can proceed as follows [49]. The  $\Delta S = 1$  currents  $J_{\pm}^{\mu} = \bar{u}\gamma^{\mu}s$ ,  $J_{\pm}^{\mu} = \bar{s}\gamma^{\mu}u$  and  $J_{\pm}^{\mu} = \frac{1}{2}(\bar{u}\gamma^{\mu}u - \bar{s}\gamma^{\mu}s)$ , have an isospin charge algebra

$$[Q_+, Q_-] = 2Q_3, \quad (226)$$

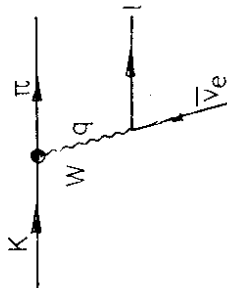


Figure 30: The decay  $\bar{K} \rightarrow \pi l \nu_l$

Here again  $q^{\mu}$  is the 4-momentum transfer and  $C$  is a Clebsch Gordan factor, which takes the values

$$C = \begin{cases} \sqrt{\frac{1}{2}} & (K^+ \rightarrow \pi^0 l^+ \nu_l) \\ 1 & (K_L^0 \rightarrow \pi^- l^+ \nu_l) \end{cases} \quad (215)$$

Since  $(p_1 - p_2)^{\mu}$ , when contracted with the leptonic tensor coming from the  $l\nu_l$  vertex in Fig 30, gives a factor of the lepton mass, for the electron decay mode only the  $f_{\pm}$  form factor is important. For this reason one considers only  $K_{e3}$  decays. For the momentum transfers involved in  $K_{e3}$  decays, the variation of  $f_{\pm}(q^2)$  with  $q^2$  is well fit by a linear formula

$$f_{\pm}(q^2) = f_{\pm}(0) [1 + \lambda_{\pm} q^2] \quad (216)$$

with the slope parameter  $\lambda_{\pm}$  fixed from the data [50].

Using Eq(214) and (216) the  $K_{e3}$  decay rate is straightforwardly computed [49]. One finds

$$\Gamma = \left[ \frac{G_F^2 M_K^5}{192\pi^3} |C f_{\pm}(0) J_{ps}|^2 \left( 1 + \frac{2\alpha}{\pi} \ln \frac{M_Z}{M_N} + \delta \right) |V_{us}|^2 \right] \quad (217)$$

The 1<sup>st</sup> factor in square brackets above is the usual 3-body ( $m = 0$ )  $\beta$ -decay rate. The 2<sup>nd</sup> factor contains hadronic effects - through  $f_{\pm}(0)$  - and phase space corrections, coming from the non zero mass of the decay by-products. Finally, the 3<sup>rd</sup> factor contains the electroweak radiative corrections, where  $\delta$  are the remaining corrections beyond the leading logarithmic ones. The phase space integrals reduce the ( $m = 0$ )  $\beta$ -decay rate by almost an order of magnitude and Leutwyler and Roos [49] find

$$J_{ps} = \begin{cases} 0.1605 \pm 0.0009 & K^+ \rightarrow \pi^0 e^+ \nu_e \\ 0.1561 \pm 0.0009 & K_L^0 \rightarrow \pi^- e^+ \nu_e \end{cases} \quad (218)$$

where the errors above are reflections of the experimental uncertainties in  $\lambda_{\pm}$ . Using the branching ratios [50]

$$\Gamma(K^+ \rightarrow \pi^0 e^+ \nu_e) = (2.565 \pm 0.282) \times 10^{-15} M e V \quad (219)$$

$$f_+^{K^0}(0) = 0.961 \pm 0.008 \quad (230)$$

where the first result is dominated by the mixing correction, while the second is purely a  $m_q$  in  $m_q$  correction. Armed with these numbers, Leutwyler and Roos [49] use Eqs(221) and (222) to extract a combined value for  $|V_{us}|$

$$|V_{us}|_{K^0} = 0.2196 \pm 0.0023 \quad (231)$$

In addition, these authors also analyze Hyperon  $\beta$ -decay. Here there are more theoretical uncertainties, since also axial current matrix elements are present. The value obtained for  $|V_{us}|$  by Leutwyler and Roos [49] in this case is somewhat larger than that given in Eq(231):

$$|V_{us}|_{\text{Hyperon}} = 0.231 \pm 0.005 \quad (232)$$

Taking both analyses into account, with an appropriate weighting, leads to a final value for  $V_{us}$

$$|V_{us}| = 0.221 \pm 0.002 \quad (233)$$

This value of  $V_{us}$  - or equivalently  $\lambda$  - is in excellent agreement with the one I quoted earlier using the unitarity of the CKM matrix and the value for  $V_{ud}$ , Eq(213). So the unitarity of the CKM matrix is actually checked experimentally, at least for the first row!

### 4.3 Heavy Quark Matrix Elements

The matrix elements  $V_{cd}$  and  $V_{cs}$  of the CKM matrix are much more accurately fixed by unitarity than by direct measurements. To  $0(\lambda^4)$  unitarity implies <sup>19</sup>

$$V_{cs} = V_{ud} = 0.9744 \pm 0.0010 \quad (234)$$

$$V_{cd} = V_{us} = 0.221 \pm 0.002 \quad (235)$$

Direct estimates for  $V_{cd}$  and  $V_{cs}$  come from neutrino deep inelastic experiments, in particular dimuon production  $\nu_\mu \bar{N} \rightarrow \mu^+ \mu^- X$ . Opposite sign muons can arise from the production and subsequent semileptonic decay of charmed states. As is shown in Fig 32, there are two possible ways to produce charm in neutrino scattering. Both these contributions turn out to be comparable, since the probability of finding a valence  $d$  quark is much greater than that of finding a sea  $s$  quark, thereby compensating the disparity between  $V_{cd}$  and  $V_{cs}$ . Furthermore, since the sea and valence distributions have a different  $x$ -dependence, one can extract  $V_{cd}$  and  $V_{cs}$  separately. This analysis has been performed by the CDHS collaboration [55] and they obtain:

$$V_{cd} = 0.207 \pm 0.024 \quad (236)$$

$$V_{cs} = 0.95 \pm 0.14 \quad (237)$$

Clearly these numbers are consistent with those obtained through unitarity, but they are much less precise.

The remaining parameters of the mixing matrix, except for the phase  $\delta$ , are fixed by  $B$  meson decays. For  $\delta$ , CP violation in the Kaon system is of primary importance but, as

<sup>19</sup>If one does include  $\lambda^4$  terms, then unitarity implies  $V_{cs} = 0.973 \pm 0.061$ .

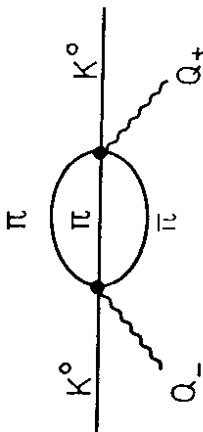


Figure 31: Dominant  $3\pi$  correction to  $f_+^{K^0}(0)$ .

where  $Q_i = f d^2 x J_i^0$ . This algebra, upon sandwiching it with  $|K^0\rangle$  states and inserting a complete set of states  $|n\rangle$ , yields a sum rule [53]

$$\sum_n |\langle K^0|Q_+|n\rangle|^2 - \sum_n |\langle K^0|Q_-|n\rangle|^2 = |\langle K^0|K^0\rangle|^2 \quad (227)$$

The states  $|n\rangle$  above have zero strangeness, while the states  $|m\rangle$  must have strangeness 2. These latter states are exotic and there is good reason to drop altogether their contribution from the sum rule. Furthermore, if  $|n\rangle$  is a  $|\pi^-\rangle$  what enters in Eq(227) is precisely  $f_+^{K^0}(0)$ . Hence one finds

$$|f_+^{K^0}(0)|^2 = 1 - \sum_{|n\rangle \neq |\pi^-\rangle} \frac{|\langle K^0|Q_+|n\rangle|^2}{|\langle K^0|K^0\rangle|^2} \quad (228)$$

The above formula, which could also be derived for other states besides Kaons is, essentially, the BSAG theorem [45] for SU(3). If one does not worry about mass singularities, then the matrix element on the RHS vanishes when  $m_s = m_u$ , so that the corrections are indeed of  $0((\frac{m_s - m_u}{m_s + m_u})^2)$ . Actually, in the case of Kaons, the corrections to  $f_+(0)$  are only of  $0((m_s - m_u)^2)$  near  $m_s = m_u$ . Otherwise, there are logarithmic modifications. The dominant contribution in the sum in Eq(228) is due to the state  $|n\rangle = |\pi^-\rangle$ . Since as  $m_u, m_d \rightarrow 0$ ,  $M_\pi$  vanishes, there are actually mass singularities when one performs the integrals over the  $|\pi^-\rangle$  to intermediate states, depicted in Fig 31. These integrals give rise to terms proportional to  $M_K^2 \ln \frac{M_K^2}{M_\pi^2}$ , which are not analytic in the quark masses. Fortunately, numerically these contributions are rather small, because the three body phase space of Fig 31 provides suppression factors of  $\frac{1}{192\pi^3}$ !

Leutwyler and Roos [49], make use of the chiral Lagrangian estimate of Gasser and Leutwyler [54] of the  $3\pi$  corrections to  $f_+(0)$ , plus the  $\pi - \eta$  mixing corrections of Eq(225), to calculate the departure of the  $K_{e3}$  form factors from unity. They find

$$\frac{f_+^{K^+}(0)}{f_+^{K^0}(0)} = 1.022 \quad (229)$$

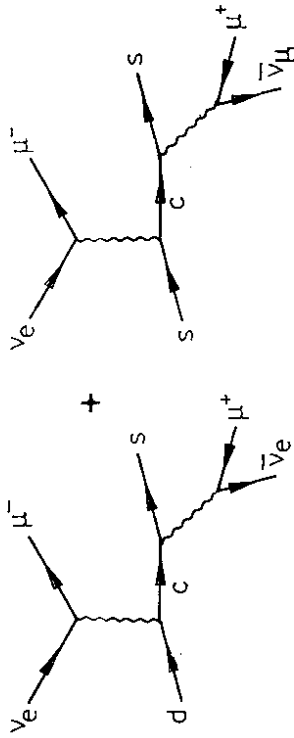


Figure 32: Processes giving rise to opposite sign dimuons in deep inelastic neutrino scattering.

I'll discuss in the next Section, also  $B - \bar{B}$  mixing imposes constraints. The ratio of  $\frac{|V_{cb}|}{|V_{cd}|}$ , which measures  $\rho$ , is determined by semileptonic  $B$  decays. The two contributions to these decays, coming from  $b \rightarrow c l^- \bar{\nu}_l$  and  $b \rightarrow u l^- \bar{\nu}_l$ , can be separated out experimentally, in principle, by the shape of the lepton spectrum near the end point. This is shown in Fig 33, where the various contributions to the lepton spectrum observed by the ARGUS collaboration [56] are depicted. The relative strength of the  $b \rightarrow u$  and  $b \rightarrow c$  transitions, which is denoted by  $R$ , is related to the ratio of  $V_{ub}$  to  $V_{cb}$ .

To actually extract a value for  $\frac{|V_{cb}|}{|V_{cd}|}$  necessitates a calculation of the end point spectrum which, in turn, depends (somewhat) on the bound state model one adopts for the  $B$  mesons. The ratio  $R$ , on the other hand, can be computed in a spectator model where, as shown in Fig 34,  $B$  decays proceeds as a free quark decay. The ratio of total rates, is after all, a very inclusive quantity and the spectator model, which is a partonic approximation, should work well in these circumstances. One has then

$$R = \frac{\Gamma(b \rightarrow u)}{\Gamma(b \rightarrow c)} = \frac{|V_{ub}|^2 \Phi(\frac{m_u}{m_b})}{|V_{cb}|^2 \Phi(\frac{m_c}{m_b})} \quad (238)$$

Here  $\Phi(x)$  is the usual three body phase space factor for the decay of a massive particle, of mass  $M$ , into a light particle, of mass  $m$ , and two massless particles, with  $x = \frac{m}{M}$ :

$$\Phi(x) = 1 - 8x^2 + 8x^6 - 24x^4 \ln x \quad (239)$$

For the case at hand, using  $\frac{m_c}{m_b} \simeq 0.3$ , the ratio of phase space factors in Eq(238) is nearly

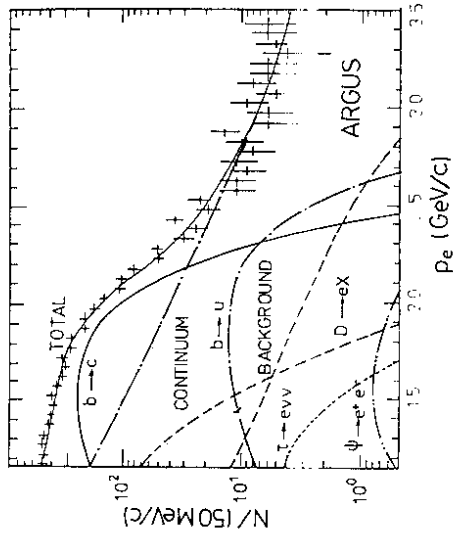


Figure 33: The electron spectrum at the  $\Upsilon(4s)$  observed by the ARGUS collaboration [56].

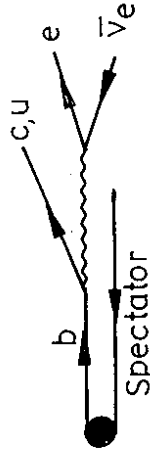


Figure 34:  $B$  decays in the spectator model.

2, so that

$$\frac{|V_{ub}|}{|V_{cb}|} \equiv \lambda \rho \simeq \sqrt{\frac{R}{2}} \quad (240)$$

Present experimental data shows no evidence for a  $b \rightarrow u$  component. This, in turn, implies a bound on  $R$ . This bound is model dependent since to calculate the spectral shape of electrons near the end point:

$$\frac{d\Gamma}{dE_e} = \Gamma(b \rightarrow u) \left| \frac{1}{\Gamma(b \rightarrow u)} \frac{d\Gamma(b \rightarrow u)}{dE_e} \right| + \Gamma(b \rightarrow c) \left| \frac{1}{\Gamma(b \rightarrow c)} \frac{d\Gamma(b \rightarrow c)}{dE_e} \right| \quad (241)$$

one has to make some assumptions on the  $B$ -meson wavefunction, to calculate the individual factors in the square brackets above. What is usually assumed [57], is that the decay rate is no longer totally independent of the spectator in Fig 34. Rather, this particle has some momentum distribution  $\Phi(p) \sim \exp[-\frac{p^2}{p_F^2}]$ , where  $p_F$  is a free parameter. What weak decays then is a virtual  $b$  quark, whose invariant mass depends on  $p$  and the mass of the spectator (another free parameter):

$$W^2 = M_B^2 + m_s^2 - 2M_B \sqrt{p^2 + m_s^2} \quad (242)$$

The free parameters  $m_{sp}$  and  $p_F$  are then fixed by fitting the spectrum of the decay electrons

$$\frac{d\Gamma_B}{dE_e} = \int p^2 dp \Phi(p) \frac{d\Gamma_b}{dE_e} \quad (243)$$

By following this procedure, or analogous steps depending on the detail of the model chosen, the various experimental collaborations arrive at a bound on  $R$ , based on the absence of a  $b \rightarrow u$  signal. The present, rather conservative, bound on  $R$  [58], is

$$R < 0.08 \quad (244)$$

which, using Eq(240), implies

$$\frac{|V_{ub}|}{|V_{cb}|} < 0.20 \quad (245)$$

and

$$\rho < 0.9 \quad (246)$$

Smaller values of  $\rho$ , however, have also been given in the literature. For instance, a recent analysis of the ARGUS data [59] gives  $\frac{|V_{ub}|}{|V_{cb}|} < 0.16$  and  $\rho < 0.73$ .

A lower bound on  $\frac{|V_{ub}|}{|V_{cb}|}$ , and therefore on  $\rho$ , can be inferred from the recent ARGUS observation of charmless  $B$  decays [60]:

$$\begin{aligned} B(B^+ \rightarrow p\bar{p}\pi^+) &= (3.7 \pm 1.3 \pm 1.4) \times 10^{-4} \\ B(B_d^0 \rightarrow p\bar{p}\pi^+\pi^-) &= (6.0 \pm 2.0 \pm 2.2) \times 10^{-4} \end{aligned} \quad (247)$$

These decay modes, however, have been looked for by CLEO and have not been found, at a level of perhaps a factor of 2-3 below that of the ARGUS claim [61]. Thus one must take the result in Eq(247) with a certain degree of caution. Apart from this controversy, which must be settled, it appears that Eq(247) provides the first evidence for a nonzero

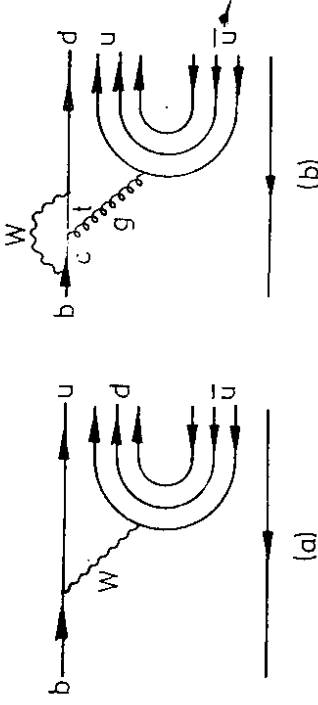


Figure 35: Diagrams contributing to charmless  $B$  decays.

$V_{ub}$ . This assertion is not trivial, since one has to make sure that the results in Eq(247) are not induced by hadronic Penguin diagrams.

There are two sources for the charmless  $B$  decays of Eq(247), as depicted in Fig 35. Either they proceed directly through a  $b \rightarrow u$  transition, or they are induced by a  $b \rightarrow d$  Penguin diagram. The Penguin contribution is (slightly) suppressed, by being a factor of  $O(\frac{m_s}{m_c} \ln \frac{m_c}{m_s})$  down relative to the direct diagram, but is of the same order in electroweak parameters:  $O(A\rho\lambda^3)$ . Thus one must have some additional evidence that the decays in Eq(247) are not Penguin induced. This evidence fortunately exists, since if Penguin effects were dominant one would expect a very large signal for  $B \rightarrow A\bar{p}\pi(\pi)$ . Such a signal has not been observed. Indeed, ARGUS [60] quotes a limit

$$\frac{B(B \rightarrow \Lambda\bar{p}\pi(\pi))}{B(B \rightarrow p\bar{p}\pi(\pi))} < 0.5 \quad (248)$$

If Penguin effects were to have dominated, since the rate associated with the  $b \rightarrow s$  Penguin is enhanced by  $O(\lambda^{-2})$  relative to the  $b \rightarrow d$  Penguin, one would have expected Eq(248) to be of order 20.

It is not easy to translate the ARGUS results into a value for  $\frac{|V_{ub}|}{|V_{cb}|}$ . The collaboration itself gives a conservative bound, as follows. They write

$$B(B \rightarrow p\bar{p}\pi(\pi)) = \frac{|V_{ub}|^2}{|V_{cb}|^2} B(B \rightarrow \text{charmless Baryons}) [P_s \cdot r_{us} \cdot r_B] \quad (249)$$

and then ask that the "fudge factors" in the square bracket be maximized. These terms correspond to:

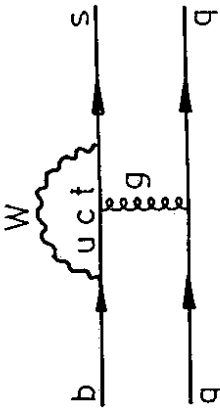


Figure 36: Penguin diagram entering in the  $b \rightarrow s g \bar{g}$  decay.

- A factor,  $P_s$ , which takes into account of the fact that the phase space for the  $b \rightarrow s$  decay is bigger. Using a quark model estimate,  $P_s \simeq 2$  as we have argued earlier [cf. Eq(240)].
- A factor  $r_{us}$  to account for the percentage of baryonic decay modes that are actually seen. ARGUS, assumes, that this is at most 10 %.
- A recombination factor, which takes into account the increase in probability that baryons are made after a  $b \rightarrow u$  transition, relative to what happens after a  $b \rightarrow c$  transition. Here what is assumed in [60] is that  $r_B \simeq 2$ .

In addition, one must make some assumption on the what is the biggest total charmed baryon rate that one can reasonably allow. ARGUS takes this as 25 %. Putting all these numbers together, then a branching ratio  $B(B \rightarrow p \bar{p} \pi(\pi)) \simeq 5 \times 10^{-4}$  implies lower bounds on  $\frac{|V_{ub}|}{|V_{cb}|}$  and  $\rho$  of [60]

$$\frac{|V_{ub}|}{|V_{cb}|} > 0.07; \quad \rho > 0.3 \quad (250)$$

One can obtain roughly the same kind of estimate for  $\rho_{\min}$ , by making use of the Penguin bound of Eq(248) [62]. The Penguin graph of Fig 36 gives rise to an effective Lagrangian which is analogous to the one which I computed when considering the photonic contribution to  $\nu_\mu e$  scattering. The only difference here is that the electric charge is now replaced by the color charge. In Fig 36 the  $u$ -quark loop is irrelevant, since  $V_{ub} V_{us}^* \sim 0(\lambda^4)$ . Furthermore, all dependence on  $\ln M_W$  disappears since the contribution of the  $t$ -quark loop  $[\sim V_{tb} V_{ts}^* = -A\lambda^2]$  cancels against that of the  $c$ -quark loop  $[\sim V_{cb} V_{cs}^* = A\lambda^2]$ . By straightforward calculation, one finds

$$L_{eff} = \frac{G_F}{\sqrt{2}} \left[ \frac{\alpha_s}{12\pi} A\lambda^2 \ln \frac{m_t^2}{m_c^2} \right] \left\{ |s\gamma^r(1 - \gamma_5)\delta| \sum_q \bar{q}\gamma_\mu \lambda_a q \right\} \quad (251)$$

In the above  $\lambda_a$  are the color matrices.

To get a lower bound on  $\rho$ , one needs an estimate of the contribution of the operator in curly brackets in Eq(251) to the decay matrix element for  $B \rightarrow \Lambda \bar{p} \pi(\pi)$ . At the most naive level, one can assume that this operator contributes the same as that appearing in the CC Lagrangian responsible for the decay of  $B \rightarrow p \bar{p} \pi(\pi)$ :

$$L^{CC} = \frac{G_F}{\sqrt{2}} [A\rho\lambda^3 \epsilon^{\delta\delta}] \left\{ |\bar{u}\gamma^r(1 - \gamma_5)\delta| [\bar{d}\gamma_\mu(1 - \gamma_5)u] \right\} \quad (252)$$

Then the ARGUS bound of Eq(248) implies a lower bound on  $\rho$ . One has

$$\frac{B(B \rightarrow \Lambda \bar{p} \pi(\pi))}{B(B \rightarrow p \bar{p} \pi(\pi))} \simeq \frac{|\frac{\alpha_s}{12\pi} A\lambda^2 \ln \frac{m_t^2}{m_c^2}|^2}{|A\lambda^3 \rho|^2} \quad (253)$$

which, using  $\alpha_s(m_b) \simeq 0.2$ ,  $m_t = 45 G e V$ , requires

$$\rho > 0.25. \quad (254)$$

which is comparable to the ARGUS limit of Eq(250).

To summarize the situation on  $\rho$  is as follows. Conservative limits on  $\rho$  put in the range:

$$0.3 < \rho < 0.9 \quad (255)$$

However, the lower limit is soft. If one believes in the ARGUS result of Eq(247), then probably  $\rho_{\min}$  could be bigger. On the other hand, the experimental result of ARGUS [60] is not supported by CLEO data [61]. Thus  $\rho_{\min}$  could also be smaller! The upper limit in eq(255) is probably too generous. Indeed, as we have indicated earlier, different analyses [59] arrive at stronger bounds for the values of  $\frac{|V_{ub}|}{|V_{cb}|}$ . I shall, nevertheless, in what follows imagine that  $\rho$  lies in the range of Eq(255), with my own working guesstimate being that  $\rho \simeq 0.6$ .

The lifetime of the  $B$  mesons, along with a measurement of the semileptonic branching ratio, can be used to estimate the parameter  $A$  which enters in CKM matrix. By definition one has

$$\tau_B^{-1} B(B \rightarrow l\nu_l X) = \Gamma(B \rightarrow l\nu_l X) \equiv \Gamma(b \rightarrow c) [1 + R] \quad (256)$$

The left hand side of this equation contains quantities that are measured and  $\Gamma(b \rightarrow c) \sim |V_{cb}|^2 \sim A^2$ . However, to extract a precise value for  $A$  one needs a good estimate of  $\Gamma(b \rightarrow c)$ . I have argued earlier that the spectator model should provide a dynamically adequate framework for calculating this rate. Unfortunately, the formula for  $\Gamma(b \rightarrow c)$  in the spectator model has another unknown beside  $A$ , namely the mass of the decaying b-quark:

$$\Gamma(b \rightarrow c)_{\text{spectator}} = \frac{G_F^2 m_b^5}{192\pi^3} \Phi\left(\frac{m_c}{m_b}\right) |V_{cb}|^2 \quad (257)$$

From Eq(257) one sees that a 10% uncertainty in  $m_b$  implies a 25 % error in  $V_{cb}$  and in  $A$ .

To avoid this large uncertainty associated with  $m_b$ , one can go back to the simple bound state model I discussed earlier [57]. In this model, after one fixes the free parameters  $m_{sp}$  and  $p_F$  by fitting the electron spectrum, then  $\Gamma(b \rightarrow c)$  is very much better determined,



since it depends only on  $M_B$ . For example, a recent analysis of Altarelli and Franzini [63] along these lines, finds

$$\Gamma(b \rightarrow c) = (4 \pm 0.6) \times 10^{13} \text{ sec}^{-1} |V_{cb}|^2 \quad (258)$$

which corresponds to an effective  $m_b$  mass, with a tiny error:  $m_b^{\text{eff}} = 4.70 \pm 0.13 \text{ GeV}$ . Using the average value of  $\tau_B$  [64] [ $\tau_B = (1.11 \pm 0.16) \times 10^{-12} \text{ sec}$ ] and of the semileptonic branching ratio [50] [ $B = 0.117 \pm 0.006$ ], Altarelli and Franzini [63] find <sup>20</sup>:

$$A = 1.05 \pm 0.17 \quad (259)$$

## 5 Particle-Antiparticle Mixing and CP Violation

All the real parameters  $\lambda, \rho$  and  $A$  in the CKM matrix are now fixed, as best as it is presently possible [cf. Eqs(233), (255) and (259)]. It remains to constrain the phase  $\delta$ . This parameter enters in the CP violating phenomena observed in Kaon decay. Furthermore, since  $V_{td} \simeq A\lambda^3(1 - \rho e^{i\delta})$ , a precise measurement of  $V_{td}$  has implications for  $\delta$ . Such a measurement is afforded by the observation of  $B_d - \bar{B}_d$  oscillations. In this section, therefore, I want to discuss both these topics.

### 5.1 Two State Formalism

Before I enter into these topics proper, it is useful to briefly discuss the formalism associated to a particle-antiparticle system (e.g.  $K^0 - \bar{K}^0$ ;  $B_d - \bar{B}_d$ ; etc) which are connected by the weak interactions. I shall denote the particle and antiparticle states, generically, by  $P$  and  $\bar{P}$ . Because, by assumption, there exist transition and decay channels which connect  $P$  and  $\bar{P}$ ; this two state system can be described by an effective Hamiltonian which is complex

$$H \begin{pmatrix} P \\ \bar{P} \end{pmatrix} = (M - i\Gamma) \begin{pmatrix} P \\ \bar{P} \end{pmatrix} \quad (260)$$

In the above, the mass matrix,  $M$ , and the decay matrix,  $\Gamma$ , are Hermitian

$$M = M^\dagger; \quad \Gamma = \Gamma^\dagger \quad (261)$$

Furthermore, the CPT theorem [66] implies that the diagonal elements of  $M$  and  $\Gamma$  are equal. Thus

$$M = \begin{pmatrix} m & M_{12} \\ M_{12}^* & m \end{pmatrix}; \quad \Gamma = \begin{pmatrix} \gamma & \Gamma_{12} \\ \Gamma_{12}^* & \gamma \end{pmatrix} \quad (262)$$

The presence of non vanishing phases in the off diagonal elements of  $M$  and  $\Gamma$  signifies CP violation [66].

Diagonalizing the  $2 \times 2$  Hamiltonian of Eq(260) one obtains the eigenstates  $|P_\pm\rangle$  of the two state system

$$|P_\pm\rangle \equiv \frac{1}{[2(1 + |\epsilon_P|^2)]^{1/2}} [(1 + \epsilon_P)|P\rangle \pm (1 - \epsilon_P)|\bar{P}\rangle] \quad (263)$$

<sup>20</sup>This number is consistent with that obtained in a new analysis of C.S. Kim [65], who, however, uses the new smaller experimental value of  $B = 0.10 \pm 0.1$  [59].

where

$$\frac{1 - \epsilon_P}{1 + \epsilon_P} = \left( \frac{M_{12} - \frac{i}{2}\Gamma_{12}^*}{M_{12} - \frac{i}{2}\Gamma_{12}} \right)^{1/2} \quad (264)$$

Clearly  $\epsilon_P \rightarrow 0$  if  $M_{12}$  and  $\Gamma_{12}$  are real, so that  $\epsilon_P$  is a measure of CP violation in the system. In the limit of good CP, then the states  $|P_\pm\rangle$  are CP eigenstates:

$$CP|P_\pm\rangle = \mp|P_\pm\rangle \quad (265)$$

The masses and widths of the eigenstate  $|P_\pm\rangle$  involve a quantity

$$Q = \left( (M_{12} - \frac{1}{2}\Gamma_{12}) \left( M_{12}^* - \frac{i}{2}\Gamma_{12}^* \right) \right)^{1/2} \quad (266)$$

and one has

$$m_\pm = m \pm Re Q; \quad \Gamma_\pm = \gamma \mp 2Im Q \quad (267)$$

The physical states  $|P_\pm\rangle$  have a well defined time dependence:

$$|P_\pm(t)\rangle = e^{-im_\pm t} e^{-\frac{\Gamma_\pm}{2}t} |P_\pm(0)\rangle \quad (268)$$

However, a state produced at  $t = 0$  as  $|P\rangle$  (or as  $|\bar{P}\rangle$ ), will be a superposition of  $|P\rangle$  and  $|\bar{P}\rangle$  at later times. That is, a state  $|P\rangle$  will oscillate into a state  $|\bar{P}\rangle$ . For a state born at  $t = 0$  as a  $|P\rangle$  one finds, at later times,

$$|P_{\text{phys}}(t)\rangle = f_+(t)|P\rangle + f_-(t) \left( \frac{1 - \epsilon_P}{1 + \epsilon_P} \right) |\bar{P}\rangle \quad (269)$$

where

$$f_+(t) = e^{-im t} e^{-\frac{\gamma}{2}t} \cos\left[ \left( \frac{\Delta m}{2} - i \frac{\Delta\Gamma}{4} \right) t \right] \quad (270)$$

and

$$f_-(t) = i e^{-im t} e^{-\frac{\gamma}{2}t} \sin\left[ \left( \frac{\Delta m}{2} - i \frac{\Delta\Gamma}{4} \right) t \right] \quad (271)$$

Here  $\Delta m = m_+ - m_-$ ;  $\Delta\Gamma = \Gamma_+ - \Gamma_-$ .

### 5.2 CP violation and $\epsilon$

In the Kaon system,  $|P_+\rangle \leftrightarrow |K_L\rangle$  and  $|P_-\rangle \leftrightarrow |K_S\rangle$ . If CP were absolutely conserved, then the decay  $K_L \rightarrow \pi^+\pi^-$  would be entirely forbidden, since  $CP|\pi^+\pi^-\rangle = |\pi^+\pi^-\rangle$ . In fact this decay, along with the  $\pi^0\pi^0$  decay mode of the  $K_L$ , has been seen. The two measured CP violating parameters  $\eta_{+-}$  and  $\eta_{00}$ , or  $\epsilon$  and  $\epsilon'$ , characterize the ratio of the decay amplitudes for  $K_L$  and  $K_S$  mesons [67]:

$$\eta_{+-} = \frac{A(K_L \rightarrow \pi^+\pi^-)}{A(K_S \rightarrow \pi^+\pi^-)} \simeq \epsilon + \epsilon' \quad (272)$$

$$\eta_{00} = \frac{A(K_L \rightarrow \pi^0\pi^0)}{A(K_S \rightarrow \pi^0\pi^0)} \simeq \epsilon - 2\epsilon' \quad (273)$$

Experimentally, it has been known for a long time that the magnitude of the above ratios are very nearly the same and [50]

$$|\eta_{+-}| \simeq |\eta_{00}| \simeq |\epsilon| = (2.28 \pm 0.02) \times 10^{-3} \quad (274)$$

Very recently the NA31 experiment at CERN has obtained the first indications of a nonzero value for  $\epsilon'$  [68].

$$\frac{\epsilon'}{\epsilon} = (3.5 \pm 1.1) \times 10^{-3} \quad (275)$$

The latest results from the Chicago Saclay experiment at Fermilab [69] are also consistent with a nonzero  $\epsilon'$ , but their result is not yet significant.

It is straightforward to relate the measured quantities  $\epsilon$  and  $\epsilon'$  to the CP violating contributions arising from the CKM model [70]. It is usual to define the decay amplitude for a  $K^0$  into a  $2\pi$  state of definite isospin  $I$  ( $I = 0, 2$ ) as

$$\langle \pi\pi; I | H_{\text{weak}} | K^0 \rangle = A_I e^{i\delta_I} \quad (276)$$

Here  $\delta_I$  is the strong interaction phase shift of the outgoing pions. The decay amplitude for a  $\bar{K}^0$  would be the same, if CP were conserved, while if CP is not conserved, then  $A_I \rightarrow A_I'$ :

$$\langle \pi\pi; I | H_{\text{weak}} | \bar{K}^0 \rangle = A_I' e^{i\delta_I'} \quad (277)$$

Using the above, along with the identification of  $|K_L\rangle$  and  $|K_S\rangle$  with  $|P_+\rangle$  and  $|P_-\rangle$  and the definitions of  $\epsilon$  and  $\epsilon'$  of Eq(272) and (273), results in the following formulas for  $\epsilon$  and  $\epsilon'$  [70]<sup>21</sup>

$$\epsilon = \epsilon_K + i \frac{\text{Im } A_0}{\text{Re } A_0} \quad (278)$$

$$\epsilon' = \frac{1}{\sqrt{2}} \epsilon^{i(\delta_2 - \delta_0 + \frac{\pi}{2})} \frac{\text{Re } A_2}{\text{Re } A_0} \left\{ \frac{\text{Im } A_2}{\text{Re } A_2} - \frac{\text{Im } A_0}{\text{Re } A_0} \right\} \quad (279)$$

In the Kaon system one finds experimentally that  $(\Delta m)_K \simeq -\frac{1}{2}(\Delta\Gamma)_K$  [50]. This implies that the quantity  $Q_K$ , defined in Eq(266) is just

$$Q_K = \frac{1}{2}(\Delta m - \frac{i}{2}\Delta\Gamma)_K \simeq \frac{\epsilon^{\frac{\pi}{4}}}{\sqrt{2}}(\Delta m)_K \quad (280)$$

Furthermore, since the CP violating effects are small, one can approximate

$$(\Delta m)_K \simeq 2\text{Re}(M_{12}) \quad (281)$$

Using the above two equations, and working only to lowest order in significant quantities, a simple calculation starting from the definition of Eq(264), yields

$$\epsilon_K \simeq \frac{\epsilon^{\frac{\pi}{4}}}{\sqrt{2}} \frac{\text{Im } M_{12}}{(\Delta m)_K} - \frac{\epsilon^{-\frac{\pi}{4}}}{\sqrt{2}} \frac{\text{Im } \Gamma_{12}}{(\Delta\Gamma)_K} \quad (282)$$

However, saturating the decay rates by the  $2\pi$  intermediate state [70] one has

$$\frac{\text{Im } \Gamma_{12}}{(\Delta\Gamma)_K} = -\frac{\text{Im } A_0}{\text{Re } A_0} \quad (283)$$

<sup>21</sup>I have dropped, in these formulas, nonleading  $\Delta I = 1/2$  suppressed terms of  $O(\frac{\text{Re } A_2}{\text{Re } A_0})$ .

Hence, putting everything together, one arrives at the following formula for  $\epsilon$

$$\epsilon \simeq \frac{1}{\sqrt{2}} \epsilon^{\frac{\pi}{4}} \left\{ \frac{\text{Im } M_{12}}{(\Delta m)_K} + \frac{\text{Im } A_0}{\text{Re } A_0} \right\} \quad (284)$$

Although the expressions for  $\epsilon$  and  $\epsilon'$ , Eqs(284) and (279), are convention independent, one can pick phase conventions to eliminate individual pieces in these formulas. For instance, in the Wu-Yang convention [71], one chooses  $\text{Im } A_0 = 0$ , thereby making the formula for  $\epsilon$  depend only on the mass matrix. In the standard model, however, this convention is not so natural, since at the quark level it is the  $\Delta I = 1/2$  amplitude  $A_0$  which has an imaginary part. Thus in what follows I shall adopt the quark phase convention, where  $\text{Im } A_2 = 0$ , and shall denote by  $\xi$  the ratio

$$\xi = \frac{\text{Im } A_0}{\text{Re } A_0} \quad (285)$$

Using the experimental ratio for the  $\Delta I = 3/2$  to  $\Delta I = 1/2$  amplitudes,  $\frac{\text{Re } A_2}{\text{Re } A_0} \simeq 0.05$ , Eqs(284) and (279) simplify to

$$\epsilon \simeq \frac{\epsilon^{\frac{\pi}{4}}}{\sqrt{2}} \left\{ \frac{\text{Im } M_{12}}{2\text{Re } M_{12}} + \xi \right\} \quad (286)$$

$$\epsilon' \simeq \frac{\epsilon^{i(\frac{\pi}{2} + \delta_2 - \delta_0)}}{\sqrt{2}} \left\{ -\frac{\xi}{20} \right\} \quad (287)$$

Remarkably, using the values of the  $\pi\pi$  phase shifts of [72] the phase factor in Eq(287) is also very close to  $\frac{\pi}{4}$ , so that the phase of  $\epsilon'$  is nearly the same as that of  $\epsilon$ . Using the value obtained by the NA31 collaboration for  $\frac{\epsilon'}{\epsilon}$ , Eq(275), implies  $|\xi| \simeq 0.1|\epsilon|$ . Hence, the second contribution in Eq(286) is a negligible correction and I shall neglect it, henceforth.

To calculate  $\epsilon$ , one needs to calculate the imaginary part of  $M_{12}$ . At the quark level, this is given by the imaginary part of the box diagram shown in Fig 37, which graphically depicts how by a  $2^{\text{nd}}$  order weak process one can transit from a  $K^0$  to a  $\bar{K}^0$ . I shall show below that the box graph contribution is equivalently described by an effective 4-Fermi interaction Lagrangian for the  $\Delta S = 2$  transition of the form [73]

$$\mathcal{L}_{\epsilon'/\epsilon}^{\Delta S=2} = A_{\text{box}} |\bar{d}\gamma^\mu (1 - \gamma_5)s| |\bar{d}\gamma_\mu (1 - \gamma_5)s| \quad (288)$$

The coefficient  $A_{\text{box}}$ , does not contain any dominant  $\ln M_W$  terms, because of the unitarity of the CKM matrix. However, it is a function of the parameters entering in this matrix.

To demonstrate that the box graph of Fig 37 is equivalent to having the interaction Lagrangian of Eq(288), it suffices to evaluate the box graph in the figure at zero external momentum. The associated amplitude, evaluated in the physical gauge for the vector bosons, is:

$$A_{\epsilon'/\epsilon} = -\frac{i}{2} \frac{\epsilon}{2\sqrt{2} \sin \Theta_W} \left( \frac{1}{i} \right)^4 \int \frac{d^4 q}{(2\pi)^4} \left\{ \frac{[\eta_{\mu\alpha} + \frac{9u^2 q_\alpha}{M_W^2}] [\eta_{\nu\beta} + \frac{9u^2 q_\beta}{M_W^2}]}{(q^2 + M_W^2)^2} \right\} \left\{ \sum_{ij} \lambda_i |\gamma^{\mu\nu} (1 - \gamma_5) \frac{(-\gamma q + m_i)}{q^2 + m_i^2} \gamma^\nu (1 - \gamma_5) \right\} \lambda_j |\gamma^\beta (1 - \gamma_5) \frac{(-\gamma q + m_j)}{q^2 + m_j^2} \gamma^\alpha (1 - \gamma_5)| \quad (289)$$

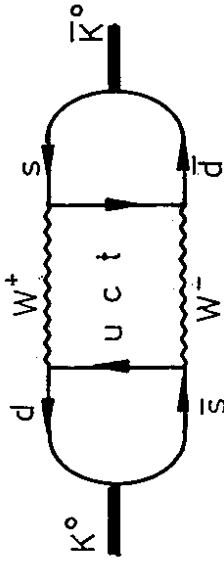


Figure 37: Box graph contributing to the 2<sup>nd</sup> order weak transition from a  $K^0$  to a  $\bar{K}^0$ .

In the above the factor of  $\frac{1}{2}$  is a combinatoric factor, while the factors in the first square brackets are associated with the vertices and propagators in the graph. Furthermore,  $\lambda_i$  is short hand for the product of CKM matrix elements:

$$\lambda_i = V_{is}^* V_{id} \quad (290)$$

Obviously, the unitarity of the CKM matrix implies that

$$\lambda_u + \lambda_c + \lambda_t = 0 \quad (291)$$

Using this constraint, one can eliminate  $\lambda_u$  entirely from the above. Thus one can rewrite the 2<sup>nd</sup> curly bracket in Eq(289) as <sup>22</sup>:

$$\begin{aligned} \{2\}^{\mu\nu\beta\alpha} &= 4[\gamma^\mu \gamma^\nu (1 - \gamma_5)] [\gamma^\beta \gamma^\alpha (1 - \gamma_5)] \\ &\cdot \left\{ \lambda_c^2 \left[ \frac{1}{(q^2 + m_c^2)^2} - \frac{2}{q^2(q^2 + m_c^2)} + \frac{1}{(q^2)^2} \right] + \lambda_t^2 \left[ \frac{1}{(q^2 + m_t^2)^2} - \frac{2}{q^2(q^2 + m_t^2)} + \frac{1}{(q^2)^2} \right] \right. \\ &\left. + 2\lambda_c \lambda_t \left[ \frac{1}{(q^2 + m_c^2)(q^2 + m_t^2)} - \frac{1}{q^2(q^2 + m_c^2)} - \frac{1}{q^2(q^2 + m_t^2)} + \frac{1}{(q^2)^2} \right] \right\} \quad (292) \end{aligned}$$

Because of the unitarity of the CKM matrix, the divergent contributions of the individual graphs are now turned into very convergent factors. A little algebra transforms the product of the two curly brackets in the integrand in Eq(289) to

$$\begin{aligned} \{1\} \cdot \{2\} &= 4 \frac{[\gamma^\mu (1 - \gamma_5)] [\gamma_\mu (1 - \gamma_5)]}{M_W^4} \left\{ 1 - \frac{3(q^2)^2}{4(q^2 + M_W^2)^2} \right\} \left\{ \lambda_c^2 \frac{m_c^4}{q^2(q^2 + m_c^2)^2} \right. \\ &\left. + \lambda_t^2 \left[ \frac{m_c^4}{q^2(q^2 + m_c^2)^2} \right] + 2\lambda_c \lambda_t \left[ \frac{m_c^2 m_t^2}{q^2(q^2 + m_c^2)(q^2 + m_t^2)} \right] \right\} \quad (293) \end{aligned}$$

<sup>22</sup>We have set  $m_c^2 = 0$  here.

The factor above which contains a  $(q^2 + M_W^2)^2$  contribution, for  $m_q \ll M_W$  will give corrections of  $O(\frac{m_q^2}{M_W^2})$ . Thus it is irrelevant except for top. I will ignore it in the discussion below, but shall restate the corrections due to this term in the final answer. Using Eq(293), it is clear that the integral over  $d^4q$  in Eq(289) is very convergent. Evaluating this integral yields a result for the amplitude  $A_{eff}$  which is precisely of the form expected from the effective Lagrangian of Eq(288), and one identifies:

$$A_{box} = \frac{G_F^2}{16\pi^2} [\lambda_c^2 m_c^2 + \lambda_t^2 m_t^2 + 2\lambda_c \lambda_t m_c^2 \ln \frac{m_c^2}{m_t^2}] \quad (294)$$

For  $\epsilon$ , since it is proportional to  $Im M_{12}$ , we need to consider the imaginary part of the effective Lagrangian of Eq(288). Using the form of the Cabibbo Kobayashi Maskawa matrix given in Eq(200) one has

$$\begin{aligned} Im \lambda_c^2 &= -2A^2 \lambda^6 \rho \sin \delta \\ Im \lambda_t^2 &= 2A^4 \lambda^{10} \rho \sin \delta (1 - \rho \cos \delta) \\ 2Im \lambda_c \lambda_t &= 2A^2 \lambda^6 \rho \sin \delta \end{aligned} \quad (295)$$

Hence

$$\begin{aligned} \mathcal{L}_{eff}^{CP \text{ viol}} &= \frac{G_F^2}{8\pi^2} [A^2 \lambda^6 \rho \sin \delta] [m_c^2 (-1 + \ln \frac{m_c^2}{m_t^2}) + A^2 \lambda^4 (1 - \rho \cos \delta) m_t^2] \\ &\cdot [(\bar{d}\gamma^\mu (1 - \gamma_5) s)(\bar{d}\gamma_\mu (1 - \gamma_5) s)] \end{aligned} \quad (296)$$

We note that:

- The CP violating contribution of Eq(296) is suppressed by the high power of  $\lambda$  entering in its common coefficient  $[A^2 \rho \lambda^6 \sin \delta]$ . This already "explains" why  $\epsilon$  is so small.

- The two terms in the second square bracket are comparable numerically if  $m_t > 45 GeV$ , even though the  $t$ -quark contribution is quite Cabibbo suppressed  $[\lambda^4]$ .

To calculate  $\epsilon$  we need to compute the contribution of  $\mathcal{L}_{eff}^{CP \text{ viol}}$  between a  $|K^0\rangle$  and a  $|\bar{K}^0\rangle$  state. One has:

$$\epsilon^{-\frac{1}{4}} \epsilon = \frac{1}{\sqrt{2}(\Delta m)_K} \langle K^0 | Im M_{12} | \bar{K}^0 \rangle = -\frac{1}{\sqrt{2}(\Delta m)_K} \langle K^0 | \mathcal{L}_{eff}^{CP \text{ viol}} | \bar{K}^0 \rangle \quad (297)$$

Unfortunately, it is not possible yet to compute the above hadronic matrix element accurately. What is done, usually, is to replace the quark matrix element in Eq(297) by

$$\langle K^0 | (\bar{d}\gamma^\mu (1 - \gamma_5) s) (\bar{d}\gamma_\mu (1 - \gamma_5) s) | \bar{K}^0 \rangle = -\frac{8}{3} f_K^2 M_K^2 B_K \quad (298)$$

Apart from  $B_K$ , this is the result one would have obtained by inserting  $|0\rangle \langle 0|$  in the above, using the definition of the Kaon decay constant ( $f_K \simeq 160 MeV$ ):

$$\langle K^0 | (\bar{d}\gamma^\mu \gamma_5 s) | 0 \rangle = i f_K p_\mu \quad (299)$$

and taking into account of color factors [74]. The uncertainty in the hadronic matrix element resides then in  $B_K$ , with  $B_K = 1$  - obviously - representing the vacuum insertion approximation. Although  $B_K$  is not really calculable, present day estimates for  $B_K$  [75] put it in the range

$$0.3 \leq B_K \leq 1 \quad (300)$$

I quote below the final formula for  $\epsilon$ , which uses the results derived above, but includes also some kinematical correction factors connected with terms of  $O(y_t = \frac{m_t}{M_K})$ , which may not be negligible if top is not light [76]. This formula, in addition, contains parameters  $\eta_i$  which are short distance QCD corrections to the effective Lagrangian of Eq(296) [77] ( $\eta_1 \simeq 0.7$ ;  $\eta_2 \simeq 0.6$ ;  $\eta_3 \simeq 0.4$ ),

$$\begin{aligned} \epsilon^{-\frac{1}{2}} \epsilon = & \frac{G_F^2 f_K^2 M_K}{6\sqrt{2}\pi^2(\Delta m)_K} B_K (A^2 \rho \lambda^6 \sin \delta) \left\{ m_c^2 [-\eta_1 + \eta_3 (\ln \frac{m_t^2}{m_c^2} + f_3(y_t))] \right. \\ & \left. + m_t^2 [\eta_2 f_2(y_t) A^2 \lambda^4 (1 - \rho \cos \delta)] \right\} \end{aligned} \quad (301)$$

Here  $f_2$  and  $f_3$  are weakly dependent functions of the top quark mass

$$f_2(y_t) = 1 - \frac{3y_t(1+y_t)}{4(1-y_t)^2} \left[ 1 + \frac{2y_t}{1-y_t} \ln y_t \right], \quad (302)$$

$$f_3(y_t) = -\frac{3y_t}{4(1-y_t)} \left[ 1 + \frac{y_t}{1-y_t} \ln y_t \right] \quad (303)$$

### 5.3 Penguin Operators and $\epsilon'$

Before I analyze the formula for  $\epsilon$ , I want to discuss the origin for  $\epsilon'$  in the standard model. I mentioned earlier, that in the standard model-adopting the natural quark phase convention - there is only an imaginary part for  $A_0$  and not  $A_2$ . That is, there is a complex weak contribution to transitions involving a change in strong isospin equal to  $\frac{1}{2}$ , but not  $\frac{3}{2}$ . Since

$$\epsilon' \sim Im < 2\pi | \mathcal{L}_{\text{weak}}^{\Delta S=1} | K^0 > \quad (304)$$

one must find complex contributions to the  $\Delta S = 1$  weak Lagrangian and show that, indeed, they affect only  $A_0$ . This is actually very easy to see, since the leading contribution in Eq(304) is that provided by the Penguin operator of Fig 38. Since this is a pure  $d \rightarrow s$  transition, one has obviously a pure  $\Delta I = \frac{1}{2}$  contribution.

Most of the work needed for the computation of the Penguin diagrams has already been done. We know already the  $\ln \frac{M_W^2}{m_c^2}$  behaviour of the individual graphs. Furthermore, I have given an example earlier of the cancellations that ensue, due to CKM unitarity, for the case of Penguins in B decay [cf Eq(251)]. For the Penguin diagrams of Fig 38, the relevant logarithmic terms are given by

$$P \sim \sum_i \lambda_i \ln \frac{M_W^2}{m_i^2} = \lambda_t \ln \frac{m_c^2}{m_t^2} + \lambda_u \ln \frac{m_c^2}{m_u^2} \quad (305)$$

where I have used Eq(291) to eliminate  $\lambda_c$ . Since  $\lambda_u$  is purely real, the contribution to  $\epsilon'$  arises only from the imaginary part of  $\lambda_t$ :

$$\lambda_t \simeq -A\lambda^5(1 - \rho e^{-i\delta}) \leftrightarrow Im \lambda_t = -A\lambda^5 \rho \sin \delta \quad (306)$$

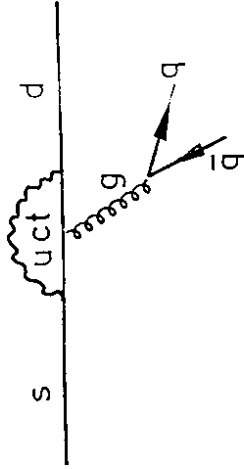


Figure 38: Penguin diagram giving rise to a  $\Delta I = \frac{1}{2}$  CP violating contribution.

One finds, for the CP violating effective Lagrangian [78]:

$$\mathcal{L}_{\text{Penguin}}^{CP \text{ viol}} = \frac{G_F}{\sqrt{2}} |A^2 \rho \lambda^5 \sin \delta| \frac{\alpha_s}{12\pi} \ln \frac{m_t^2}{m_c^2} \{ (\bar{s} \gamma^\mu (1 - \gamma_5) \lambda_c d) \sum_q (\bar{q} \gamma_\mu \lambda_q q) \} \quad (307)$$

This expression is slightly modified by QCD corrections [79] and by  $y_t = \frac{m_t^2}{M_W^2}$  effects. The net result of incorporating these modifications is to replace the  $2^{nd}$  function in the square brackets in Eq(307) by an effective coefficient  $C_P$ :

$$\frac{\alpha_s}{12\pi} \ln \frac{m_t^2}{m_c^2} \rightarrow C_P = 0.085 \pm 0.035 \quad (308)$$

The numerical value above is that estimated by a recent analysis of these effects by Altarelli and Franzini [80].

To calculate  $\epsilon'$ , according to Eq(287), one needs to calculate the ratio  $\xi$  of  $Im A_0$  to  $Re A_0$ . Calling the operator in the curly brackets in Eq(307)  $O_P$ , one has

$$Im A_0 = - < \pi \pi; I = 0 | \mathcal{L}_{\text{Penguin}}^{CP \text{ viol}} | K^0 > = - |A^2 \rho \lambda^5 \sin \delta| < \pi \pi; I = 0 | \frac{G_F}{\sqrt{2}} \lambda C_P O_P | K^0 > \quad (309)$$

On the other hand,  $Re A_0$  is just given by the matrix element of the  $\Delta S = 1$  current-current Lagrangian:

$$Re A_0 = - < \pi \pi; I = 0 | \frac{G_F}{\sqrt{2}} \lambda \bar{s} \gamma^\mu (1 - \gamma_5) u \bar{u} \gamma_\mu (1 - \gamma_5) d | K^0 > \quad (310)$$

Using Eqs(309) and (310) and Eq(287), one finds

$$\begin{aligned} \epsilon' &= -\frac{1}{\sqrt{2}} \frac{1}{20} |e^{i(\frac{\delta}{2} + \delta_2 - \delta_0)} \xi| \\ &= -0.032 e^{i(\frac{\delta}{2} + \delta_2 - \delta_0)} |A^2 \rho \lambda^5 \sin \delta| |H| \end{aligned} \quad (311)$$

Here  $H$  contains the ratio of the hadronic matrix elements entering in Eq(309) and (310):

$$H = \frac{\langle \pi\pi; I = 0 | C_P O_P | K^0 \rangle}{\langle \pi\pi; I = 0 | \bar{s}\gamma^\mu(1 - \gamma_5)u\bar{u}\gamma^\mu(1 - \gamma_5)d | K^0 \rangle} \quad (312)$$

Several remarks are in order:

1. Independent of a precise evaluation of  $H$ , one sees that  $\epsilon'$  is numerically small, both because of the  $\Delta I = \frac{1}{2}$  suppression factor of 0.032 and as a result of the high powers of  $\lambda$  entering in its coefficient  $[A^2\rho\lambda^4 \sin\delta]$ .
2. The hadronic matrix element ratio  $H$  is slightly dependent on  $m_t$  through  $C_P$ . However, here the dependence is only logarithmic. Unfortunately this ratio is theoretically quite poorly estimated. For instance, the recent analysis of Altarelli and Franzini [80] gives the range

$$-0.43 \leq H \leq -0.03 \quad (313)$$

3. The sign of Eq(313) implies that the quantity multiplying the phase factor in  $\epsilon'$  is positive, so that  $\epsilon' > 0$ . This sign agrees with that determined experimentally by the NA31 collaboration [68]. It is also in accord with some general arguments of Hagelin [81].

Unfortunately, given the large uncertainty in  $H$ , in my opinion the beautiful measurement of  $\epsilon'$  does little to determine the phase  $\delta$ . However, the NA31 result [68], Eq(275), is **perfectly consistent** with the standard model. For instance, if one uses the central values for  $\lambda$ ,  $A$ ,  $\rho$  and  $H$  [ $\lambda = 0.22$ ,  $A = 1.05$ ,  $\rho = 0.6$ ,  $H = 0.23$ ] one finds

$$|\epsilon'| = 1.9 \times 10^{-5} \sin\delta \quad (314)$$

while, experimentally, using Eqs(274) and (275) one has

$$|\epsilon'|_{\text{exp}} = (0.8 \pm 0.3) \times 10^{-5} \quad (315)$$

To get an estimate of the phase  $\delta$ , it is much better to use  $\epsilon$  and the recent new information on  $B_d - \bar{B}_d$  oscillations, to which I now turn.

### 5.4 $B_d - \bar{B}_d$ Mixing

I discussed earlier how through 2nd order weak effects a particle-antiparticle transmutation can occur. A state which starts originally as a  $B^0$  can, via mixing, become in time a superposition of  $B^0$  and  $\bar{B}^0$  states [cf. Eq. (269)]:

$$|B_{\text{phys}}^0(t)\rangle = f_+(t)|B^0\rangle + f_-(t)\left(\frac{1 - \epsilon_B}{1 + \epsilon_B}\right)|\bar{B}^0\rangle \quad (316)$$

<sup>23</sup>Recall that the phases in  $\epsilon'$  and  $\epsilon$  are approximately the same.

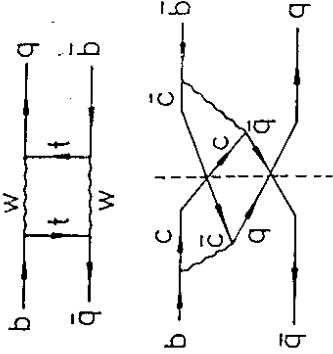


Figure 39: Mass and decay mixing in the  $B - \bar{B}$  complex.

where  $f_{\pm}(t)$  are given in Eqs(270) and (271). For  $B$  mesons the mass matrix  $M_{12}$  dominates over the decay matrix  $\Gamma_{12}$ . Hence the function  $f_{\pm}(t)$  can be approximated by

$$\begin{aligned} f_+(t) &= e^{-imt} e^{-\frac{\Delta m}{2}t} \\ f_-(t) &= ie^{-imt} e^{-\frac{\Delta m}{2}t} \sin \frac{\Delta m}{2}t \end{aligned} \quad (317)$$

with the characteristic parameter of the oscillation being  $x = \frac{\Delta m}{\Gamma}$ .

The fact that  $M_{12} \gg \Gamma_{12}$  for the  $B$  system is easily understood by comparing the graphs contributing to  $B - \bar{B}$  transitions shown in Fig. 39. Clearly one sees from the figure that for the  $B_q - \bar{B}_q$  system

$$\Delta m \sim m_t^2 |V_{tb}^* V_{tq}|^2 \quad (318)$$

while

$$\Delta \Gamma \sim m_b^2 |V_{cb}^* V_{cq}|^2 \quad (319)$$

Although the Kobayashi Maskawa matrix elements are comparable, one can neglect  $\Delta \Gamma$  relative to  $\Delta m$  because of the phase space difference:  $m_b^2$  versus  $m_t^2$ .

Normally a  $B_d^0 \sim (bd)$  state has a semileptonic decay into an  $l^+ \nu_l X$ . However, with  $B_d^0 - \bar{B}_d^0$  mixing one expects also semileptonic decays into an  $l^- \nu_l X$ ,

$$B_d^0 \xrightarrow{\text{mix}} \bar{B}_d^0 \rightarrow l^- \nu_l X \quad (320)$$

The ratio <sup>24</sup>

$$r_d = \frac{\Gamma(B_d^0 \rightarrow l^- \nu_l X)}{\Gamma(B_d^0 \rightarrow l^+ \nu_l X)} = \frac{\int_0^\infty |f_-(t)|^2 dt}{\int_0^\infty |f_+(t)|^2 dt} = \frac{x_d^2}{2 + x_d^2} \quad (321)$$

measures the amount of  $B_d^0 - \bar{B}_d^0$  mixing, with the parameter  $x_d$

$$x_d = \frac{(\Delta m)_{B_d}}{(\Gamma)_{B_d}} = \tau_{B_d} (\Delta m)_{B_d} \quad (322)$$

<sup>24</sup>For the  $B_d$  system,  $\epsilon_{B_d}$  is negligible in magnitude and can be neglected.

the formula for  $x_d$ . In particular, the large mixing observed implies that top cannot be too light. Although one cannot make an absolute pronouncement on this, the results of very many detailed studies [86] suggest that

$$(m_t)_{\text{theor}} > 50 \text{ GeV}, \quad (327)$$

which is comparable to the UA1 bound of Eq(162). Furthermore, at least in the 3 generation CKM model, also  $V_{td}$  cannot be too small. Now

$$|V_{td}|^2 = A^2 \lambda^6 [1 + \rho^2 - 2\rho \cos \delta], \quad (328)$$

so the mixing is largest when  $\rho$  is large and  $\delta \rightarrow \pi$ . However,  $\delta$  is not really allowed to get to  $\pi$ , because then all CP violation disappears in the CKM model!

As the last point in these lectures, I want to give the results of a combined fit, made in collaboration with Krawczyk, London and Steger [85], of the  $x_d$  and  $\epsilon$  formulas to determine the allowed area in the  $\rho - \delta$  plane, for given values of  $m_t$ , and of the hadronic uncertainties  $B_K$  and  $f_{B_d}^2 B_{B_d}$ . In the analysis of [85]  $f_{B_d}^2 B_{B_d}$  was taken in the range of Eq(326),  $B_K$  in the range of Eq(300) and we assumed  $40 \text{ GeV} < m_t < 180 \text{ GeV}$ . Our results are shown in Fig. 41. As one can see from the figure, the allowed regions are "moons" in the  $\rho - \delta$  plane, which fatten up as one increases the theoretical uncertainty. Knowledge of the top mass would greatly reduce the allowed region in  $\rho - \delta$  space, even in the case depicted in Fig. 42 in which the whole range of theoretical uncertainty assumed is allowed.

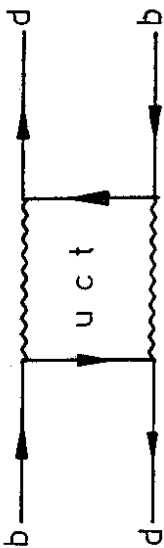


Figure 40: Box graph contributing to  $x_d$ .

being a function of the CKM matrix elements. The ARGUS collaboration in 1987 discovered that there was substantial mixing in the  $B_d$  system [82]. They had the good fortune to actually detect an event with two fully reconstructed  $B_d$ 's, thereby obtaining explicit evidence for mixing. To actually extract the mixing parameter quantitatively, they studied their data sample for the presence of same sign leptons and of reconstructed  $B_d$ 's associated with leptons of the wrong sign. From both these signals ARGUS deduced that [82]:

$$\frac{\Gamma(B_d^0 \rightarrow l^- \bar{\nu}_l X)}{\Gamma(B_d^0 \rightarrow l^+ \nu_l X)} = 0.21 \pm 0.08 \quad (323)$$

which implies that  $x_d = 0.73 \pm 0.18$ . Very recently the ARGUS result has been confirmed by CLEO [83], with the combined results leading to a mixing parameter

$$x_d = 0.70 \pm 0.13 \quad (324)$$

To calculate  $x_d$  theoretically, one is invited to calculate the box graph of Fig. 40. This calculation proceeds in an analogous fashion to the one in the Kaon system, done earlier in these lectures. Here, however, after having made use of the unitarity of the CKM matrix, one need only retain the  $t$  loop contribution, since both  $c$  and  $u$  loops are of  $O(\lambda^6)$  and  $m_i^2 \gg m_c^2$ . One finds [84]:

$$x_d = \tau_{B_d} \frac{G_F^2 M_B}{6\pi^2} [f_{B_d}^2 B_{B_d} \eta_B |m_t f_d(y_t)| |V_{td}|^2] \quad (325)$$

In the above  $\eta_B \simeq 0.85$  [84] is a QCD correction factor, while  $f_{B_d}^2 B_{B_d}$  is the analogue for the  $B_d$  system of  $f_K^2 B_K$ . A reasonable range for this hadronic uncertainty is [85]:

$$100 \text{ MeV} < (f_{B_d}^2 B_{B_d})^{\frac{1}{2}} < 200 \text{ MeV} \quad (326)$$

Because the ARGUS result for  $x_d$  [82] turned out to be bigger than theorists expected prior to the measurement, one needed to push upwards the various factors appearing in

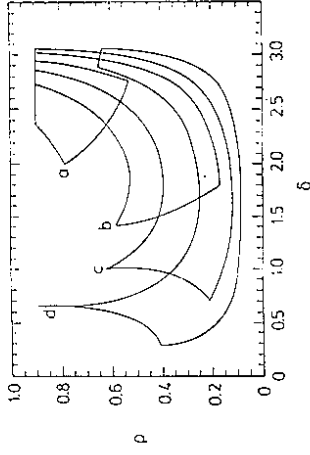


Figure 42: Allowed regions in the  $\rho - \delta$  plane for fixed values of  $m_t$ , but for the full theoretical uncertainty. Regions  $a - d$  correspond to  $m_t = 60, 90, 120, 180 \text{ GeV}$ , respectively. From [85].

## References

- [1] S.L. Glashow, Nucl. Phys. 22 (1961) 579; A. Salam in *Elementary Particle Theory*, ed. N. Svarthelm (Almqvist and Wiksell, Stockholm, 1968); S. Weinberg, Phys. Rev. Lett. 19 (1967) 1264
- [2] See for example, E. Abers and B.W. Lee, Phys. Rept. 9C (1973) 1
- [3] N. Cabibbo, Phys. Rev. Lett. 10 (1963) 531; M. Kobayashi and T. Maskawa, Prog. Theo. Phys. 49 (1973) 652
- [4] C. Llewellyn Smith, Nucl. Phys. B228 (1983) 205
- [5] CDHS Collaboration H. Abramowicz et al., Phys. Rev. Lett. 57 (1986) 298
- [6] CHARM Collaboration J.V. Allaby et al., Phys. Lett. 177B (1986) 446
- [7] CCFRR Collaboration P.G. Reutens et al, Phys. Lett. 152B (1985)404
- [8] FMM Collaboration D. Bogert et al., Phys. Rev. Lett. 55 (1985) 1969
- [9] U. Amaldi et al., Phys. Rev. D36 (1987) 1385
- [10] G. Costa et al., Nucl. Phys. B297 (1988) 244
- [11] CDHS Collaboration H. Abramowicz et al., Z. Phys. C 28 (1985) 51
- [12] CHARM Collaboration M. Jonker et al., Phys. Lett. 99B (1981) 265; 103B (1981) 469(E)

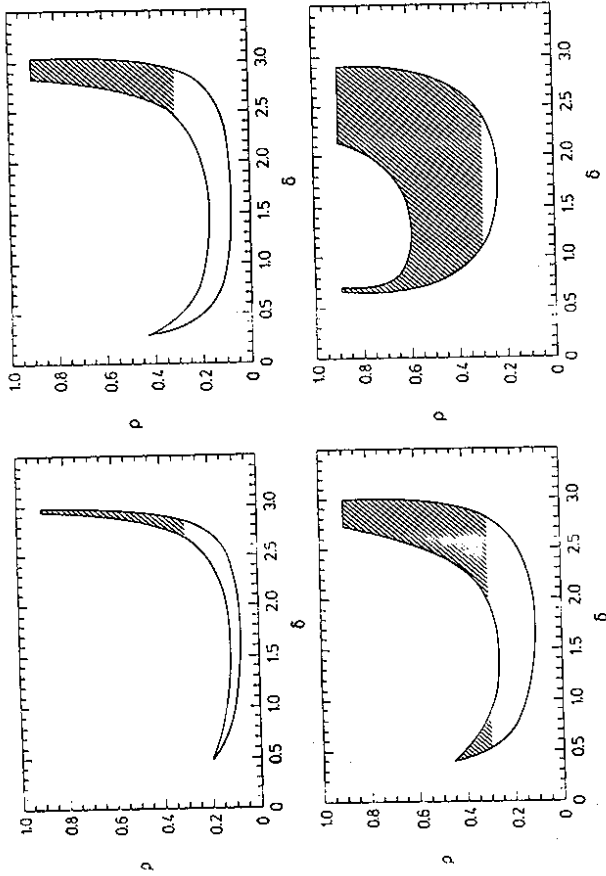


Figure 41: Summary of the present information on the CP violating phase  $\delta$ . In all curves the whole  $m_t$  uncertainty is allowed. In the top left curve  $f_{B_d}^2 B_{B_d} = 150 \text{ MeV}$  and  $B_K = 1$ . In the other curves  $f_{B_d}^2 B_{B_d}$  was taken in the full range of uncertainty and  $B_K = 1, \frac{2}{3}, \frac{1}{3}$ . From [85].

[32] E. Ma and J. Okada, *Phys. Rev. Lett.* 41 (1978) 287; See also G. Barbiellini, B. Richter and J.L. Siegrist, *Phys. Lett.* 106B (1981) 414

[33] K.J.F. Gaemers, R. Gastmans and F.M. Renard, *Phys. Rev. D* 19 (1979) 1605

[34] ASP Collaboration, C. Hearty et al., *Phys. Rev. Lett.* 58 (1987) 1711

[35] CELLO Collaboration, H.J. Behrend et al., *Phys. Lett.* 215B (1988) 179

[36] UA1 Collaboration, C. Albajar et al., *Phys. Lett.* 98B (1987) 271

[37] UA2 Collaboration, R. Ansari et al., *Phys. Lett.* 186B (1987) 440

[38] P. Colas, D. Denegri and C. Stubenrauch, *Zeit. Phys.* C40 (1988) 527

[39] See, for example, the recent global analysis by A. Ali and F. Barreiro, DESY preprint DESY 88-075

[40] A. Blondel et al., in **Physics at LEP** ed. by J. Ellis and R.D. Peccei, CERN Yellow Report CERN 86-02

[41] L. Maiani, *Phys. Lett.* B62 (1976) 183

[42] L. Wolfenstein, *Phys. Rev. Lett.* 51 (1983) 1945

[43] A. Sirlin, in **Proceedings of the 1987 International Symposium on Lepton and Photon Interactions at High Energy**, Hamburg, ed. W. Bartel and R. Ruckl, Nucl. Phys. B (Proc. Suppl.) 417 (1988)

[44] S.S. Gershtein and Ya. B. Zeldovich, *JETP* 29, 698 (1955); *Soviet Physics JETP* 2, 576 (1958), translation; E.C.G. Sudarshan and R.E. Marshak, *Proc. Padua-Venice Conf. on Mesons and Recently Discovered Particles (1957) V-14*. Reprinted in P.K. Kabir, **Development of the Weak Interaction Theory** (Gordon and Breach, New York 1963) p. 118; R.P. Feynman and M. Gell-Mann, *Phys. Rev.* 109, 193 (1958)

[45] R. Behrends and A. Sirlin, *Phys. Rev. Lett.* 4 (1960) 186; M. Ademollo and R. Gatto, *Phys. Rev. Lett.* 13 (1964) 264

[46] A. Sirlin, *Phys. Rev.* D35 (1987) 3423

[47] V.T. Koslowsky et al., in **Proceedings of the Seventh International Conference on Atomic Masses and Fundamental Constants**, ed. O. Klepper (GSI, Darmstadt, 1984)

[48] N. Cabibbo, *Phys. Rev. Lett.* 10 (1963) 531

[49] H. Leutwyler and M. Roos, *Z. Phys.* C25 (1984) 91

[50] *Particle Data Book*, *Phys. Lett.* 170B (1986) 1

[51] For a review, see for example H. Pagels, *Phys. Rept.* 16C (1975) 219; See also, J. Gasser and H. Leutwyler, *Ann. Phys.* (N.Y.) 158 (1984) 142

[52] See for example, J. Gasser and H. Leutwyler, *Phys. Rept.* 87 (1982) 77

[13] P. Jenni, in **Proceedings of the 1987 International Symposium on Lepton and Photon Interactions at High Energy**, Hamburg, ed. W. Bartel and R. Ruckl, Nucl. Phys. B (Proc. Suppl.) 3 (1988) 341

[14] W. Marciano and A. Sirlin, *Phys. Rev. D* 12 (1980) 2695; D29 (1984) 945; M. Consoli, S. Lo Presti and L. Maiani, *Nuc. Phys.* B223 (1983) 474; Z. Hioki, *Prog. Theor. Phys.* 68 (1982) 2134; *Nuc. Phys.* B229 (1983) 284

[15] A. Sirlin, *Phys. Rev. D* 22 (1980) 971

[16] W. Marciano, *Phys. Rev. D* 20 (1979) 274; F. Antonelli and L. Maiani, *Nucl. Phys. B* 186 (1981) 269; For a very nice discussion, see also, L. Maiani in the **TASI Lectures 1984**, Univ. of Michigan, Ann Arbor, Michigan.

[17] See for example, C. Itzykson and J.B. Zuber **Quantum Field Theory** (McGraw Hill, N.Y. 1980)

[18] W. Marciano and A. Sirlin, *Phys. Rev. D* 29 (1984) 945

[19] For a discussion of renormalization group methods to sum QCD corrections to weak process, see for example, G. Altarelli, R.K. Ellis, L. Maiani and R. Petronzio *Nucl. Phys. B* 88 (1975) 215

[20] M. Veltman, *Nucl. Phys. B* 123 (1977) 89

[21] W. Marciano and A. Sirlin, *Phys. Rev. D* 22 (1980) 2695

[22] See for example, P. Baillon et al. in **Physics at LEP** ed. J. Ellis and R.D. Peccei CERN Yellow Report CERN 86-02

[23] P. Langacker in **Neutrino Physics** ed. H.V. Klapdor (Springer, Berlin, 1988)

[24] JADE Collaboration, W. Bartel et al., *Phys. Lett.* 146B (1984) 437

[25] S.L. Wu in **Proceedings of the 1987 International Symposium on Lepton and Photon Interactions at High Energy**, Hamburg, ed. W. Bartel and R. Ruckl, Nucl. Phys. B (Proc. Suppl.) 3 (1988) 39

[26] T. Kamae, to appear in the **Proceedings of the XXIV Int. Conference on High Energy Physics**, Munich, West Germany, Aug. 1988

[27] H. Kichimi, to appear in the **Proceedings of the 8th Physics in Collision Conference**, Capri, Italy, Oct. 1988

[28] UA1 Collaboration, C. Albajar et al., *Zeit. Phys.* 37C (1988) 505

[29] G. Altarelli, M. Diemoz, G. Martinelli and P. Nason, *Nucl. Phys. B* 308 (1988) 724

[30] P. Nason, S. Dawson and R.K. Ellis, *Nucl. Phys. B* 303 (1988) 607

[31] J. Yang, M.S. Turner, G. Steigman, D.N. Schramm and K.A. Olive, *Astrophys. J.* 281 (1984) 443



- [53] G. Furlan, F. G. Lammoy, C. Rossetti, G. Segre, Nuovo Cim. 38 (1965) 1747
- [54] J. Gasser and H. Leutwyler, Nucl. Phys. B250 (1984) 465, 517, 539
- [55] CDHS Collaboration H. Abramowicz et al, Zeit. Phys. C15 (1982) 19
- [56] ARGUS Collaboration H. Schröder, Proceedings of the International Conference on Hadron Spectroscopy, ed. S. Oneda (AIP, New York, 1985)
- [57] G. Altarelli, N. Cabibbo, G. Corbo, L. Maiani and G. Martinelli, Nucl.Phys. B 208 (1982) 365
- [58] M. Gilchriese, in Proceedings of the XXIII International Conference on High Energy Physics, Berkeley, USA (1986)
- [59] ARGUS Collaboration H. Schröder, to appear in the Proceedings of the XXIV International Conference on High Energy Physics, Munich, West Germany, August 1988; See also, CLEO Collaboration R. Fulton et al, preprint CBX-88-13 (1988)
- [60] ARGUS Collaboration H. Albrecht et al., Phys. Lett. 209B (1988) 119
- [61] CLEO Collaboration D. Kreinek, to appear in the Proceedings of the XXIV International Conference on High Energy Physics, Munich, West Germany, August 1988
- [62] For a similar discussion, see also, M. Gronau and J. Rosner, Phys. Rev. D37 (1988) 688
- [63] G. Altarelli and P. Franzini, Z. Phys. C37 (1988) 271
- [64] D.M. Ritson, in Proceedings of the XXIII International Conference on High Energy Physics, Berkeley, ed. S. Loken (World Scientific, Singapore, 1987)
- [65] C. S. Kim, private communication. See also, G. Belanger et al, to appear in the Proceedings of the 1988 Snowmass Summer Study on High Energy Physics in the 1990's, Snowmass, Colorado, USA, July 1988
- [66] T. D. Lee and C. S. Wu, Ann. Rev. Nucl. Sci. 16 (1966) 511
- [67] K. Kleinknecht, Ann. Rev. Nucl. Sci. 26 (1976) 1
- [68] NA31 Collaboration H. Burkhardt et al., Phys. Lett. 206B (1988) 169
- [69] M. Woods et al, Phys. Rev. Lett. 60 (1988) 1695
- [70] L. Wolfenstein, Ann. Rev. Nucl. Sci. 36 (1986) 137
- [71] T. T. Wu and C. N. Yang, Phys. Rev. Lett. 13 (1964) 380
- [72] T. T. Devlin and J. O. Dickey, Rev. Mod. Phys. 51 (1979) 237
- [73] B. W. Lee and M. K. Gaillard, Phys. Rev. D10 (1974) 897
- [74] R.E. Shrock and S. B. Treiman, Phys. Rev. D19 (1979) 2148
- [75] For a discussion of various determinations of  $B_K$ , see for example, L. Wolfenstein, Ann. Rev. Nucl. Sci. 36 (1986) 137
- [76] A. J. Buras, W. Slominski and H. Steger, Nucl. Phys. B 238 (1984) 529
- [77] F. Gilman and M. Wise, Phys. Rev. D27 (1983) 1128
- [78] F. Gilman and M. Wise, Phys. Lett. 83B (1979) 83
- [79] B. Guberina and R. D. Peccei, Nucl. Phys. B 163 (1980) 289; F. Gilman and M. Wise, Phys. Rev. D20 (1979) 2392
- [80] G. Altarelli and P. Franzini, Cern Th 4914/87, to appear in the Proceedings of the Symposium on Present Trends, Concepts and Instruments of Particle Physics, Rome, Nov 1987
- [81] J. Hagelein, in Proc. Moriond Workshop on Electroweak Interactions and Unified Theories, ed J. Tran Thanh Van (Editions Frontiers, 1984); L. Wolfenstein, Comments Nucl. Part. Phys. 14 (1985) 135
- [82] ARGUS Collaboration H. Albrecht et al, Phys. Lett. 192B (1987) 245
- [83] CLEO Collaboration A. Jawahery, to appear in the Proceedings of the XXIV International Conference on High Energy Physics, Munich, West Germany, August 1988
- [84] A. J. Buras, W. Slominski and H. Steger, Nucl. Phys. B 245 (1984) 369; J. Hagelein, Nucl. Phys. B 193 (1981) 123
- [85] P. Krawczyk, D. London, R.D. Peccei and H. Steger, Nucl. Phys. B 307 (1988) 19
- [86] G. Altarelli and P. Franzini, Z. Phys. C37 (1988) 271; J. Donoghue, T. Nakada, E. Paschos and D. Wyler, Phys. Lett. 195B (1987) 285; J. Ellis, J. Hagelein and S. Rudaz, Phys. Lett. 192B (1987) 201; I. I. Bigi and A. I. Sanda, Phys. Lett. 194B (1987) 307; J. Maalampi and M. Roos, Phys. Lett. 195B (1987) 489; V. Barger, T. Han, D. V. Nanopoulos and R. J. N. Phillips, Phys. Lett. 194B (1987) 312